INVESTIGATING SPATIAL REPRESENTATION OF MICROMETEOROLOGICAL FLUX MEASUREMENTS OVER AGROECOSYSTEMS

by

Amanda M. Taylor

A Thesis
Submitted to the Faculty of Graduate Studies of
The University of Manitoba
In partial fulfillment of the requirements for the degree of

DOCTOR OF PHILOSOPHY

Department of Soil Science
University of Manitoba
Winnipeg, Manitoba

ABSTRACT

Taylor, Amanda M. Ph.D., The University of Manitoba, October, 2017. Investigating Spatial Representation of Micrometeorological Flux Measurements over Agroecosystems. Major Professor; Brian D. Amiro.

A challenge with micrometeorological flux measurements is determining whether they represent field spatial variability. Often only one tower characterizes agricultural fluxes, so we used three towers (co-located, 50 m, and 100 m apart) to evaluate the spatial capability of eddy covariance to measure net ecosystem exchange (NEE), latent heat flux (LE), and sensible heat flux (H) over a forage and a spring wheat crop. Regression comparisons of NEE decreased slightly as towers moved apart at the forage and was not reliable at the wheat because of senescence. LE varied little amongst separations, and H maintained a consistently high r^2 at all tower locations on both fields whether examined over the short- or long-term. Georeferenced, gridded leaf area index values within tower footprints were representative of the whole field. Overall, H field variability was captured within 10 W m^{-2}, LE ranged 15 – 60 W m^{-2}, and NEE was 23 – 33% RMSE over the forage. Many farms have known heterogeneity that can come from forage, grains, and cattle operations within the same agroecosystem, and cattle movement is a challenge when measuring farm budgets. With two eddy covariance towers and static-vented chamber campaigns we measured NEE, methane (CH_4), and nitrous oxide (N_2O) fluxes for a year over a beef cattle farm. Enteric CH_4 was used as a tracer to separate cattle respiration fluxes from the farm landscape NEE. Chamber measurements on bale locations after winter grazing were hotspots for N_2O emission the following spring and summer, while pasture fluxes were minimal elsewhere. When all sources of greenhouse

gas measurement were combined, field and cattle respiration and CH_4 dominated, and the farm was a carbon source of 46 t CO_2 equivalent ha^{-1} y^{-1}. Flux research would benefit from quantifying field spatial variability to ensure that eddy covariance measurements are representative. Incorporating flux towers and chambers can help estimate greenhouse gas budgets of spatially variant agroecosystems.

ACKNOWLEDGEMENTS

Thank you to my PhD advisory committee, Dr. Brian D. Amiro, Dr. Paul Bullock, and Dr. Karin Wittenberg. A special thanks to Dr. Amiro for the mentor he became through the years, and the example he is of someone in life I aspire to be like. I could always count on him for encouragement, kindness, understanding, and laughter.

Thank you for the funding provided by the Natural Sciences and Engineering Research Council (NSERC), Agriculture and Agri-Food Canada Agricultural Greenhouse Gas Program, The Canadian Foundation for Innovation, Manitoba Graduate Fellowship (UMGF), and the University of Manitoba Graduate Enhancement of the Tri-Council Stipends (GETS). Without their support this research and my doctoral work would not have been possible.

Thank you to the researchers and technicians who helped in field and in the lab: H. Block, K. Buckley, J. Bieganski, R. Thiessen from the AAFC Brandon Research centre for site support, expertise, and use of the Johnson Farm for our research site; M. Gervais, B. Sparling, K. Hanis, J. Yorick, V. Bondar, for technical support; all the soilies and staff in the Department of Soil Science for help, encouragement, and comradery; Z. Nesic, A. Barr, M.-A. Giasson, K. Morgenstern, T.A. Black, N. Kljun, R. Clement, and B. Chen, researchers who've developed MATLAB flux algorithms; the University of British Columbia and A. Glenn for lending us equipment; K. Ominski and S. McGinn for project advice for Chapter 4; M. Tenuta and the National Centre for Livestock and the Environment for expertise and use of their site for our field experiment, and for part of

the data used in Chapter 3 and 4; and Scott Smith for allowing us to conduct research on his farm in Oakbank, Manitoba.

Thank you very much to the reviewers who gave feedback on the Chapter 4 paper submission.

Lastly, thank you to my spouse Chris for mental and emotional support, and for all the evenings and weekends he joined me in the field or troubleshot code with me. Wouldn't be where or who I am without him.

FOREWORD

This thesis was organized in accordance with the Department of Soil Science of the University of Manitoba guidelines.

Chapter 4 was published and incorporated feedback from anonymous reviewers:

Taylor, A.M., Amiro, B.D., Tenuta, M., Gervais, M. 2017. Direct whole-farm greenhouse gas flux measurements for beef cattle operations. Agric. Ecosyst. Environ. **239**: 65-79.

Amanda Taylor collected, processed, and analysed the flux data, and wrote the initial drafts of this paper (80% contribution).

In the near future, versions of Chapter 2 and 3 will be submitted for publication.

TABLE OF CONTENTS

LIST OF TABLES

LIST OF FIGURES

1. INTRODUCTION

1.1 Measuring fluxes with eddy covariance and chambers

Eddy covariance is a micrometeorological technique that continuously measures surface-atmosphere fluxes of gas or energy *in situ* without disrupting the environment, and provides time-averaged, area-integrated measurements (Baldocchi et al. 1988; Baldocchi 2003). It measures the covariance between the fluctuations of a given gas (c') and vertical wind velocity (w') to provide the mean flux (F), where primes ($'$) are deviations from the mean and overbars are time averaged values (Baldocchi 2003).

$$F = \overline{w'c'}$$

Measurements are made with fast responding sonic anemometers and gas analysers, usually recorded at 5 – 20 Hz and typically averaged over half-hour time periods. The technique measures a flux footprint several hundred metres upwind depending on the height of the instrument tower. Accompanying meteorological variables like photosynthetically active radiation, soil and air temperature, soil heat flux, and water vapour flux are measured in parallel with the gas flux for use in corrections, characterization, and gap-filling. It is the preferred micrometeorological technique for providing direct, independent measurements of fluxes because it has fewer simplifying assumptions compared to most other techniques (Denmead 2008).

FLUXNET uses micrometeorology and eddy covariance to measure gas and turbulent fluxes at more than 650 research stations the world over. The work has helped characterize and understand processes on peatlands (e.g., Lafleur et al. 2003; Glenn et al. 2006), marshes (e.g., Strachan et al. 2015), boreal forests both new and old (e.g., Amiro

et al. 2006; Dunn et al. 2007), grasslands (e.g., Soussana et al. 2007; Flanagan et al. 2002), pasture (e.g., Mudge et al. 2011), multiple crops (e.g., Alberti et al. 2010; Taylor et al. 2013) for multiple years (e.g., Aubinet et al. 2009; Béziat et al. 2009), in Arctic regions (e.g., Hanis et al. 2015) and more.

During the past century non-steady-state chambers have also been used to measure gases, with methodologies updated by Matthias et al. (1980) and Hutchinson and Mosier (1981). Static-vented, closed chambers allow a target gas to accumulate in the headspace volume (V_C) over a set deployment time (t) on the chamber's surface area (A_S), using concentration differences between measurement time intervals (C_{t1}, C_{t2}) to determine the gas flux (F_G) (Hutchinson and Mosier 1981).

$$F_G = \frac{V_C}{A_S \Delta t} [C_{t2} - C_{t1}] \quad [1.1]$$

Chambers are simple to construct and operate (Denmead 2008), and cost less than micrometeorological techniques, but require many chambers to account for a site's spatial variability (Bolan et al. 2004; McGinn 2006; Denmead 2008). Closed chambers are preferred because they can measure smaller fluxes, and gases like N_2O are often below the detection levels of open chambers (Hutchinson and Mosier 1981). A vented chamber helps eliminate disturbances associated with air pressure and temperature changes between the chamber headspace and the external atmosphere (Hutchinson and Mosier 1981; Hutchinson and Livingston 2001). Chamber techniques can alter the environment being studied (McGinn 2006; Rochette and Eriksen-Hamel 2008; Muñoz et al. 2011) and are difficult to get continuous, long-term measurements (Baldocchi et al. 1988), but they can help account for landscape heterogeneity that micrometeorology may miss,

particularly for spatial analysis of non-homogeneous sites and to contextualize temporal differences (Molodovskaya et al. 2011).

1.2 Challenges of spatial variability

Ecological processes have spatial variability that can make measurement site comparison difficult (Oksanen 2001). Surface properties like topography, soil moisture, vegetation, and climatic drivers like air temperature and vapour pressure deficit can influence directional flux characteristics and the magnitude of fluxes within the footprints measured (Griebel et al. 2016). Many sites only use one eddy covariance tower to characterize ecosystems or processes, essentially using pseudoreplication (Hurlbert 1984). Furthermore, advection and large scale atmospheric processes can cause imbalances in turbulent flux energy measurements, as can eddies from local or landscape heterogeneity (Foken 2008; Anderson and Wang 2014). If a measurement site lacks surface homogeneity, measurements violate the eddy covariance technique assumption that the measured landscape is homogeneous and this can increase measurement uncertainty (Mauder et al. 2013).

1.3 Agricultural systems and greenhouse gases

Agricultural systems are of particular interest when measuring greenhouse gases because of how human intervention modifies the processes and landscape features depending on what managements, animals, or amendments are used. Carbon dioxide (CO_2), methane (CH_4), and nitrous oxide (N_2O) are three of the greenhouse gases whose

cycles are more heavily impacted by agriculture. Agriculture contributes to atmospheric greenhouse gases which drive climate change (Ciais et al. 2013).

1.3.1 CO_2 fluxes

Atmospheric CO_2 concentrations have increased 25% in the last fifty years alone (Tans and Keeling 2015). CO_2 fluxes have strong seasonality and temperature dependence (Hynšt et al. 2007) regulated by the landscape over which they cycle. Agroecosystems can follow a different pattern of carbon dioxide uptake and emission; annual crops have periods of fallow in the spring and fall, and perennials are grazed or hayed, each resulting in removal of carbon from the farm (Taylor et al. 2013). On-farm CO_2 emissions also come from field work, haulage, electricity, heating, machinery, and fertilizer application (Vergé et al. 2008). Different stages of cattle production (Beauchemin et al. 2011) and grazing pressures also modify carbon flux through excreta effecting mineralization and nitrogen cycling, defoliation/treading by animals (Soussana et al. 2007), and animal consumption and respiration.

1.3.2 CH_4 fluxes

CH_4 is second only to CO_2 in contributing to human-induced global warming. Historical changes in atmospheric CH_4 are closely linked to changes in atmospheric temperature (Montzka et al. 2011). Too complex to naturally form in the atmosphere, CH_4 is released from earth-bound processes like enteric fermentation (Ehhalt and Schmidt 1978), whereby CO_2 and H_2 combine to produce CH_4 and H_2O. Generally agricultural fields are small net sinks of CH_4, but are relatively insignificant compared to

that produced by ruminants through enteric fermentation. Agriculture produces 50% of the anthropogenic CH_4 globally (Kebreab et al. 2006).

Beef cattle CH_4 emissions primarily result from enteric fermentation and manure (Johnson et al. 2007; Vergé et al. 2008), with global ruminant livestock emissions contributing 87 – 94 Tg CH_4 $year^{-1}$ (Ciais et al. 2013). The amount of CH_4 produced depends on rate and method of weight gain (Desjardins et al. 2012), feed quality and quantity, feed intake and rumination (Harper et al. 1999; Dijkstra et al. 2011), environmental factors, and feed conversion efficiency (Kebreab et al. 2006). High animal-to-animal variation in CH_4 emission increases uncertainty, as does how much of a herd can be captured in a flux measurement footprint (Laubach and Kelliher 2005). Low accuracy of whole farm CH_4 prediction models (Dijkstra et al. 2011) necessitates measurements that examine different management strategies attempting to capture all farm activities.

1.3.3 N_2O fluxes

Agriculture is a major source of N_2O because of increasing nitrogen fertilizer use and livestock manure, with agricultural intensification accounting for ~80% of atmospheric increases in N_2O (Ciais et al. 2013). Most agricultural N_2O emissions result from fertilizer, through denitrification after mineralisation (Bremner 1997; Bolan et al. 2004), which are influenced by soil pH, temperature (Knowles 1982; Wagner-Riddle and Thurtell 1998; Rochette and Eriksen-Hamel 2008), soil water, available organic matter, substrate oxygen levels, NO_3^- levels, (Knowles 1982; Bremner 1997; Brown et al. 2002; Bolan et al. 2004), and C:N ratios (Dijkstra et al. 2011). Spatial and temporal variation in

conditions like wetting or drying, fertilizers, plant type, and organic matter affect nitrifying/denitrifying activity and can be difficult to quantify in field (Knowles 1982), and the resulting emissions have large uncertainties (Ciais et al. 2013).

In cattle systems, N_2O emissions also relate to the amount of solids in manure (Kebreab et al. 2006), nutrient surplus in faeces, and urine (Dijkstra et al. 2011). Cattle retain up to 20% of total N consumed, losing the rest through urine and faeces, depositing more where they congregate depending on the N-content of feed and their stocking behaviour (Oenema et al. 1997; Bolan et al. 2004). Soil moisture, degree of trampling, and temperatures change can influence N_2O fluxes more than the amount of N in faeces and urine (Salomon and Rodhe 2011). The nitrogen from animal excreta and organic manures can be upwards of 30% of beef cattle greenhouse gas emissions (Beauchemin et al. 2010). Challenges stemming from variation and subsequent upscaling of anthropogenic N_2O flux measurements contribute further to uncertainty in flux estimates (Bolan et al. 2004).

1.3.4 Challenges with management and fluxes

CO_2, CH_4, and N_2O uptake and emission change based on management and time of year. For example, forages generally take up more carbon but may result in higher CH_4 emission when consumed by cattle, while grains are more easily digested and result in lower enteric CH_4 emissions (Harper et al. 1999), but use more fertilizer that have higher N_2O emissions (Vergé et al. 2008; Desjardins et al. 2012). Livestock use plants and landscapes unsuitable for crops to make products for human consumption. With demand for animal protein and dairy increasing globally (Lemaire et al. 2014) our capability to

accurately measure and understand how cattle farms change greenhouse gas cycles spatially and temporally is important to monitor and predict the impact agriculture has and will have in the future.

Eddy covariance can be used to measure agricultural greenhouse gases, and may be applied to multiple, homogeneous point sources, like CH_4 emitted from grazing livestock (McGinn 2006) or feedlots. Instrumentation needs to be high enough to treat the gas as a uniformly emitted source (Harper et al. 2011) whose footprint includes all cattle in the pasture to reduce uncertainty.

1.4 Thesis organization

This thesis examines how agricultural landscape heterogeneity complicates measuring the gas and energy fluxes that originate from them. Chapter 2 explores the influence of spatial variability on two agricultural fields, comparing three identical towers using eddy covariance to measure CO_2 fluxes and evaluating the potential drivers of variability and patchiness with leaf area index (LAI). Chapter 3 examines sensible heat (H) and latent heat (LE) fluxes over two agricultural fields, comparing short-term data from three towers on the same field to determine if a single tower is sufficient to represent the turbulent fluxes. A second dataset is used to evaluate a longer period and larger dataset, comparing four towers on the same field over four years. Chapter 4 looks at the whole farm variability of a backgrounding beef cattle operation, measuring CO_2 and CH_4 with eddy covariance and static-vented chambers, and N_2O with chambers alone. Over one year, we measured the greenhouse gas emissions of cattle and the agroecosystem during winter bale grazing, cow-calf grazing, confinement, pasture

grazing, and swath grazing. The measurements allowed us to estimate whole farm CO_2-equivalent emissions and examine our ability to capture mobile sources like cattle. The fourth chapter is published, while the second and third will be submitted in the near future. Combined, these three research chapters tackle some of the spatial challenges of measuring gas and energy fluxes over agricultural systems.

1.5 References

Alberti, G., Vedove, G.D., Zuliani, M., Peressotti, A., Castaldi, S., Zerbi, G. 2010. Changes in CO_2 emissions after crop conversion from continuous maize to alfalfa. Agric. Ecosyst. Environ. 136: 139-147.

Amiro, B.D., Barr, A.G., Black, T.A., Iwashita, H., Kljun, N., McCaughey, J.H., Morgenstern, K., Murayama, S., Nesic, Z., Orchansky, A.L., Saigusa, N. 2006. Carbon, energy and water fluxes at mature and disturbed forest sites, Saskatchewan, Canada. Agric. For. Meteorol. 136: 237-251.

Anderson, R.G., Wang, D. 2014. Energy budget closure observed in paired eddy covariance towers with increased and continuous daily turbulence. Agric. For. Meteorol. 184: 204-209.

Aubinet, M., Moureaux, C., Bodson, B., Dufranne, D., Heinesch, B., Suleau, M., Vancutsem, F., Vilret, A. 2009. Carbon sequestration by a crop over a 4-year sugar

beet/winter wheat/seed potato/winter wheat rotation cycle. Agric. For. Meteorol. 149: 407-418.

Baldocchi, D. D. 2003. Assessing the eddy covariance technique for evaluating carbon dioxide exchange rates of ecosystems: past, present and future. Global Change Biol. 9: 479-492

Baldocchi, D.D., Hicks, B. B., Meyers, T.P. 1988. Measuring biosphere-atmosphere exchanges of biologically related gases with micrometeorological methods. Ecology 69: 1331-1340.

Beauchemin, K.A., Janzen, H.H., Little, S.M., McAllister, T.A., McGinn, S.M. 2010. Life cycle assessment of greenhouse gas emissions from beef production in western Canada: A case study. Agric. Sys. 103: 371-379.

Beauchemin, K.A., Janzen, H.H., Little, S.M., McAllister, T.A., McGinn, S.M. 2011. Mitigation of greenhouse gas emissions from beef production in western Canada – Evaluation using farm-based life cycle assessments. Anim. Feed Sci. Technol. 166-167: 663-677.

Béziat, P., Ceschia, E., Dedieu, G. 2009. Carbon balance of a three crop succession over two cropland sites in South West France. Agric. For. Meteorol. 149: 1628-1645.

Bolan, N.S., Saggar, S., Luo, J., Bhandral, R., Singh, J. 2004. Gaseous emissions of nitrogen from grazed pastures: Processes, measurements and modelling, environmental implications, and mitigation. Adv. Agron. 84: 37-120.

Bremner, J.M. 1997. Sources of nitrous oxide in soils. Nutr. Cycling Agroecosyst. 49: 7-16.

Brown, H.A., Wagner-Riddle, C., Thurtell, G.W. 2002. Nitrous oxide flux from a solid dairy manure pile using a micrometeorological mass balance method. Nutr. Cycling Agroecosyst. 62: 53-60.

Ciais, P., Sabine, C., Bala, G., Bopp, L., Brovkin, V., Canadell, J., Chhabra, A., DeFries, R., Galloway, J., Heimann, M., Jones, C., Le Quéré, C., Myneni, R.B., Piao, S., Thornton, P. 2013. Carbon and other biogeochemical cycles. In: *Climate change 2013: The physical science basis. Contribution of Working Group I to the Fifth Assessment Report of the Intergovernmental Panel on Climate Change* [Stocker, T.F., Qin, D., Plattner, G.-K., Tignor, M., Allen, S.K., Boschung, J., Nauels, A., Xia, Y., Bex, V., Midgley, P.M. (eds.)]. Cambridge University Press, Cambridge, United Kingdom and New York, NY, USA.

Denmead, O.T. 2008. Approaches to measuring fluxes of methane and nitrous oxide between landscapes and the atmosphere. Plant Soil 309: 5-24.

Desjardins, R.L., Worth, D.E., Vergé, X.P.C., Maxime, D., Dyer, J., Cerkowniak, D. 2012. Carbon footprint of beef cattle. Sustainability. 4: 3279-3301.

Dijkstra, J., Oenema, O., Bannink, A. 2011. Dietary strategies to reducing N excretion from cattle: implications for methane emissions. Curr. Opin. Environ. Sustain. 3: 414-422.

Dunn, A.L., Barford, C.C., Wofsy, S.C., Goulden, M.L., Daube, B.C. 2007. A long-term record of carbon exchange in a boreal black spruce forest: means, responses to interannual variability, and decadal trends. Global Change Biol. 13: 577-590.

Ehhalt, D.H, Schmidt, U. 1978. Sources and sinks of atmospheric methane. Pure Appl. Geophys. 116: 452-464.

Flanagan, L.B., Wever, L.A., Carlson, P.J. 2002. Seasonal and interannual variation in carbon dioxide exchange and carbon balance in a northern temperate grassland. Global Change Biol. 8: 599-615.

Foken, T. 2008. The energy balance closure problem: An overview. Ecol. App. 18: 1351-1367.

Glenn, A.J., Flanagan, L.B., Syed, K.H., Carlson, P.J. 2006. Comparison of net ecosystem CO_2 exchange in two peatlands in western Canada with contrasting dominant vegetation, *Sphagnum* and *Carex*. Agric. For. Meteorol. 140: 115-135.

Griebel, A., Bennett, L.T., Metzen, D., Cleverly, J., Burba, G., Arndt, S.K. 2016. Effects of inhomogeneities within the flux footprint on the interpretation of seasonal, annual, and interannual ecosystem carbon exchange. Agric. For. Meteorol. 221: 50-60.

Hanis, K.L., Amiro, B.D., Tenuta, M., Papakyriakou, T., Swystun, K.A. 2015. Carbon exchange over four growing seasons for a subarctic sedge fen in northern Manitoba, Canada. Arctic Sci. 1: 27-44.

Harper, L.A., Denmead, O.T., Freney, J.R., Byers, F.M. 1999. Direct measurements of methane emissions from grazing and feedlot cattle. J. Anim. Sci. 77: 1392-1401.

Harper, L.A., Denmead, O.T., Flesch, T.K. 2011. Micrometeorological techniques for measurement of enteric greenhouse gas emissions. Anim. Feed Sci. Technol. 166-167: 227-239.

Hurlbert, S.H. 1984. Pseudoreplication and the design of ecological field experiments. Ecolog. Monogr. 54: 187-211.

Hutchinson, G.L., Livingston, G.P. 2001. Vents and seals in non-steady-state chambers used for measuring gas exchange between soil and the atmosphere. Eur. J. Soil Sci. 52: 675-682.

Hutchinson, G.L., Mosier, A.R. 1981. Improved soil cover method for field measurement of nitrous oxide fluxes. Soil Sci. Soc. Am. J. 45: 311-316.

Hynšt, J., Miloslav, Š., Brůček, P., Petersen, S.O. 2007. High fluxes but different patterns of nitrous oxide and carbon dioxide emissions from soil in a cattle overwintering area. Agric. Ecosyst. Environ. 120: 269-279.

Johnson, J.M.-F., Franzluebbers, A.J., Weyers, S.L., Reicosky, D.C. 2007. Agricultural opportunities to mitigate greenhouse gas emissions. Environ. Pollut. 150: 107-124.

Kebreab, E., Clark, K., Wagner-Riddle, C., France, J. 2006. Methane and nitrous oxide emissions from Canadian animal agriculture: A review. Can. J. Anim. Sci. 86: 135-158.

Knowles, R. 1982. Denitrification. Microbiol. Rev. 46: 43-70.

Lafleur, P.M., Roulet, N.T., Bubier, J.L., Frolking, S., Moore, T.R. 2003. Interannual variability in the peatland-atmosphere carbon dioxide exchange at an ombrotrophic bog. Global Biogeochem. Cycles 17: 1:14.

Laubach, J., Kelliher, F.M. 2005. Methane emissions from dairy cows: Comparing open-path laser measurements to profile-based techniques. Agric. For. Meteorol. 135: 340-345.

Lemaire, G., Franzluebbers, A., Carvalho, P.C.F., Dedieu, B. 2014. Integrated crop-livestock systems: Strategies to achieve synergy between agricultural production and environmental quality. Agric. Ecosys. Environ. 190:4-8.

Matthias, A.D., Blackmer, A.M., Bremner, J.M. 1980. A simple chamber technique for field measurement of emission of nitrous oxide from soil. J. Environ. Qual. 9: 251-256.

Mauder, M., Cuntz, M., Drüe, C., Graf, A., Rebmann, C., Schmid, H.P., Schmidt, M., Steinbrecher, R. 2013. A strategy for quality and uncertainty assessment of long-term eddy-covariance measurements. Agric. For. Meteorol. 169: 122-135.

McGinn, S.M. 2006. Measuring greenhouse gas emissions from point sources in agriculture. Can. J. Soil Sci. 86: 355-371.

Molodovskaya, M., Warland, J., Richards, B.K., Öber, G., Steenhuis, T.S. 2011. Nitrous oxide from heterogeneous agricultural landscapes: source contribution analysis by eddy covariance and chambers. Soil Sci. Soc. Am. J. 75: 1829-1838.

Montzka, S.A., Dlugokencky, E.J., Butler, J.H. 2011. Non-CO_2 greenhouse gases and climate change. Nature 476: 43-59.

Mudge, P.L., Wallace, D.F., Rutledge, S., Campbell, D.I., Schipper, L.A., Hosking, C.L. 2011. Carbon balance of an intensively grazed temperate pasture in two climatically contrasting years. Agric. Ecosyst. Environ. 144: 271-280.

Muñoz, C., Saggar, S., Berben, P., Giltrap, D., Jha, N. 2011. Influence of waiting time after insertion of base chambers into soil on produced greenhouse gas fluxes. Chil. J. Agr. Res. 71(4): 610-614.

Oenema, O., Velthof, G.L., Yamulki, S., Jarvis, S.C. 1997. Nitrous oxide emissions from grazed grassland. Soil Use Manage. 13: 288-295.

Oksanen, L. 2001. Logic of experiments in ecology: is pseudoreplication a pseudoissue? Oikos 94: 27-38.

Rochette, P., Eriksen-Hamel, N.S. 2008. Chamber measurements of soil nitrous oxide flux: are absolute values reliable? Soil Sci. Soc. Amer. J. 72: 331-342.

Salomon, E., Rodhe, L. 2011. Losses of N_2O, CH_4 and NH_3 from a grass sward used for overwintering beef heifers. Anim. Feed Sci. Technol. 166-167: 147-154.

Soussana, J.F., Allard, V., Pilegaard, K., Ambus, P., Amman, C., Campbell, C., Ceschia, E., Clifton-Brown, J., Czobel, S., Domingues, R., Flechard, C., Fuhrer, F., Hensen, A.,

Horvath, L., Jones, M., Kasper, G., Martin, C., Nagy, Z., Neftel, A., Raschi, A., Bartoni, S., Rees, R.M., Skiba, U., Stefani, P., Manca, G., Sutton, M., Tuba, Z., Valentini, R. 2007. Full accounting of greenhouse gases (CO_2, N_2O, CH_4) budget of nine European grassland sites. Agric. Ecosyst. Environ. 121: 121-134.

Strachan, I.B., Nugent, K.A., Crombie, S., Bonneville, M.-C. 2015. Carbon dioxide and methane exchange at a cool-temperate freshwater marsh. Environ. Res. Lett. 10: 065006.

Tans, P., NOAA/ESRL (www.esrl.noaa.gov/gmd/ccgg/trends/) Keeling, R. 2017. Scripps Institution of Oceanography (scrippsco2.ucsd.edu/). 'Trends in Atmospheric Carbon Dioxide'. Accessed: April 28, 2017

Taylor, A.M., Amiro, B.D., Fraser, T.J. 2013. Net CO_2 exchange and carbon budgets of a three-year crop rotation following conversion of perennial lands to annual cropping in Manitoba, Canada. Agric. For. Meteorol. 182-83: 67-75.

Vergé, X.P.C, Dyer, J.A., Desjardins, R.L., Worth, D. 2008. Greenhouse gas emissions from the Canadian beef industry. Agric. Syst. 98: 126-134.

Wagner-Riddle, C., Thurtell, G.W. 1998. Nitrous oxide emissions from agricultural fields during winter and spring thaw as affected by management practices. Nutr. Cycl. Agroecosyst. 52: 151-163.

2. EVALUATING THE SPATIAL VARIABILITY OF EDDY COVARIANCE CARBON DIOXIDE FLUXES OVER TWO AGRICULTURAL FIELDS

2.1 Abstract

Eddy covariance is used to measure carbon dioxide (CO_2) fluxes over agroecosystems and can help quantify carbon dynamics for management, budgeting, and modelling. One flux tower is often used to represent an entire field. A continuous crop can seem homogeneous, but we need to assess whether a flux tower's footprint is able to capture the representative spatial variability of a field's net ecosystem exchange (NEE). We used three towers on a perennial forage (Forage) and a spring wheat (Wheat) field in 2014 to investigate this. One tower remained stationary (Centre), while the other two (North and South) were moved to distances of 50 m and then 100 m away from it. Regression r^2 values amongst fields ranged from 0.67 to 0.92 and were lower when towers were further apart at Forage, but not Wheat. Root-mean-square error (RMSE) among towers at Forage was ~4 μmol m^{-2} s^{-1} with a mean NEE of -15 μmol m^{-2} s^{-1}. Spring wheat measurements were later in the season and had smaller NEE (mean -7.5 μmol m^{-2} s^{-1}) with an RMSE of 2 μmol m^{-2} s^{-1}. Mean NEE significant differences at Wheat were primarily driven by the senescing crop at all separations. Leaf area index (LAI) measurements were done in a 50 m georeferenced grid of each field, and semivariograms of each field's LAI had a range of 200 m at Forage and 80 m at Wheat. There were no significant differences amongst the mean LAI of each flux footprint at any tower at any separation. LAI field means of Wheat and Forage were similar to footprint LAI. Instrument uncertainty was also examined. Tower sonic anemometer friction

velocity regressions were similar amongst tower locations, while the infrared gas analyser CO_2 standard deviation changed as towers moved apart. This suggests that NEE differences were driven by spatial CO_2 concentration differences across the field. For NEE fluxes at Forage, the RMSE among towers was ~30% no matter the location, suggesting that sampling with a single tower would have been sufficient. Crop senescence at Wheat caused very small fluxes that made it difficult to evaluate the impact of spatial variation.

2.2 Introduction

There can be huge variability among fields when measuring agricultural fluxes with eddy covariance, based on local climate, soil type, and management practice (Moors et al. 2010). Current measurement techniques still need to improve our ability to characterise and account for on-site variability when measuring carbon fluxes (Loescher et al. 2006). Spatial variation within a site can potentially cause variations in carbon flux measurements of 10 – 20% (Baldocchi et al. 1988).

Eddy covariance CO_2 flux systems have systematic and random errors that contribute to their uncertainty. Systematic errors may come from instrument calibration issues, calculation errors, or experimental design. Random measurement errors can have several sources, including turbulent transport, stochastic turbulence, statistical errors resulting from the measurement site, and assuming the flux footprint is constant or that it is homogeneous (Moncrieff et al. 1996; Hollinger and Richardson 2005; Mauder et al. 2013; Post et al. 2015).

To minimize systematic errors, experiments should be conducted over flat terrain, in steady environmental conditions, and with a homogeneous surface upwind of the tower, while using fast-responding anemometers and CO_2 analysers to prevent errors from slow response (Baldocchi 2003). Complex terrain can increase uncertainty when measuring CO_2 flux due to advection and horizontal flux divergence (Sun et al. 2007). Towers with low heights may be affected more greatly by small eddy transfer and increase peak transfer frequency (Davis et al. 2010).

Flux footprint source areas are larger at night when the atmosphere is stable than during the day when it is more turbulent and unstable. Source footprints also vary season-to-season as vegetation and groundcover change, depending on how they influence atmospheric turbulence (Chen et al. 2009). Footprint variation affects the uncertainty of long-term flux datasets by 5 – 60% depending on a site's heterogeneity (Chen et al. 2009). Even if a site looks uniform, variable soil, plant, or nutrient characteristics must be considered when estimating the random error of NEE, because flux footprints will sample different locations based on tower placement (Post et al. 2015). Multiple independent observations made in one place can evaluate sampling error (Finkelstein and Sims 2001), but spatial sampling is necessary to ground truth and identify drivers of variability.

Using an extended two tower approach, random errors were found to vary more when eddy covariance towers were on different landscapes, and were greater during stable atmospheric conditions (40 – 50%) than unstable (15 – 20%) (Kessomkiat et al. 2013). The variability of surface roughness and thermal stability upwind of a measurement tower affects local advection and how the fluxes generated from them move in the atmosphere (Leclerc and Thurtell 1990). When multiple towers of differing height

were compared over heterogeneous terrain in Colorado, CO_2 flux variability was less during the day than at night (Sun et al. 2007); however, variability was greater during the day when two towers in identical conditions were compared in Maine (Hollinger and Richardson 2005). Furthermore, random uncertainties are not constant and are generally greater during the growing season (Hollinger and Richardson 2005).

Research has been conducted to evaluate uncertainty of carbon fluxes using the eddy covariance method. A comparison in 1989 found CO_2 fluxes from four instruments agreed within 10%, that instrument calibration errors may change the regression slope when comparing instruments, and that signal noise may also explain variability in flux measurements (Moncrieff et al. 1992). Two open-path and two closed-path eddy covariance systems duplicated at four sites found plant stage greatly impacted surface fluxes even if crops were the same (Moncrieff et al. 1997a).

Unique systems over three inhomogeneous vegetation sites confirmed that surface cover and soil variability may produce differences in short-term flux measurements because of differences in footprints (Lloyd et al. 1997), contributing to the difficulty of comparing processes and management practises, or using such data for modelling. Furthermore, the amount of variability in surface cover and soil moisture didn't allow instrument error to be separated from the contributing factors of surface variability. Finkelstein and Sims (2001) found that normalized errors over a variety of forests and low canopy agricultural crops were 25 – 30% for trace gases. Hollinger and Richardson (2005) characterized the random error in flux measurements using a two-tower system in Maine, USA, and were able to show that uncertainty in measurements could be characterized by binning the data according to daytime and meteorological conditions to

allow for analysis on single-tower systems. This approach had towers with nearly identical meteorological conditions, but with flux footprints that didn't overlap. It assumed that the paired systems were identical, having ongoing calibration verification, but footprint differences created uncertainty in the comparison (Billesbach 2011). Kessomkiat et al. (2013) expanded on the two-tower approach studying sensible and latent heat with data from sites in Italy, Germany, and the USA, and acknowledged that even if there is similar vegetation on comparison sites, local factors like soil type and precipitation could result in systematic differences.

With only one tower used in many instances, the potential for variation and uncertainty from systemic, random, and time-integrated errors from various sources can affect data interpretation. Any site-to-site comparisons may be suspect to greater amounts of uncertainty without research to determine if eddy covariance systems accurately represent the fields and sites they are measuring,

Agroecosystems can be ideal for eddy covariance systems to measure CO_2 fluxes because they generally have a uniform plant cover that helps meet eddy covariance assumptions. We examined whether multiple eddy covariance towers increased our ability to capture the NEE spatial variability of an agricultural field, and if not, investigate whether variability among towers was driven by differences in LAI within flux tower footprint areas.

2.3 Methods

2.3.1 Experimental design

Two different fields were identified to evaluate the capability of eddy covariance to capture spatial variability over agricultural fields in Southern Manitoba. A perennial forage and an annual spring wheat field were chosen, since perennials are able to uptake carbon earlier in the year while annuals are still maturing. Measurements were conducted May through September when carbon fluxes and temperatures are highest. The perennial field (Forage) (49°54'36.72" N 96°49'41.28 W, 243 m.a.s.l.) was a private producer's 60 ha field split between seed alfalfa (*Medicago sativa*) and seed trefoil (*Lotus corniculatus*), and measurements were conducted from June 13 through July 22, 2014. The annual field (Wheat) was at the Glenlea Research Farm (49°38'48.48" N 97°09'21.09" W 235 m.a.s.l.) on 50 ha of hard red spring wheat (*Triticum aestivum. L.* 'Carberry'), and measurements were from July 23 through September 5, 2014.

Three eddy covariance towers were co-located side-by-side on each field, approximately 1 – 2 m apart. Two towers (North and South) were calibrated against one central tower (Centre) that remained stationary throughout the study. Towers were moved from co-location, to 50 m separation, to 100 m separation from the Centre tower (Figure 2.1) with one to three weeks at each, depending on instrument performance and weather. Towers were moved along a north-south line to minimize trampling and provide field access at on both fields, moving along the crop divide at Forage (Figure 2.1). The north-south arrangement also aimed to minimize turbulence interference amongst towers, given that winds are predominantly from the northwest and west at Glenlea June through September (Environment Canada 2016).

The towers ran daily from 6 a.m. to 10 p.m. to measure the greatest flux dynamics during highest atmospheric turbulence, while also taking advantage of smaller flux footprints to ensure measurements originated within the cropping fields. The battery banks from each tower were exchanged each morning. Each day of data provided up to 32 half-hourly averaged data points from each analyzer.

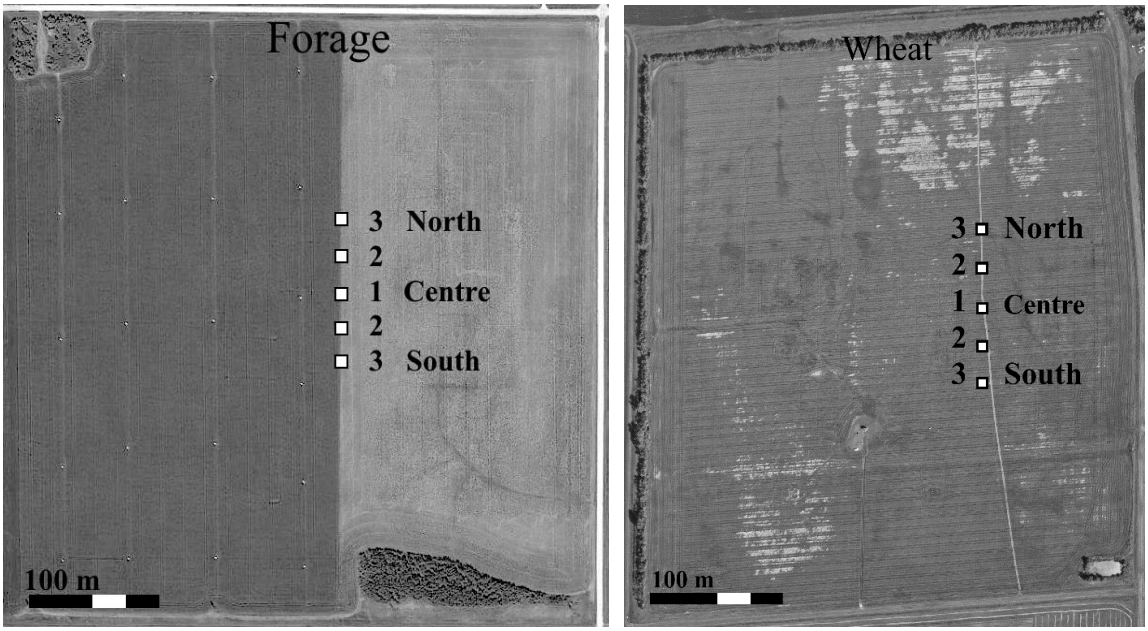

Figure 2.1 Forage and Wheat fields and the location of the towers on each; (1) towers were co-located with the Calibration tower; (2) 50 m distance (3) 100 m distance from it. Forage had two crops, seed alfalfa on the west and trefoil on the east side of the field. Forage image from July 1, 2013 (Google, DigitalGlobe 2015), Wheat aerial photograph taken August 28, 2014.

2.3.2 Site characterization

Both sites were fine textured, Lacustrine Fine Clays of the Red River Association, well to intermediately drained Red River Clay and poorly drained Osborne Clay (Ehrlich et al. 1956). Soil characterization on the Forage field was measured on July 17, 2014, with samples taken every 75 m north-south along eight east-west transects each ~175 m

apart, for 64 total. Samples from each transect were bulked into one bag, resulting in 8 bulked samples from each depth of 0 – 15 cm and 15 – 30 cm. Characterization was previously conducted at the Wheat field in 2008 in conjunction with ongoing research there (Glenn et al. 2010; Glenn et al. 2011).

On the Forage field 0 – 15 cm and 15 – 30 cm depths respectively, total organic carbon was 40 and 30 g kg^{-1}dry soil, pH_{water} was 7.8 and 8.0, and NO_3-N was 11.4 and 8.2 mg kg^{-1}. Electric conductivity was 0.6 mS cm^{-1} and SO_4-S was 0.67 mg kg^{-1} at both depths, while P and K were 8.9 and >255 mg kg^{-1}, respectively, at the 0 – 15 cm depth.

Total organic carbon of the Wheat field was 38, 30 and 19 g kg^{-1} dry soil at 0 – 10 cm, 10 – 20 cm, and 20 – 40 cm. The Wheat field had a bulk density in the topsoil (0 – 20 cm) of 1.2 Mg m^{-3}, a pH_{water} of 6.2, and was 60% clay, 35% silt, and 5% sand (Glenn et al. 2010). The Wheat field NH_4-N and NO_3-N were 2.0 and 11.1 mg kg^{-1} at the 0 – 30 cm depth on July 11, 2014.

Georeferenced LAI measurements (LAI-2000 Plant Canopy Analyzer, LI-COR Biosciences, Lincoln, NE, USA) were taken in a 50 m grid of each field, using the 90° viewing cap facing directly away from the rod. The locations of each measurement were recorded with a handheld GPS (GPSmap 60, Garmin Ltd., Olathe, KS, USA), with Forage n= 237 and Wheat n = 212. Samples were taken through morning and midday with an umbrella used to shield the sensor and canopy if it was not overcast. Sampling was done between July 2 – 14, 2014 at Forage and August 12 – 17, 2014 at Wheat. Each sample point consisted of one reading above the canopy and four below it within ~1 m of where the researcher stood, across the row (ABBBB sampling pattern, where A is above canopy and B is below). Below-canopy readings were taken as close to the soil surface as

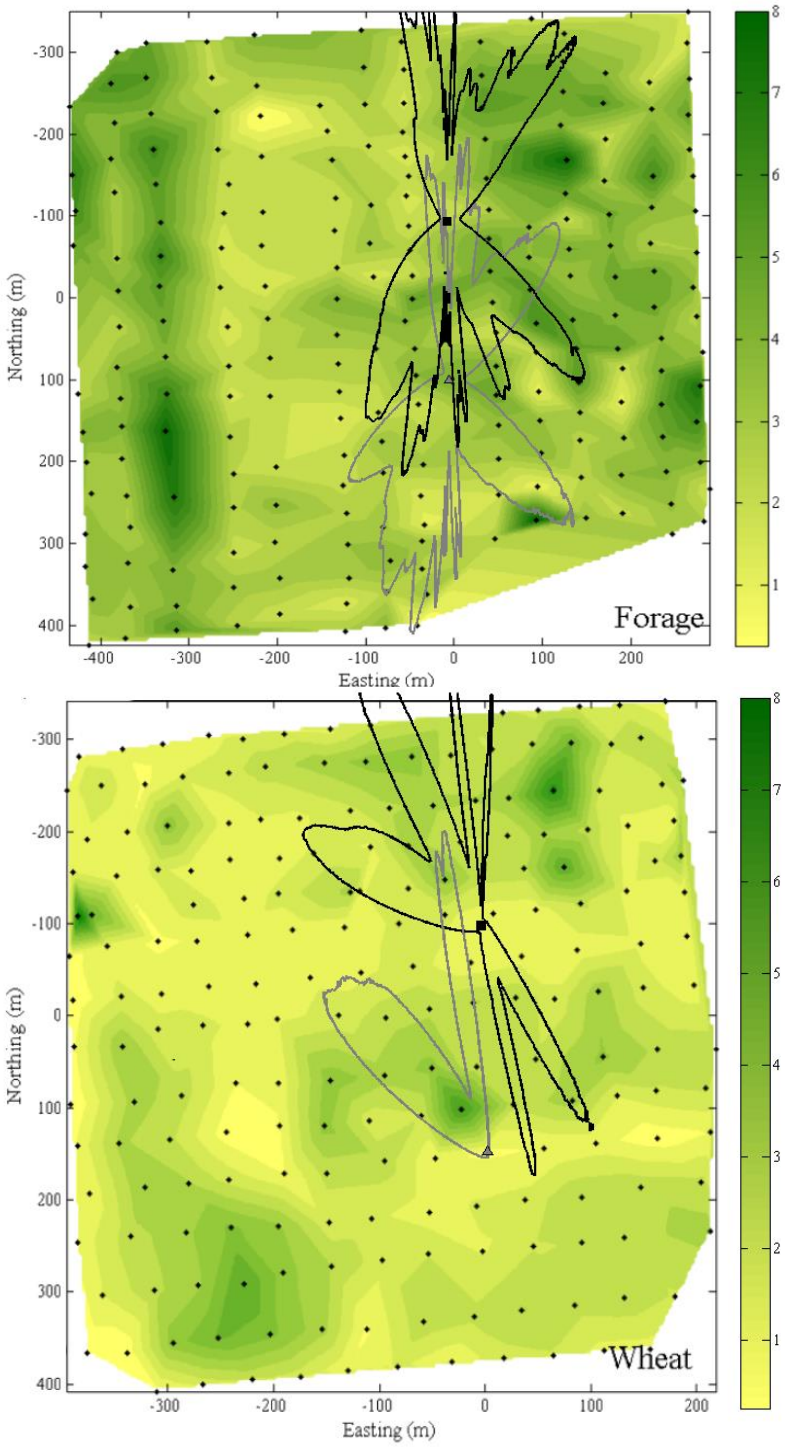

Figure 2.2 LAI contours (colour bar) at the 100 m separation with tower 95% contour footprints for North (black) & South (grey) towers. Dots are LAI sample point locations.

possible while remaining level and dry and were measured across row in a diagonal pattern, with each reading approximately 1 m apart. Standing water and active leafcutter beehives on the Forage field resulted in some samples deviating from the 50 m grid referred to above. LAI data points and their corresponding GPS coordinates were combined to create a spatial map of LAI coverage at each field (Figure 2.2).

A semivariogram (Schwanghart 2009) of each field's LAI was generated in MATLAB (Mathworks Inc.) to characterize field variability (Figure 2.3). Forage had a range = 200 m, a sill = 2.05, and a nugget = 0.21, whereas Wheat had a range = 80 m, a sill = 0.87, and a nugget = 0.42. Forage's higher sill corresponds to higher variance in the LAI values, and its larger range means that autocorrelation occurs at a further distance than at Wheat.

2.3.3 Meteorological flux measurements

Each micrometeorological tower was a 2.5 m tall tripod tower with a west-facing anemometer-thermometer (CSAT3, Campbell Scientific Inc., Logan, UT, USA) and a factory calibrated closed-path CO_2/H_2O gas analyzer (IRGA LI-7000 CO_2/H_2O Analyzer, LI-COR Biosciences) in a temperature controlled protective housing (University of British Columbia, Biometeorology Group). Air samples were drawn through an intake, down 4 m of Bev-A-Line IV 3.18mm I.D. tubing (Cole-Parmer, Vernon Hills, IL, USA), and through a volume buffer via a diaphragm pump (KNF UN828 KNDC 12V, KNF Neuberger Inc., Trenton, NJ, USA) at a rate of 9-11 L min^{-1}. There was an in-line particle filter at the analyzer. Data were recorded at 10 Hz by a data logger (CR1000, Campbell Scientific Inc.), with raw data and cross-products saved to storage (NL 115 card reader,

Campbell Scientific Inc.) and collected each morning. The three towers were configured on a north/south line as shown (Figure 2.1). The North tower Li7000 experienced technical problems from June 18 to July 23, 2014, and a replacement Li7000 was used from June 30 to July 23, 2014. However, at each field a consistent instrument package was used.

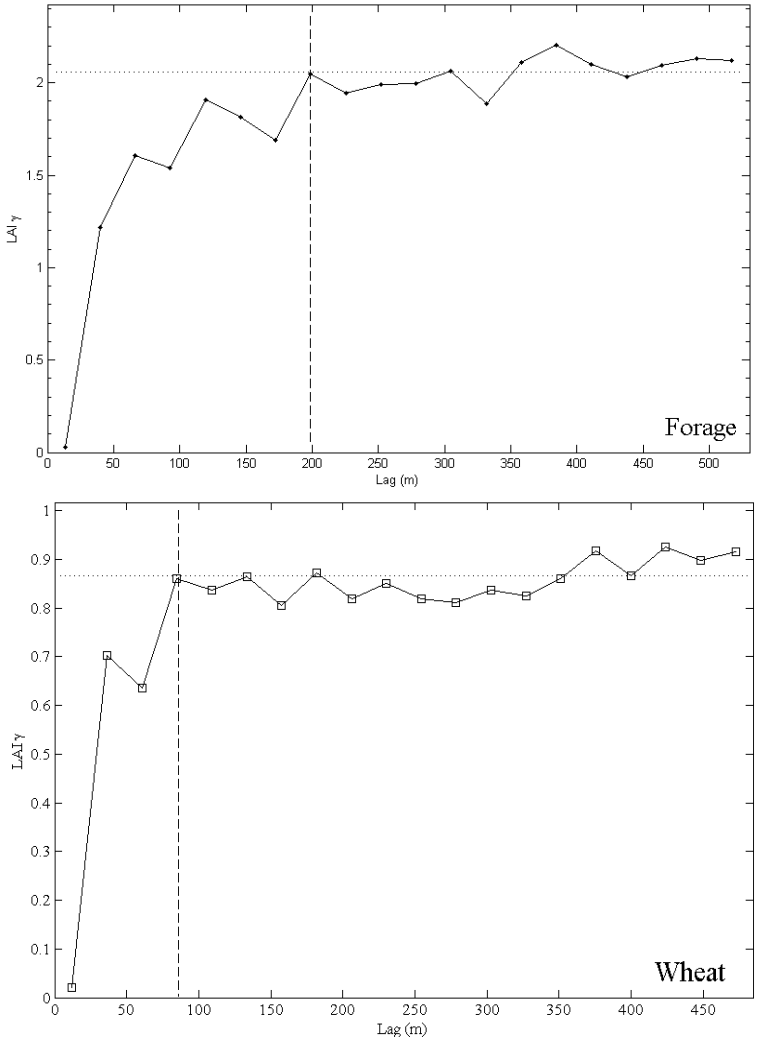

Figure 2.3 LAI semivariograms showing the sill (horizontal line) and the range (vertical line). Data fit a normal distribution within a histogram. Forage (alfalfa and trefoil included) had a 200 m range, 2.05 sill, and 0.21 nugget, whereas Wheat had an 80 m range, 0.87 sill, and 0.42 nugget. Nugget is the y-intercept.

The towers were each powered by a bank of three batteries (12V Deep Cycle Gel battery, Trojan Battery Company, Santa Fe Springs, CA, USA) that were exchanged each morning on measurement days and charged off site. The IRGAs were factory calibrated prior to the experiment and checked in lab to confirm both CO_2 and H_2O had a 1:1 slope when compared to a zero-CO_2 and a span CO_2 (398 μmol mol^{-1}) calibration gas and a dew point generator (LI-610 Portable Dew Point Generator, LI-COR Biosciences) at three dewpoint temperatures (10, 15, 20°C). The same calibration gases were used in field to determine a calibration slope for each IRGA, while a dew point generator provided calibration slope values for H_2O using three dew point temperatures that varied by day depending on actual air temperature. These calibration values were recorded once every week or two depending on weather and accessibility and the corrections were applied to each IRGA prior to flux calculation.

MATLAB (Mathworks Inc.) was used to process the data. High frequency data were split into 30-minute files, despiked, and had delays adjusted for flux maximization. Half-hourly cross-products were generated and coordinate rotations applied to the wind vectors (Tanner and Thurtell 1969). Carbon flux was calculated as net ecosystem exchange (NEE),

$$NEE = \overline{w'CO_2'} \qquad [2.1]$$

where w = vertical wind velocity and CO_2 = concentration of carbon dioxide. Overbars denote time-averaged values and primes are deviations from the mean.

Spectral corrections were computed for NEE on a half-hourly basis using spectral transfer functions (Moore 1986; Moncrieff et al. 1997b; Massman 2000), which typically increased fluxes by 40-50%. Site visits, battery changes, calibration times, set up periods,

equipment moves, and rainy periods were excluded. Data were also excluded when CSAT3 missing data count > 5%, vertical mean velocity was > 0.5 or < -0.5 m s^{-1}, when winds came from behind the tower (45° < wind direction < 135° where north is zero), when CO_2 concentration was < 290 μmol mol^{-1} or > 600 μmol mol^{-1}, and when CO_2 - variance > 50 μmol mol^{-1} (based on a histogram of variance values). One clock correction was applied to correct disparity among the three towers. No friction velocity (u*) threshold was applied and no gap-filling was done.

A regression analysis of each North or South tower versus the Centre tower when all were co-located was done for NEE. Measurement values were then multiplied by the regression slope and had the offset applied to minimize systematic differences among instrument packages and focus on other sources of variability. Each tower pair was then compared in a regression analysis. Measurement data populations from each tower were tested for normality with Shapiro-Wilks (Ben Saïda 2009). The majority were non-normal and were not improved by simple transformations, so a rank sum was used for paired towers. Comparisons among three towers had disparate sample sizes, so a Kruskal-Wallis ANOVA was used. Statistical analysis was done in MATLAB (Mathworks Inc., Natick, MA, USA). A similar method was used when investigating instrument contributions, using the standard deviation of the CO_2 concentration (σCO_2) and u*.

The footprint model developed by Chen et al. (2009), based on the analytical model of Kormann and Meixner (2001), was used to generate 30-min footprints using data from each tower. Model inputs were air temperature and pressure, relative humidity, NEE, sensible and latent heat flux, wind speed and direction, friction velocity, and the standard deviation of the transverse wind speed. All values were measured or calculated

through our experiment, except for air pressure, which was set to 98 kPa. The model domain was 500x500m, pixel size = 1, canopy height = 0.5 m, and roughness height = 0.05 m.

GPS coordinates and LAI field measurements were combined with the footprint analysis in MATLAB (Figure 2.2). The mean values of all LAI points from within each tower campaign's 95^{th} percentile footprint were assumed to be representative of each flux footprint (co-located, 50 m, or 100 m separation). A rank sum test was used to compare each footprint's mean LAI to the Centre tower, and a Kruskal-Wallis ANOVA was used when three towers were compared.

2.4 Results

2.4.1 Tower regression comparisons

After calibration (Section 2.3.1), a regression analysis compared the North and South towers to the stationary Centre tower during each campaign: co-located, 50 m, and 100 m from Centre. When systems were co-located (Figure 2.4) towers compared well and had relatively high r^2 values (0.89 – 0.92) and slope = 1 (Table 2.1) at Forage and Wheat North-Centre. Wheat South-Centre had the lowest $r^2 = 0.69$ of any tower location.

When moved 50 m apart, the tower regression (Figure 2.5) at Forage and Wheat North-Centre maintained a high r^2 (0.89 – 0.91) (Table 2.1), and Wheat South-Centre $r^2 = 0.79$. Slopes at the 50 m separation deviated most from the 1:1 line at Wheat North-Centre. There was no 50 m North-Centre comparison at Forage due to instrumentation problems. The Forage comparison had a wider range of values (-40 to 10 μmol m^{-2} s^{-1}),

while North and South towers at Wheat formed two distinct clusters of points along their respective regression lines.

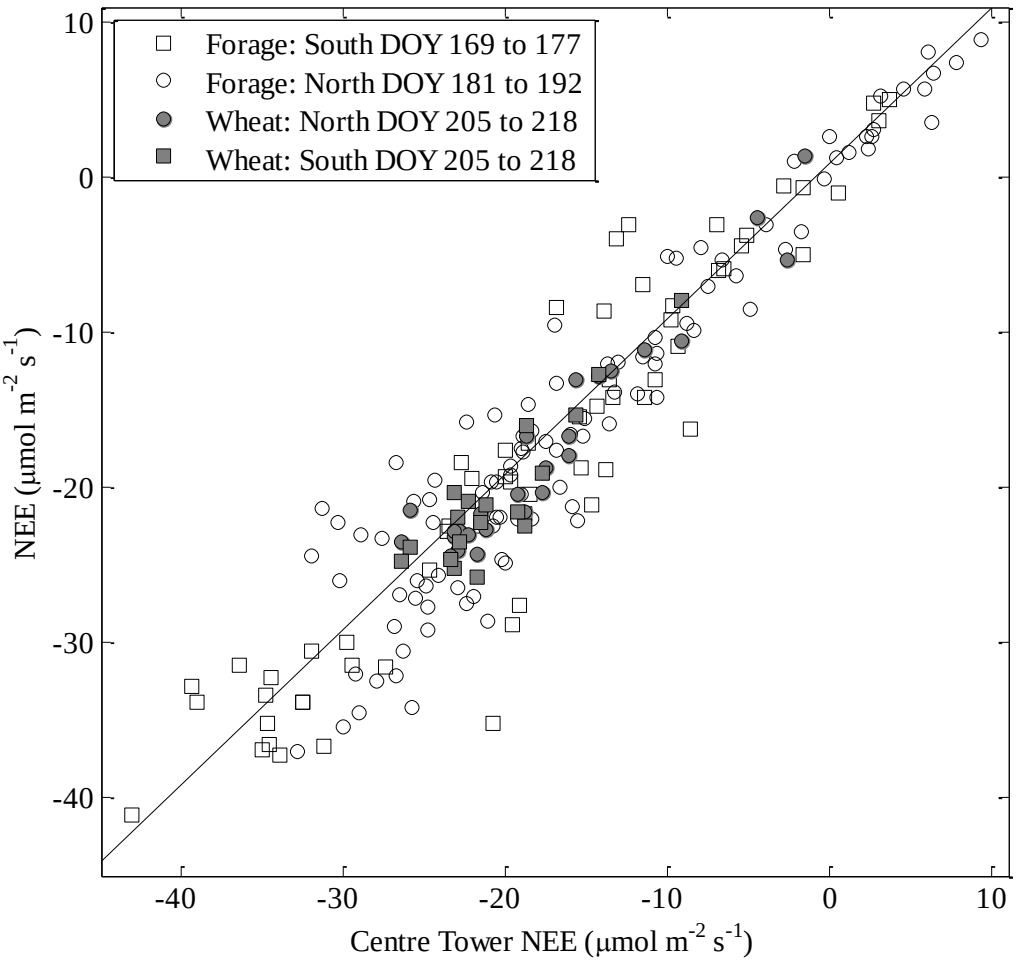

Figure 2.4 Regression analyses during calibration period when the towers were co-located. 1:1 reference line shown.

Forage had more scatter and a lower r^2 at the South tower once the towers were 100 m apart (Figure 2.6) (0.81), but unchanged at the North tower (0.89). The r^2 was lower at Wheat North-Centre (0.75), while Wheat South-Centre was unchanged compared to 50 m (0.79) (Table 2.1). Slopes generally departed further from 1 the further towers got away (Table 2.1).

Table 2.1 NEE regression coefficients and means for each field and tower separation.

Forage	DOY	y	y mean NEE (μmol m^{-2} s^{-1})	x	x mean NEE (μmol m^{-2} s^{-1})	r^2	Slope	Intercept (μmol m^{-2} s^{-1})	RMSE (μmol m^{-2} s^{-1})	n
Co-located	181 - 192	North	-15.28	Centre	-15.28	0.90	1	0	3.64	100
Co-located	169 - 177	South	-18.56	Centre	-18.56	0.89	1	0	4.26	62
50 m	177 - 192	South	-14.27	Centre	-14.27	0.90	1.05	0.68	3.98	83
100 m	192 - 204	North	-14.11	Centre	-14.84	0.89	0.99	0.61	3.70	113
100 m	192 - 204	South	-12.68	Centre	-12.67	0.81	0.68	-0.41	4.22	100
Wheat									3.96	
Co-located	205 - 218	North	-17.4	Centre	-17.4	0.92	1	0	2.01	26
Co-located	205 - 218	South	-20.49	Centre	-20.49	0.69	1	0	2.97	21
50 m	218 - 232	North	-3.22	Centre	-4.72	0.91	1.29	2.87	2.01	178
50 m	218 - 232	South	-3.82	Centre	-4.21	0.79	1.04	1.25	1.88	60
100 m	232 - 248	North	2.62	Centre	0.65	0.75	1.18	1.85	1.28	64
100 m	232 - 248	South	1.95	Centre	0.61	0.79	1.24	0.10	1.35	40

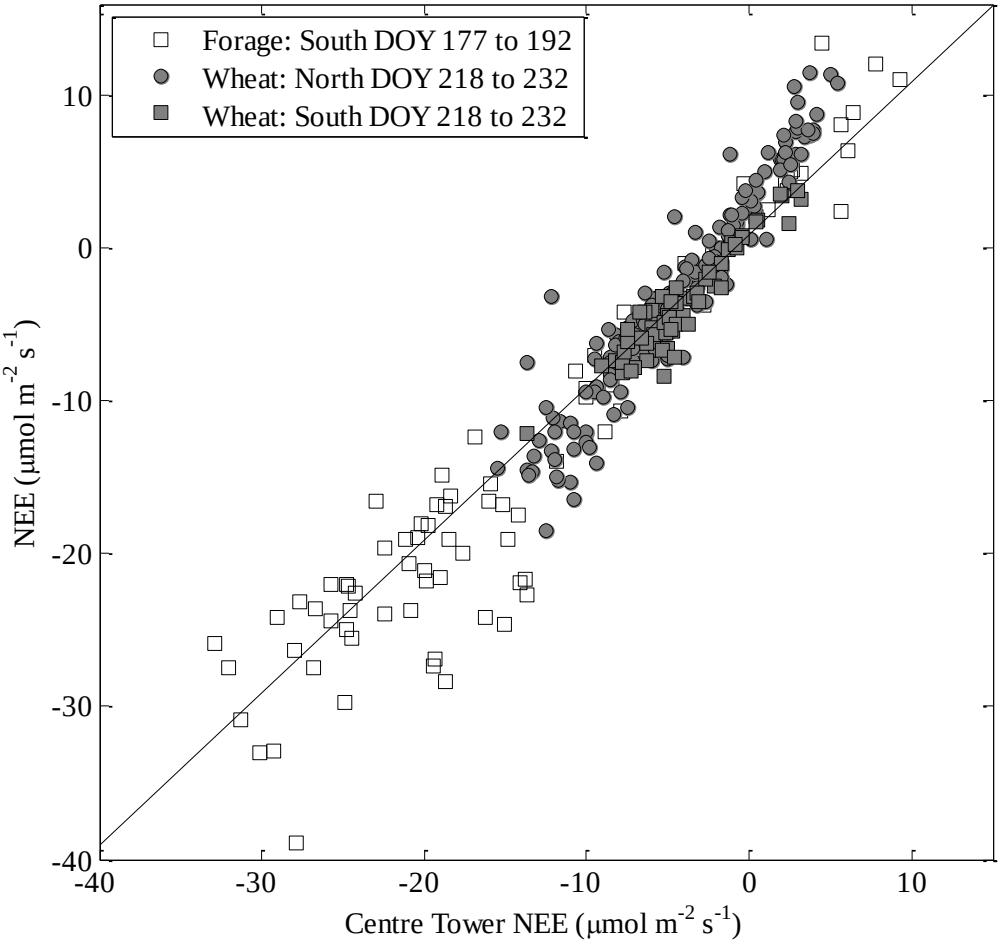

Figure 2.5 Regression analyses when the towers were separated by 50 m. North and South towers were originally calibrated to the Centre tower. 1:1 reference line shown.

Wheat North and South regression points were clustered together, while Forage values had greater magnitude and wider scatter as values grew more negative. Data collected at Wheat were later in the growing season (July through August), thus NEE values switched from uptake to emission during the course of measurement. Having a small dynamic range may contribute to a poor comparison.

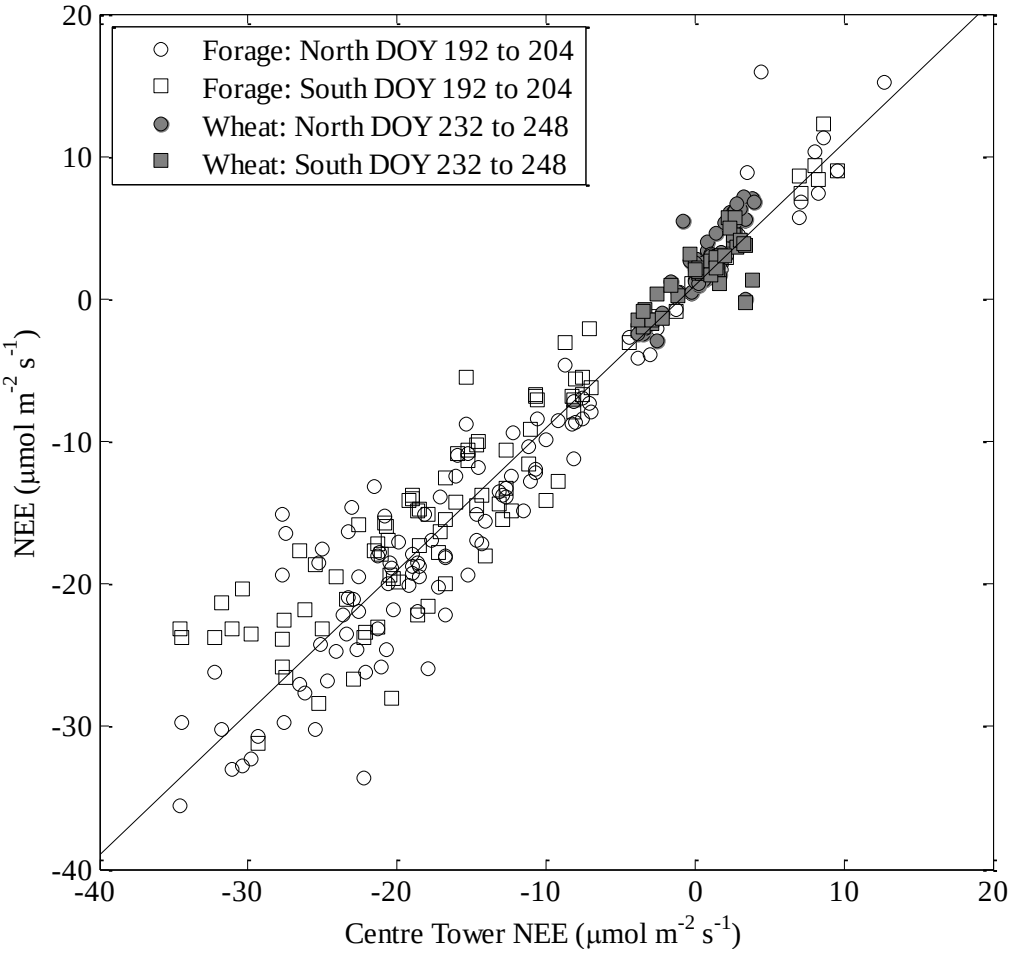

Figure 2.6 Regression analyses when the towers were separated by 100 m. North and South towers were originally calibrated to the Centre tower. 1:1 reference line shown.

Percent RMSE (RMSE / Centre NEE value, based on Table 2.1) ranged 23 – 33% at Forage and remained relatively consistent across separations. At Wheat, percent RMSE generally increased as towers were moved further apart, 12 – 14% at co-located, 43 – 45% at 50 m, and 197 – 221% at 100 m.

NEE populations from each tower were compared with a Kruskal-Wallis ANOVA and Tukey-Kramer post hoc or rank sum for 3- or 2-tower comparisons, respectively. At Forage, there were no significant differences. At Wheat, there were significant differences at all separations: North was significantly greater from Centre and South when co-located ($p < 0.001$), North was also significantly greater than Centre at the tower 50 m separation ($p < 0.05$). Centre was significantly less than North or South at the 100 m separation ($p < 0.001$). Whether these differences resulted from field vegetation variability or from instrument uncertainty were examined.

2.4.2 Quantifying field variability with LAI and flux footprints

Footprints were generated when each respective tower had data, and may include different time periods. At each separation and tower, Forage preferentially sampled from the northwest, northeast, southwest, and southeast, creating four distinct lobes in the footprint models. At Wheat, the co-located South tower preferentially sampled southeast, whereas the North tower had a more evenly distributed footprint. At 50 m footprints were similar, preferentially sampling northeast, northwest, and southwest, while at 100 m both heavily sampled from north and northwest, but the North tower sampled southeast as well. At both Forage and Wheat, each tower and separation footprint had more similarities when co-located than when 100 m away from Centre, primarily because of

tower position. We focused on when the North and South towers were 100 m away from Centre, where tower position resulted in different portions of the field being sampled (Figure 2.2). An LAI contour map with 95% flux footprints superimposed on each field (Figure 2.2) shows the variability present. Tower placement resulted in a wide range of LAI values within each tower's footprints at both Forage and Wheat.

The mean LAI of the subsampled points within each tower's footprint was calculated to compare the footprint source area variability (Table 2.2). Forage mean LAI ranged from 3.08 – 3.79 with a max value of 6.48 across all tower locations. LAI was consistently lower at Forage South (3.08 – 3.28) tower than North (3.41 – 3.79), which is apparent in the LAI contours (Figure 2.2). Wheat mean LAI had a lower mean tower LAI (1.72 – 2.50) with a max value of 5.23. Mean LAI (Table 2.2) and SEM were relatively

Table 2.2 Mean LAI for each tower's 95th percentile footprint during each campaign. Footprint specific LAI values are weighted according to the percent of the fluxes that the footprint itself represents (95%). No significant differences were found in a rank sum comparison of paired towers or a Kruskal-Wallis and a Tukey-Kramer post hoc amongst three towers. Forage co-located is separated due to temporally separate campaigns for North (N) and South (S). SEM is standard error of the mean.

		Forage						Wheat				
		mean	SEM	min	max	n*		mean	SEM	min	max	n*
Co-located	North	3.79	0.28	1.95	6.32	20	North	1.94	0.21	1.12	2.80	9
	N-Centre	3.41	0.20	1.61	5.34	27	Centre	1.72	0.16	1.10	2.80	13
	S-Centre	3.08	0.19	1.19	5.34	33						
	South	3.28	0.20	1.43	5.34	28	South	1.80	0.28	1.12	2.80	6
50 m	North	--	--	--	--	--	North	2.05	0.16	1.00	3.34	20
	Centre	3.45	0.26	1.61	6.48	25	Centre	1.97	0.14	1.00	3.16	23
	South	3.38	0.24	1.61	4.88	17	South	2.07	0.15	0.68	3.20	21
100 m	North	3.71	0.27	1.95	5.41	19	North	2.50	0.41	1.08	5.23	9
	Centre	3.55	0.24	1.61	5.34	23	Centre	2.23	0.33	1.16	3.20	7
	South	3.57	0.30	1.61	5.34	19	South	2.33	0.26	1.71	3.16	5
Whole field		3.50	0.09	0.21	8.39	219		1.94	0.06	0.42	6.77	205

* n = number of LAI sample points within the given footprint.

similar across towers at both fields. There were no significant differences among footprint LAI on any field or separation. Higher LAI values at Forage come from a denser canopy present at Forage than at Wheat.

The subsampled tower means of both fields were similar to whole field means, where Forage = 3.50 and Wheat = 1.94. There were no significant differences amongst tower subsample means or whole field means (Table 2.2). However, there was greater range of LAI over the entire field than within each sampling footprint. Other avenues of uncertainty were explored to determine where measured NEE variability originated.

2.4.3 Differentiating between measurement uncertainty and site variability

Absolute normalized values of NEE and LAI difference of each spatial separation were compared to try and separate measurement uncertainty from field sampling variability. These were calculated from tower means for each NEE and LAI, where the normalized value = (| (Tower LAI or NEE – Centre tower LAI or NEE) / Centre tower LAI or NEE|). There was broad scatter and no pattern in the regression comparison of normalized NEE to LAI difference ($r^2 = 0.09$). This suggests that LAI was not the main source of the NEE variability seen in the regression comparisons in Table 2.1.

Regression analyses of the CO_2 concentration standard deviation (σCO_2) and u* were performed (Table 2.3) to examine the instrument contributions of the IRGA and CSAT3 to flux uncertainty. σCO_2 was larger at Forage than at Wheat, as reflected in NEE (Table 2.1), while having smaller RMSE when co-located than at Wheat, which was undergoing senescence. When compared, σCO_2 r^2 values were relatively high and similar between separations, ranging from 0.77 – 0.99 when co-located, 0.89 – 0.94 at 50 m, and

0.87 – 0.94 at 100 m. Slopes were within the same range at all separations (0.87 – 1.3). Intercepts departed from zero as the towers moved further apart and was largest at the 100 m Wheat separation (Table 2.3). Comparatively, u* values were consistent across all fields and separations; RMSE were consistent too, and r^2 were consistently high and ranged from 0.83 – 0.96 when co-located, 0.92 – 0.98 at 50 m, and 0.94 – 0.98 at 100 m. Slopes and intercepts for u* regressions changed little, ranging from 0.97 – 1.05 and -0.03 – 0.05 m s^{-1} respectively.

Table 2.3 Regression coefficients and means for each field and tower separation for σCO_2 and u*. Note that initial calibrations were done when co-located.

Forage σCO_2	DOY	y	y mean σCO_2 (μmol mol^{-1})	x	x mean σCO_2 (μmol mol^{-1})	r^2	Slope	Intercept (μmol mol^{-1})	RMSE (μmol mol^{-1})	n
Co-located	181 - 192	North	3.06	Centre	3.06	0.99	1	0	0.13	174
Co-located	169 - 177	South	3.51	Centre	3.51	0.98	1	0	0.19	97
50 m	177 - 192	South	3.13	Centre	3.06	0.94	1	0.07	0.3	168
100 m	192 - 204	North	2.5	Centre	2.59	0.91	0.87	0.24	0.33	176
100 m	192 - 204	South	2.45	Centre	2.52	0.89	0.89	0.17	0.37	168
Wheat σCO_2										
Co-located	205 - 218	North	2.91	Centre	2.91	0.83	1	0	0.48	174
Co-located	205 - 218	South	2.93	Centre	2.93	0.77	1	0	0.57	164
50 m	218 - 232	North	1.15	Centre	1.42	0.89	1.08	-0.38	0.32	226
50 m	218 - 232	South	1.02	Centre	1.37	0.93	1.27	-0.73	0.26	150
100 m	232 - 248	North	0.33	Centre	0.86	0.93	1.1	-0.6	0.31	115
100 m	232 - 248	South	-0.06	Centre	0.67	0.94	1.27	-0.9	0.18	83
Forage u*	**DOY**	**y**	**y mean u* (m s^{-1})**	**x**	**x mean u* (m s^{-1})**	**r^2**	**Slope**	**Intercept (m s^{-1})**	**RMSE (m s^{-1})**	**n**
Co-located	181 - 192	North	0.34	Centre	0.34	0.89	1	0	0.06	166
Co-located	169 - 177	South	0.37	Centre	0.37	0.88	1	0	0.04	90
50 m	177 - 192	South	0.4	Centre	0.38	0.98	0.97	0.03	0.02	127
100 m	192 - 204	North	0.39	Centre	0.37	0.94	1.05	0.001	0.05	166
100 m	192 - 204	South	0.42	Centre	0.39	0.96	1.03	0.02	0.04	145
Wheat u*										
Co-located	205 - 218	North	0.21	Centre	0.21	0.83	1	0	0.06	66
Co-located	205 - 218	South	0.21	Centre	0.21	0.96	1	0	0.03	48
50 m	218 - 232	North	0.29	Centre	0.31	0.95	0.99	-0.02	0.03	239
50 m	218 - 232	South	0.29	Centre	0.31	0.92	1.03	-0.03	0.04	143
100 m	232 - 248	North	0.39	Centre	0.42	0.95	1	-0.03	0.04	88
100 m	232 - 248	South	0.48	Centre	0.48	0.98	1.02	-0.01	0.03	48

Kruskal-Wallis ANOVA and rank sum were used to compared the tower u* and the σCO_2 at the 50 m and 100 m separations to identify if the IRGA or CSAT3 were

responsible the NEE differences in Section 2.4.1. There were no significant differences among u* values at any separation on either field. The only significant differences were for σCO_2 values at the Wheat 50 m and 100 m separations ($p < 0.001$), much like was found when comparing mean tower NEE in Section 2.4.1.

2.5 Discussion

2.5.1 NEE variability at both Forage and Wheat fields

NEE fluxes were most disparate co-located at Wheat, where the $r^2 = 0.69$ at the South-Centre comparison (Table 2.1). This location only had 21 data points contributing to the comparison, which partially account for the poor regression despite how large the fluxes were. Examined in conjunction with the other towers, scatter at co-located Wheat South was greater than at both Forage towers. More data may have helped ameliorate this.

Wheat 50 m and 100 m had lower r^2 than the Forage regressions. NEE at Wheat during this time had small means (-4.72 to 2.62) and small dynamic range (RMSE ranged 1.28 – 2.01) (Table 2.1, Figure 2.5, 2.6), compared to Forage's range of 40 – 50 μmol m^{-2} s^{-1}. The small dynamic range must be considered when comparing regression differences. The wheat crop underwent senescence during our measurement period, demonstrating how uncertainties increase because of the narrow magnitude of fluxes during seasonal or crop transition periods. Mean NEE measurements were significantly different at Wheat, but not at Forage, which had larger flux magnitudes throughout the measurement period. The alfalfa and trefoil were actively growing and flowering through measurement, and were not cut while our towers were on field.

While regression comparisons focused on goodness of fit, percent RMSE provides a measure of the variability among tower separations. Percent RMSE was consistent at Forage (23 – 33% RMSE) no matter the tower location. Wheat percent RMSE ranged from 12 – 14% when co-located, 43– 45% at 50 m, and 197 – 221% at the 100 m separation. Note that the large percent difference at the last separation resulted from very low mean fluxes, indicating percent RMSE is not suited for comparing fluxes as they approach zero. A field experiment in Kansas, USA, showed two open-path and two closed-path analysers that were co-located agreed within 15%, while similar instruments agreed within 5% (Moncrieff et al. 1992). Differences ranged from 10 – 25% when two towers were compared by Kessomkiat et al. (2013), though towers were 300 – 1000 m apart and over differing land types, which can cause greater differences. Mean differences between two 30-m towers 775 m apart were only ~5% over two years in Hollinger and Richardson (2005)'s forest comparison. Multiple eddy covariance towers did not improve our ability to capture the NEE variability present on the Forage field, primarily because of greater canopy closure and denser vegetation. This was not the case at the Wheat field, where senescence and low fluxes increased percent RMSE but absolute flux values were small, making it difficult to differentiate spatial uncertainty.

2.5.2 Sources of NEE variability

Small changes in LAI can have large effects on carbon fluxes, because during the growing season daytime NEE is driven by photosynthesis (Zenone et al. 2015; Griebel et al. 2016). For LAI values up to 2, the relationship between LAI and GPP is relatively linear, and becomes asymptotic as LAI gets larger (Zenone et al. 2015). Comparing the

LAI contours (Figure 2.2) of both fields and their corresponding semivariograms (Figure 2.3) show that Forage had an overall higher and more dynamic LAI range than Wheat. At Forage and Wheat the range of mean footprint LAI ranged from 3.08 – 3.79 and 1.72 – 2.50, respectively (Figure 2.2, Table 2.2). Differences in leaf and stem morphology between alfalfa and wheat can impact leaf density and gap fraction; alfalfa is multi-foliolate and can have multiple stems (Teuber and Brick 1988) making the canopy more likely to close, while wheat has flat bladed leaves on tillers (Lersten 1987) and may have more gaps. Fields with higher LAI correspond to higher NEE uptake (larger negative values) into the ecosystem and higher photosynthetic rates than lower LAI (Moncrieff et al. 1997a). Across the whole field, forage LAI (Figure 2.3, Table 2.2) values ranged from 0.21 – 8.39 and had more numerous, higher LAI hotspots than Wheat, which ranged from 0.42 – 6.77 and was more uniform.

LAI measurements at Forage were split according to crop, and the two separate semivariograms (not shown) had the same sill but different ranges, where alfalfa range = 200 m and trefoil range = 60 m. The alfalfa patchiness resulted from partially flooded portions, tire tracks from where leaf cutter beehives were kept, and from where the producer manually sprayed herbicide to kill weeds. This variability in LAI was subsequently reflected in the whole-field semivariogram of Forage (Figure 2.3), resulting in the higher range of the alfalfa dominating and a greater distance needed for spatial autocorrelation. As well, fluxes were excluded from behind the towers to minimize tower airflow interference, resulting in less data originating from over the trefoil crop.

The crop at Wheat went through senescence during our measurement campaign, resulting in a smaller dynamic range for LAI as the crop dried, corresponding with a

decline in NEE magnitude. During measurement, portions of the field were still visibly green and less matured, which could influence field patchiness by having higher photosynthetic rates. When transitioning through senescence, the wheat plant and leaf structure remained relatively constant, but colour, dryness, and potential transmissivity may change. This may result in a similar value for LAI, while NEE has changed. Our 'snap shot' LAI measurements may have not captured this temporal transition and may not be representative of all the field conditions over which NEE measurements occurred. Wheat NEE and LAI could have provided a different picture if measurements were earlier in the summer when the crop was still actively growing.

Generally differences in CSAT3's vertical wind variance have been <5% when co-located (Mauder et al. 2007). By comparison, our co-located towers had a range of 12-24% RMSE based on u^* regression (Table 2.3), although the regression slopes at all separations were within 3%. This amount of uncertainty was maintained at both fields and across tower separations. This suggests that while the CSAT3s contributed to random measurement error, they were not the main source of NEE variability among towers and separations. Consistent and scheduled calibration upkeep of sonic anemometers may help reduce these random errors.

The contribution of the gas analysers was also examined in Table 2.3. $\sigma CO_2\ r^2$ values were less when co-located at Wheat, while highest at Forage. Differences generally increased at both fields as towers moved apart, from 4 – 15% RMSE at Forage and 16 – 300% RMSE at Wheat. This pattern is similar to that seen with NEE as the towers moved apart, supporting that spatial variability in CO_2 source or sinks were likely the main source of NEE variation amongst towers. These differences also show the

impact that smaller flux magnitudes can have on the amount of uncertainty in measurements.

2.6 Conclusions

The nature of field variability within eddy covariance experiments needs to be identified to understand measurement confidence for comparing sites and using field data in models. Comparing CO_2 flux systems over agricultural fields with a monocrop eliminates plant-type driven variation. In a regression analysis, NEE r^2 values were highest when towers were co-located and decreased slightly at Forage. Forage NEE RMSE remained at ~30% no matter the tower location. At the 100 m Wheat separation, uncertainty was 197 – 221% RMSE, mostly due to small flux magnitude. Measurement uncertainty from the CSAT3 (u*) was relatively consistent among fields and towers, while IRGA (σCO_2) percent difference increased as towers moved further apart. This supports that separation differences originated from carbon dioxide concentrations, though low fluxes at Wheat may have exacerbated this. However, vegetation quantity as measured through LAI was not significantly different among towers, and was similar to their respective field means. Field maximums and minimums were higher than for each individual footprint, highlighting a different tower placement may impact measured NEE.

Using corresponding spatial statistics to evaluate the vegetation and soil moisture variability of eddy covariance research sites could aid in determine whether there are differences among tower footprints, what degree of heterogeneity is present, and if measurements capture within-field variability. Research comparing the variability present for different crops, fields, and years may help characterize uncertainty associated with

seasonality, specific crop types, and how differences in their LAI affects NEE. These issues may be compounded in ecosystems that have greater vegetation complexity.

2.7 References

Baldocchi, D. D. 2003. Assessing the eddy covariance technique for evaluating carbon dioxide exchange rates of ecosystems: past, present and future. Global Change Biol. 9: 479-492

Baldocchi, D.D., Hicks, B.B., Meyers, T.P. 1988. Measuring biosphere-atmosphere Exchanges of biologically related gases with micrometeorological methods. Ecology 69: 1331-1340.

Ben Saïda, A. 2009. Shapiro-Wilk and Shapiro-Francia normality test function. MATLAB Inc. 2012b. Available online: [https://www.mathworks.com/matlabcentral/fileexchange/13964-shapiro-wilk-and-shapiro-francia-normality-tests/content/swtest.m]

Billesbach, D.P. 2011. Estimating uncertainties in individual eddy covariance flux measurements: A comparison of methods and a proposed new method. Agric. For. Meteorol. 151: 394-405.

Chen, B., Black, T.A., Coops, N.C., Hilker, T., Trofymow, J.A.T., Morgenstern, K. 2009. Assessing tower flux footprint climatology and scaling between remotely sensed and eddy covariance measurements. Boundary-Layer Meteorol. 130: 137-167.

Davis, P.A., Brown, J.C., Saunders, M., Lanigan, G., Wright, E., Fortune, T., Burke, J., Connolly, J., Jones, M.B., Osborne, B. 2010. Assessing the effects of agricultural management practices on carbon fluxes: Spatial variation and the need for replicated estimates of net ecosystem exchange. Agric. For. Meteorol. 150: 564-574.

Ehrlich, W.A., Poyser, E.A., Pratt, L.E., Ellis, J.H. 1953. Report of Reconnaissance Soil Survey of Winnipeg and Morris map sheet areas. Manitoba Soil Survey, Manitoba Department of Agriculture. Available: http://sis.agr.gc.ca/cansis/publications/surveys/mb/mb5/index.html [Online]

Environment Canada. 2016. Canadian Climate Normals 1971-2000, Available: http://climate.weather.gc.ca/climate_normals/index_e.html#1971 [Online]

Finkelstein, P.L., Sims, P.F. 2001. Sampling error in eddy correlation flux measurements. J. Geophys. Res. 106: 3503-3509.

Glenn, A.J., Amiro, B.D., Tenuta, M., Stewart, S.E., Wagner-Riddle, C. 2010. Carbon dioxide exchange in a northern Prairie cropping system over three years. Agric. For. Meteorol. 150: 908-918.

Glenn, A.J., Amiro, B.D., Tenuta, M., Wagner-Riddle, C., Drewitt, G., Warland, J. 2011. Contribution of crop residue carbon to total soil respiration at a northern Prairie site using stable isotope flux measurements. Agric. and For. Meteorol. 151: 1045-1054.

Griebel, A., Bennett, L.T., Metzen, D., Cleverly, J., Burba, G., Arndt, S.K. 2016. Effects of inhomogeneities within the flux footprint on the interpretation of seasonal, annual, and interannual ecosystem carbon exchange. Agric. For. Meteorol. 221: 50-60.

Hollinger, D.Y., Richardson, A.D. 2005. Uncertainty in eddy covariance measurements and its application to physiological models. Tree Physiol. 25: 873-885.

Kessomkiat, W., Franssen, H-J.H., Graf, A., Vereecken, H. 2013. Estimating random errors of eddy covariance data: An extended two-tower approach. Agric. For. Meteorol. 171-172: 203-219.

Kormann, R., Meixner, F.X. 2001. An analytical footprint model for non-neutral stratification. Boundary-Layer Meteorol. 99: 207-224.

Leclerc, M.Y., Thurtell, G.W. 1990. Footprint prediction of scalar fluxes using a Markovian analysis. Boundary-Layer Meteorol. 52: 247-258.

Lersten, N.R. 1987. Morphology and Anatomy of the Wheat Plant. In: Heyne, E.G. (ed). Wheat and Wheat Improvement. American Society of Agronomy, Madison, WI. pp. 33-75.

Lloyd, C.R., Bessemoulin, P., Cropley, F.D., Culf, A.D., Dolman, A.J., Elbers, J., Heusinkveld, B., Moncrieff, J.B., Monteny, B., Verhoef, A. 1997. A comparison of surface fluxes at the HAPEX-Sahel fallow bush sites. J. Hydrol. 188-189: 400-425.

Loescher, H.W., Law, B.E., Mahrt, L., Hollinger, D.Y., Campbell, J., Wofsy, S.C. 2006. Uncertainties in, and interpretation of, carbon flux estimates using the eddy covariance technique. J. Geophys. Res. 111:D21S90.

Massman, W.J. 2000. A simple method for estimating frequency response corrections for eddy covariance systems. Agric. For. Meteorol. 104: 185-198.

Mauder, M., Cuntz, M., Drüe, C., Graf, A., Rebmann, C., Schmid, H.P., Schmidt, M., Steinbrecher, R. 2013. A strategy for quality and uncertainty assessment of long-term eddy-covariance measurements. Agric. For. Meteorol. 169: 122-135.

Mauder, M., Oncley, S.P., Vogt, R., Weidinger, T., Ribeiro, L., Bernhofer, C., Foken, T., Kohsiek, W., De Bruin, H.A.R., Liu, H. 2007. The energy balance experiment EBEX-2000. Part II: Intercomparison of eddy-covariance sensors and post-field data processing methods. Boundary-Layer Meteorol. 123: 29-54.

Moncrieff, J.B., Verma, S.B., Cook, D.R. 1992. Intercomparison of eddy correlation carbon dioxide sensors during FIFE 1989. J. Geophys. Res. 97(D17): 18725-18730.

Moncrieff, J.B., Malhi, Y., Leuning, R. 1996. The propagation of errors in long-term measurements of land-atmosphere fluxes of carbon and water. Global Change Biol. 2: 231-240.

Moncrieff, J.B., Monteny, B., Verhoef, A., Friborg, Th., Elbers, J., Kabat, P., de Bruin, H., Soegaard, H., Jarvis, P.G., Taupin, J.D. 1997a. Spatial and temporal variations in net carbon flux during HAPEX-Sahel. J. Hydrol. 188-189: 563-588.

Moncrieff, J.B., Massheder, J.M. , de Bruin, H, Elbers, J., Friborg, T., Heusinkveld, B., Kabat, P., Scott, S., Soegaard, H., Verhoef, A. 1997b. A system to measure surface fluxes of momentum, sensible heat, water vapour and carbon dioxide. J. Hydrol. 188-189: 589-611.

Moore, C.J. 1986. Frequency response corrections for eddy correlation systems. Boundary-Layer Meteorol. 37: 17-35.

Moors, E.J., Jacobs, C., Wilma, J., Supit, I., Kutsch, W.I., Bernhofer, C., Béziat, P., Buchmann, N., Carrara, A., Ceschia, E., Elbers, J., Eugster, W., Kruijt, B., Loubet, B.,

Magliulo, E., Moureaux, C., Olioso, A., Saunders, M., Soegaard, H. 2010. Variability in carbon exchange of European croplands. Agric. Ecosyst. Environ. 139: 325-335.

Post, H., Franssen, H.J.H., Graf, A., Schmidt, A., Vereecken, H. 2015. Uncertainty analysis of eddy covariance CO_2 flux measurements for different EC tower distances using an extended two-tower approach. Biogeosci. 12: 1205-1221.

Schwanghart, W. 2009. Semi-Variogram function. MATLAB Inc. 2012b. Available online: [https://www.mathworks.com/matlabcentral/fileexchange/20355-experimental--semi---variogram/content/variogram.m]

Sun, J., Burns, S.P., Delany, A.C., Oncley, S.P., Turnipseed, A.A., Stephens, B.B., Lenschow, D.H., LeMone, M.A., Monson, R.K., Anderson, D.E. 2007. CO_2 transport over complex terrain. Agric. For. Meteorol. 15: 1-21.

Tanner, C.B., Thurtell, G.W. 1969. Sensible heat flux measurements with a yaw sphere and thermometer.TR Ecom 66-G22-F.Department of Soil Science, University of Wisconsin, Madison, Wisconsin.

Teuber, L.R, Brick, M.A. 1988. Morphology and anatomy. In A.A. Hanson, D.K. Barnes and R.R. Hill,Jr. (ed.) Alfalfa and alfalfa improvement. ASA-CSSA-SSSA, Madison, WI. pp. 125-162.

Zenone, T., Fischer, M., Arriga, N., Broeckx, L.S., Verlinden, M.S., Vanbeveren, S., Zona, D., Ceulemans, R. 2015. Biophysical drivers of the carbon dioxide, water vapor, and energy exchanges of a short-rotation polar coppice. Agric. For. Meteorol. 209-210: 22-35.

3. THE SPATIAL VARIABILITY OF TURBULENT ENERGY FLUXES OVER AGRICULTURAL FIELDS IN THE SHORT AND LONG TERM

3.1 Abstract

Eddy covariance can be used to measure the turbulent fluxes of sensible (H) and latent (LE) heat over agricultural systems. One tower is often used to measure fluxes and it's uncertain whether that is enough to represent field variability. We used two datasets to assess whether one tower's H and LE is representative of a field's variability. Three identical towers measured H and LE over a perennial Forage and a Wheat field in Southern Manitoba in 2014, two of which (North and South) moved 50 m and then 100 m away from a stationary central tower (Centre). North and South were compared in regression against Centre at each separation. H had consistently high regression r^2 values (0.8 – 0.97) at both fields. LE scatter was consistent as towers moved apart, with r^2 ranging from 0.76 – 0.82. At both fields, H RMSE (root-mean-square error) was ~10 W m^{-2} and average mean was ~18 W m^{-2}. LE RMSE among towers was ~44 W m^{-2} and mean LE averaged ~210 W m^{-2} at Forage. Wheat measurements were later in the growing season resulting in LE RMSE ~25 W m^{-2} and mean LE averaged ~140 W m^{-2}. To examine whether spatial variation affected energy partitioning, we looked at the Bowen ratio (H/LE) of all three towers at the 100 m separation for two consecutive days over the forage field. The Bowen ratios of all towers remained close together throughout the diurnal trend, suggesting that energy partitioning was consistent. Four towers of virtual heat flux data from four years in Southern Manitoba were examined, where each tower was compared to the average of all towers. Across all years there were very high r^2 values

(0.95 - 0.98). The towers were also compared during only July of each year. Slopes and root mean squared error (RMSE) were lower the year corn was planted because of crop height, smaller flux footprint source areas, and proximity to the measurement instrumentation. Uncertainty remained similar amongst separations for both H and LE, indicating that we did not capture extra variability with more measurement towers. Differences between H and LE were ameliorated when energy partitioning was evaluated with the Bowen ratio.

3.2 Introduction

Sensible heat flux (H) and latent heat flux (LE) flux are primarily driven by temperature and water vapour exchange through evapotranspiration. Measuring these fluxes over agricultural systems helps us better understand water and energy movement through surface exchange processes. Generally, a single eddy covariance tower measures a larger region through a surface footprint where H and LE originate. The footprint of this measurement depends on the measurement height, distance between sensors and sources, and atmosphere turbulence characteristics (Schmid 1997). How in-field vegetation varies both temporally and spatially locally will influence H and LE, and also how they are partitioned. H and LE also change in conjunction with one another; for example, high stomatal conductance results in high evapotranspiration, which lowers leaf surface temperatures and H, but causes an increase in LE.

The confidence in H and LE measurements affects the conclusions derived about field characterization. Errors in eddy covariance measurements are also part of the problem with energy balance closure (Foken 2008; Leuning et al. 2012; Kessomkiat et al.

2013). Generally, the measured sum of net incoming and outgoing radiation, soil heat flux, and ground heat storage are larger than the combined measurements H and LE, resulting in an incomplete closure of the energy balance at the earth's surface (Foken 2008). Vegetation borders and heterogeneity not captured by towers can influence air circulation and measured fluxes (Foken et al. 2011). In-field spatial variability may contribute to the difficulty in accurately measuring turbulent fluxes (Mauder et al. 2010), and quantifying the uncertainty created may help address the problem of energy balance closure. As well, patchiness in flux footprints might create deficits in the energy balance closure because of differences in radiative and evaporative properties which influence turbulent exchange (Guo et al. 2008).

Previous work relating H, LE, and the Bowen-ratio (H/LE) to spatial phenomena has primarily relied on modelling and remote sensing using scales coarser than field measurements and may not have evaluated if H and LE varied spatially at the field scale. For example, modelling in-field scintillometer measurement and remote sensing were compared (Kite and Droogers 2000) and could not be reconciled as to which was more accurate, but each had unique complexity and insight. Melesse and Nangia (2005) estimated energy fluxes from LANDSAT data (30 – 120 m resolution) of agricultural fields over multiple years, comparing LE and the Bowen ratio to crop yields. H and LE both have seasonal variability driven by changes in vegetation and soil water, with H more prevalent in dry periods and LE when there is adequate moisture (Krishnan et al. 2012). Neglecting the effect of seasonal and spatial variability on H and LE may also inaccurately predict the Bowen ratio for different heterogeneous landscapes (Friedrich et al. 2000). Generally though, few have measured the spatial variation of fields in

conjunction with eddy covariance energy flux measurements or combined multiple towers on the same field.

Flux tower footprint areas depend on atmospheric turbulence and wind direction, and may only measure a fraction of the desired source area depending on tower placement and campaign length (e.g., Amiro 1998). Variability in moisture and leaf area index (LAI) can contribute to heterogeneity in energy balance components like H and LE, which single tower measurements may not capture; this increases uncertainty of conclusions drawn or modelling based on those measurements (Alfieri and Blanken 2012). Random errors in eddy covariance systems are found to range 10 – 25%, decreasing as both fluxes and radiation increase (Hollinger and Richardson 2005; Kessomkiat et al. 2013). If multiple, independent measurement systems are used in one field, confidence levels of eddy covariance measurements could be evaluated (Finkelstein and Sims 2001).

Through two separate research campaigns we evaluated if a flux tower footprint captures the spatial variability of H and LE over an agricultural field. We also explored how potential field variability affected energy partitioning through the Bowen ratio and if it were different than H and LE individually.

3.3 Experimental design & research sites

Two research campaigns provided data for this paper: the short-term campaign used three towers over a perennial and annual field in 2014, and the long-term campaign used four towers over 4 years from one field with different crops each year. They are described and analysed separately.

3.3.1 Short-term experiment, summer 2014

A perennial forage field (Forage) and an annual spring wheat crop (Wheat) (Figure 2.1) were used for our experiment, from June 13 through July 22, 2014 at Forage and July 22 through September 5, 2014 at Wheat. The Forage field (49°54'36.72" N 96°49'41.28 W, 243 m.a.s.l.) was a 60 ha producer's field east of Winnipeg, MB, Canada with a 60/40 split of seed alfalfa (*Medicago sativa*) and trefoil (*Lotus corniculatus*). The Wheat field was on the Glenlea Research Farm (49°38'48.48" N 97°09'21.09" W 235 m.a.s.l.) south of Winnipeg, MB Canada, and was on 50 ha of hard red spring wheat (*Triticum aestivum. L. '*Carberry'). It is the same research site as Chapter 2 and will draw upon data and conclusions analysed within it.

Three eddy covariance towers were installed at Forage and subsequently Wheat (Figure 2.1) during the summer of 2014. The towers were equipped with sonic anemometer-thermometer CSAT3's as well as a closed-path, factory calibrated CO_2/H_2O gas analyzers (IRGA LI-7000 CO_2/H_2O Analyzer, LI-COR Biosciences, Lincoln, NE, USA) in protective temperature-controlled housing (University of British Columbia, Biometeorology Group) to enable calculation of LE and H. These towers were moved across the field (Figure 2.1) from co-location, to 50 m apart, to 100 m apart, along a north-south line. For a more in depth description of the experimental design and set-up, see Section 2.3.

3.3.2. Long-term experiment, TGAS 2012-2015

The Glenlea Research Farm is also home to the Trace Gas Manitoba (TGAS) field research site, currently operational since 2006, and has had a variety of crops in the

intervening years. It is the same farm field where Wheat was measured in 2014 (Figure 2.1), with measurement towers west of where our three-tower comparison were.

Four sonic-anemometer-temperature sensors (CSAT3, Campbell Scientific Inc., Logan, UT, USA) were mounted 2 m above the soil surface (Figure 3.1), each ~200 m apart from one another and whose data were used to calculate virtual H (H_v) for 2012 – 2015. For a more in-depth description of the TGAS experimental design and previous research outcomes, see Glenn et al. (2010), Glenn et al. (2011), Glenn et al. (2012), Maas et al. (2013), and Tenuta et al. (2016).

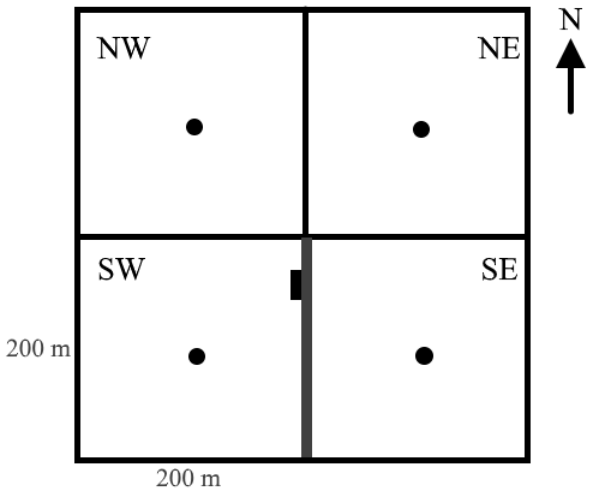

Figure 3.1 TGAS research site, where circles are the CSAT3 measurement towers, black rectangle is the weather station, and the thick grey line is a grassed access path to a research trailer in the centre.

Four years of data from TGAS, 2012 – 2015 were analysed. Corn (*Zea mays*, 'DKC26-79') was planted in on May 3, 2012 and harvested October 18, 2012. Round-up ready soybeans with inoculant (*Glycine max*, 'Variety-Syngenta S00-W3 & Cruiser Max') were planted May 28, 2013 and harvested October 9, 2013. Hard red spring wheat (*Triticum aestivum. L.* 'Carberry') was planted May 29, 2014 and harvested September

15, 2014. Round-up ready soybean was planted again on May 13, 2015 and harvested Sept 29, 2015. During the remainder of the periods, the field was fallow, with snow cover typically extending November through March.

3.3.3 Data processing and quality controls

Data from both research campaigns were processed in MATLAB (Mathworks Inc. Natick, MA, USA). No gap-filling was done on any of the data.

3.3.3.1 Three-tower comparison, summer 2014

Raw high-frequency data were split into half-hourly files, which were de-spiked, cross-products calculated, had delays removed through flux optimization, and wind vectors underwent coordinate rotation (Tanner and Thurtell 1969). Turbulent 3D sensible heat flux (H) was calculated as:

$$H = \left((c_d\,\rho_d) + (c_v\,\rho_v)\right)\overline{w'T_a'} \qquad [3.1]$$

where c_d = specific heat dry air (J kg^{-1} K^{-1}), ρ_d = dry air density (kg m^{-3}), c_v = specific heat of water vapour (J kg^{-1} K^{-1}), ρ_v = water vapour density (kg m^{-3}), and $w'T_a'$ = turbulent air temperature flux (K m s^{-1}) , which was calculated from:

$$w'T_a' = \overline{w'T_s'} - T_a\left(\overline{w'C_v'}\,/\left(\overline{C_v}\right)\right) \qquad [3.2]$$

where $w'T_s'$ = rotated turbulent CSAT3 temperature flux corrected for vapour pressure (K m s^{-1}) , T_a = vapour-corrected mean ambient air temperature derived from the CSAT3 (K), $w'C_v'$ = rotated turbulent vertical vapour flux (mmol m^{-2} s^{-1}), and C_v = water vapour concentration (mmol m^{-3}). Overbars denote means over a 30-minute period and primes ($'$) are deviations from the mean.

The latent heat flux (LE) was calculated by:

$$LE = \lambda \overline{w' C_v'} \quad [3.3]$$

where λ = latent heat of vapourization using corrected ambient air temperature (J $mmol^{-1}$), and $w'C_v'$ = rotated turbulent vertical vapour flux density (mmol m^{-2} s^{-1}) .

Known instrument disruptions such as site visits, instrument failure, tower movement, shut-downs, rainy periods, and calibration times were removed from the 2014 three-tower data. Periods when winds came from behind the tower (> 45° or < 135°) and when the mean of the vertical wind velocity was > 0.5 m s^{-1} or < -0.5 m s^{-1} were also removed. A friction velocity (u*) threshold of 0.2 m s^{-1} was applied to both H and LE to focus on turbulent conditions. Spectral corrections were applied to LE based on half-hourly model spectra transfer functions (Moore 1986; Moncrieff et al. 1997; Massman 2000) after all other quality controls were applied. LE < 50 W m^{-2} was excluded, in particular to limit the range when calculating the Bowen ratio and focus on higher flux periods.

To minimize the impact of instrument error, we calibrated the North and South tower against the Centre through regression analysis when co-located, prior to further analysis. The regression statistics from each pair (North-Centre or South-Center) and separation were applied, whereby H or LE were multiplied by the regression slope, and the offset was added.

When comparing mean values of H and LE, tower data were tested for normality using Shapiro-Wilk (Ben Saïda 2009), were found to be not normal, and could not be transformed due to negative numbers. In MATLAB, rank sum was used for two-tower comparisons and Kruskal-Wallis was used for three-tower comparisons.

3.3.3.2 TGAS four-tower comparison, 2012 to 2015

High-frequency data (10 Hz) were collected from each tower via datalogger (Model CR1000, Campbell Scientific Inc.) and resulted in 30-minute averages of data and cross-products. To test for stationarity, 30-minute periods were removed if any 5-minute period within the half hour had a standard deviation of the vertical wind velocity >30% different from the whole 30-minutes (Foken et al. 2004). This ensured that half-hourly values are representative of the conditions present during the measurement period. A u* cut-off of 0.15 m s^{-1} was applied based on the standard protocol for carbon dioxide flux measurements at this site (Glenn et al. 2010). No water vapour flux measurement was available for density corrections, so the virtual heat flux (H_v) was calculated from each tower's respective CSAT3 values:

$$H_v = (c_d\, \rho_d)\overline{w'T_s'} \qquad [3.4]$$

A model (Chen et al. 2009) was used to generate footprints based on crop height to compare source area differences, based on original work by Kormann and Meixner (2001).

3.4 Results

3.4.1 Turbulent flux three-tower comparison at Wheat and Forage fields in 2014

Regression analyses were done of each North and South tower against a stationary Centre tower to evaluate the uncertainty in sampling the spatial variability of field-scale turbulent fluxes. We evaluated LE and H separately, and then looked at the Bowen ratio to examine energy partitioning. Measurements were during summer 2014 because both H and LE have greater magnitude than through frozen, snow-covered winters. LE in

particular increases through early summer, peaking mid-summer, before generally declining late in the season in Manitoba.

3.4.1.1 Regression comparison of LE. When towers were co-located (Figure 3.2) LE r^2 = 0.69 and 0.90 at Forage and 0.89 at both Wheat towers (Table 3.1). Note that the low r^2 value from the Forage North-Centre comparison was largely caused by four outlying points. RMSE was larger at Forage North-Centre (35 – 59 W m^{-2}) than any other co-located comparison, and percent RMSE as determined by RMSE/Centre LE was higher at North than South (29% RMSE compared to 17% RMSE). Tower populations of LE at Forage North-Centre were not significantly different from one another ($p = 0.16$), while South-Centre were ($p = 0.006$). North was significantly different from both Centre and South at Wheat ($p < 0.001$), though had quite low sample populations ($n = 18$) comparatively.

When towers were moved 50 m away from Centre, Forage South-Centre had higher flux values and wider scatter, while Wheat values clustered more tightly with the 1:1 line (Figure 3.3). The sole 50 m Forage South-Centre comparison had an r^2 lower than when co-located ($r^2 = 0.78$) and a slope = 1, while the intercept = 19.98 W m^{-2} (Table 2.1). Wheat r^2 values were both relatively high (0.80 and 0.94) at 50 m separation, while intercepts were negative, ranging -18.26 to -9.07 W m^{-2}. Forage South-Centre were significantly different ($p = 0.03$).Wheat Centre LE was also significantly higher than South ($p = 0.007$). At both fields, percent RMSE were similar to when co-located (12 – 24% RMSE).

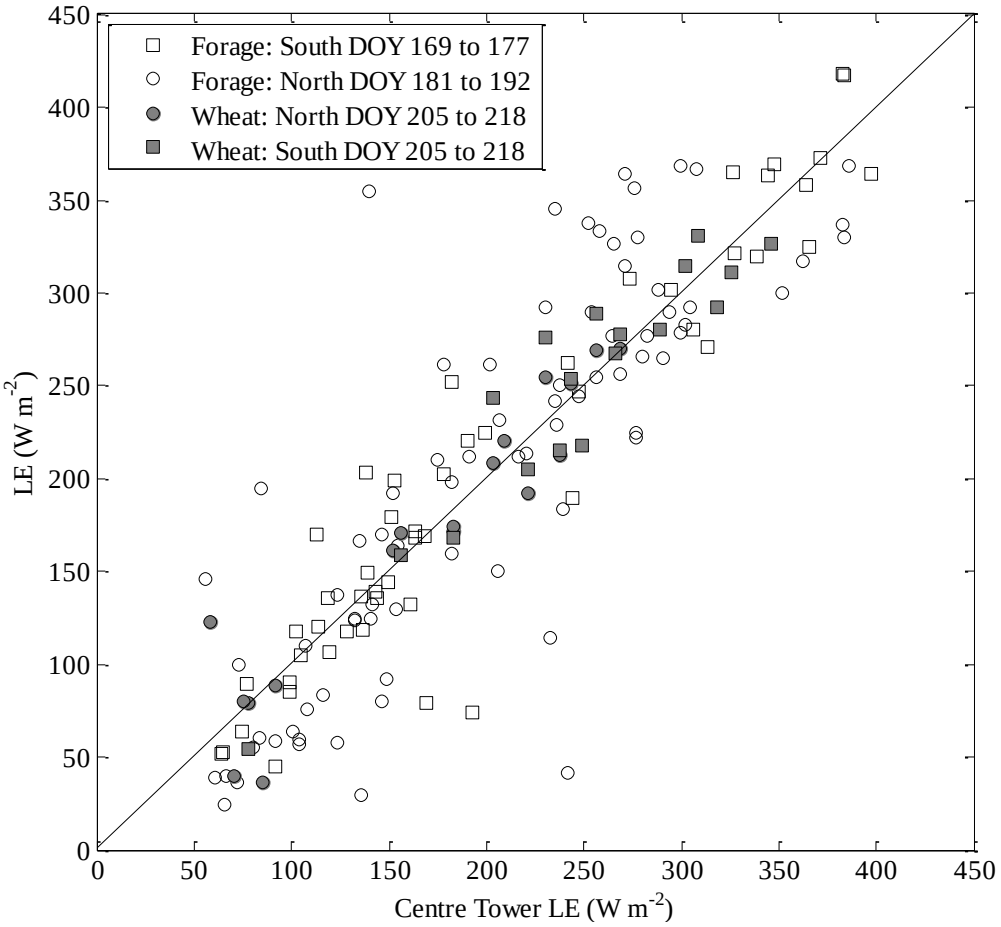

Figure 3.2 Co-located three tower regression comparison of LE when co-located in 2014. The black line is a 1:1 reference.

Table 3.1 Regression comparisons and means for LE in 2014. RMSE is root mean squared error.

Forage	DOY	y	y mean LE (W m^{-2})	x	x mean LE (W m^{-2})	r^2	Slope	Intercept (W m^{-2})	RMSE (W m^{-2})	n
Co-located	169 - 177	North	203.32	Centre	203.32	0.69	1	0	58.80	78
Co-located	181 - 192	South	201.95	Centre	201.95	0.90	1	0	34.96	51
50 m	177 - 192	South	235.15	Centre	256.02	0.78	1.00	19.98	46.18	74
100 m	192 - 204	North	205.31	Centre	204.64	0.82	1.13	-25.15	39.93	97
100 m	192 - 204	South	203.69	Centre	213.34	0.76	0.92	6.43	39.78	87
Wheat										
Co-located	205 - 218	North	166.79	Centre	166.79	0.89	1	0	25.71	18
Co-located	205 - 218	South	248.96	Centre	248.96	0.89	1	0	24.31	18
50 m	218 - 232	North	147.44	Centre	141.40	0.80	1.11	-9.07	31.85	127
50 m	218 - 232	South	120.70	Centre	136.04	0.94	1.02	-18.26	16.69	48
100 m	232 - 248	North	87.88	Centre	103.20	0.54	0.83	2.32	25.28	46
100 m	232 - 248	South	76.66	Centre	108.15	0.64	1.19	-51.96	27.08	24

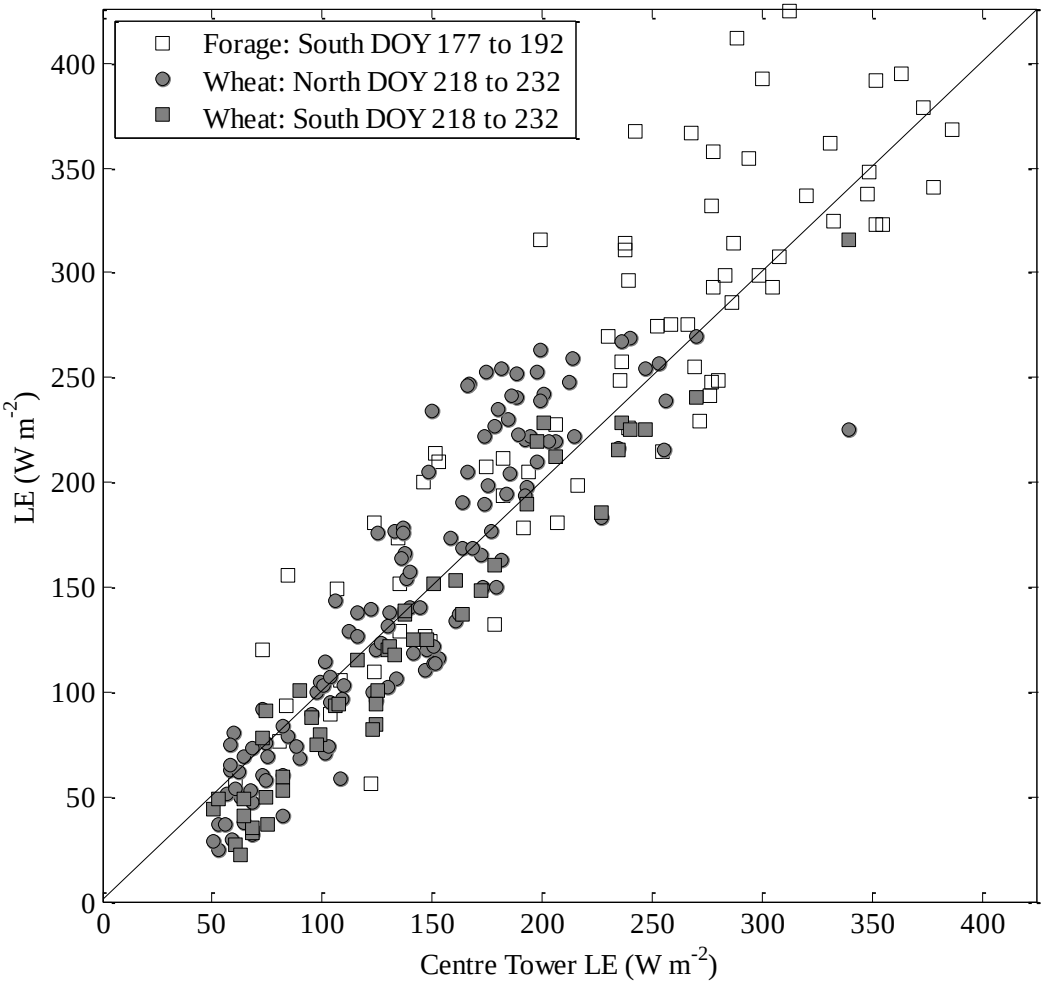

Figure 3.3 Regression three tower comparison of LE at 50 m separation in 2014. The black line is a 1:1 reference.

When towers were 100 m apart r^2 values ranged from 0.76 – 0.82 at Forage and 0.54 – 0.64 at Wheat (Table 3.1). LE at Wheat North and South were both significantly lower than Centre LE ($p = 0.007$), while there were no differences amongst Forage ($p = 0.87$). The dynamic range of Wheat LE was lesser (~50 – 200 W m^{-2}) when towers were 100 m apart than when co-located (~50 – 350 W m^{-2}) because of the later time of year, while Forage LE maintained the same range of values (~50 – 400 W m^{-2}). Overall, there

was wide scatter in r^2 values and consistent percent difference (RMSE/Centre LE) at Wheat (12 – 25% RMSE) and Forage (17 – 29% RMSE).

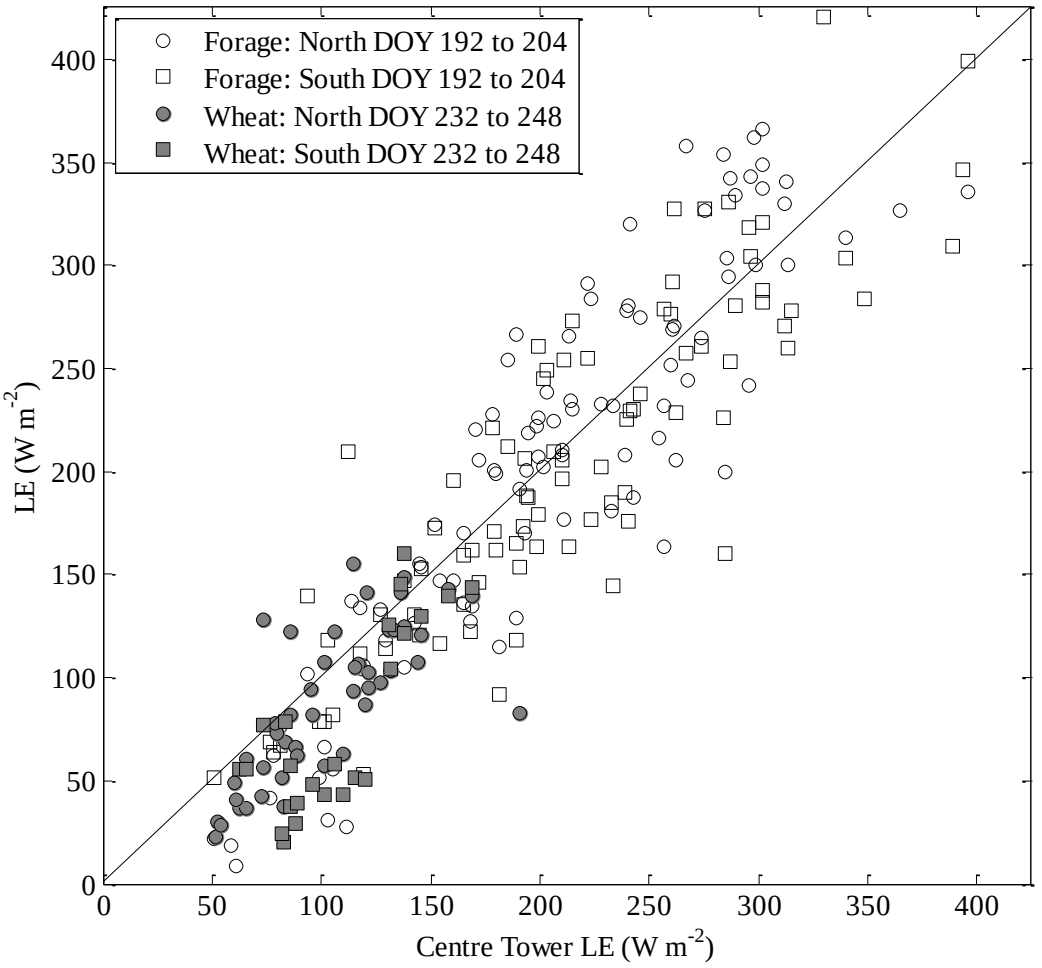

Figure 3.4 Regression three tower comparison of LE at 100 m separation in 2014. The black line is a 1:1 reference.

3.4.1.2 Regression comparison of H. When towers were co-located (Figure 3.5), H r^2 values were high (0.94 – 0.97) at both fields (Table 3.2), though Forage South-Centre had more scatter and an $r^2 = 0.80$. The Wheat North and South tower H were significantly different ($p < 0.001$). There were no significant difference between co-located Forage

towers (North-Centre p =0.58, South-Centre p = 0.73). Percent RMSE was not used for H because of small and negative values.

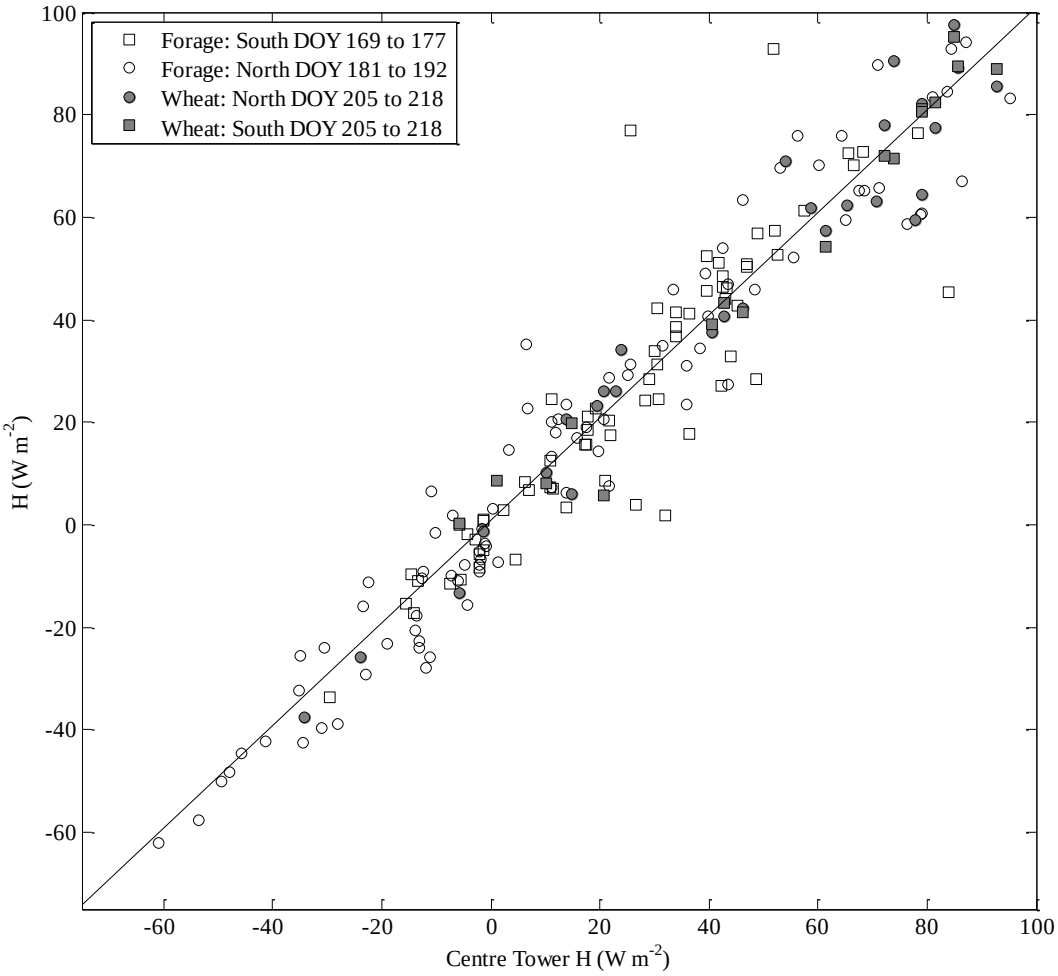

Figure 3.5 Co-located three tower regression comparison of H in 2014. The black line is a 1:1 reference.

At the 50m separation (Figure 3.6), r^2 values remained high at both fields, ranging from 0.91 – 0.95 (Table 3.2). Slopes remained near to 1 (0.97 – 1.1). Intercepts departed more at the Wheat field, from -5.38 to -1.65 W m^{-2} compared to 1.70 W m^{-2} at Forage. There were no significant differences between tower H at either field (Forage p = 0.8, Wheat p = 0.72).

Table 3.2 Regression comparisons and means for H in 2014. RMSE is root mean squared error.

Forage	DOY	y	y mean H ($W m^{-2}$)	x	x mean H ($W m^{-2}$)	r^2	Slope	Intercept ($W m^{-2}$)	RMSE ($W m^{-2}$)	n
Co-located	169 - 177	North	15.90	Centre	15.90	0.94	1	0	9.69	90
Co-located	181 - 192	South	25.24	Centre	25.24	0.80	1	0	12.25	69
50 m	177 - 192	South	9.01	Centre	11.62	0.93	1.10	1.70	12.24	74
100 m	192 - 204	North	12.68	Centre	6.47	0.94	1.16	5.13	12.33	100
100 m	192 - 204	South	23.48	Centre	10.72	0.93	0.97	13.00	11.5	92
Wheat										
Co-located	205 - 218	North	43.86	Centre	43.86	0.95	1	0	8.49	28
Co-located	205 - 218	South	51.86	Centre	51.86	0.97	1	0	6.14	17
50 m	218 - 232	North	12.25	Centre	16.51	0.94	1.07	-5.38	11.42	134
50 m	218 - 232	South	15.39	Centre	17.60	0.95	0.97	-1.65	9.96	65
100 m	232 - 248	North	2.13	Centre	2.22	0.93	1.00	-0.09	10.59	29
100 m	232 - 248	South	-12.07	Centre	-5.34	0.96	1.07	-6.33	7.88	17

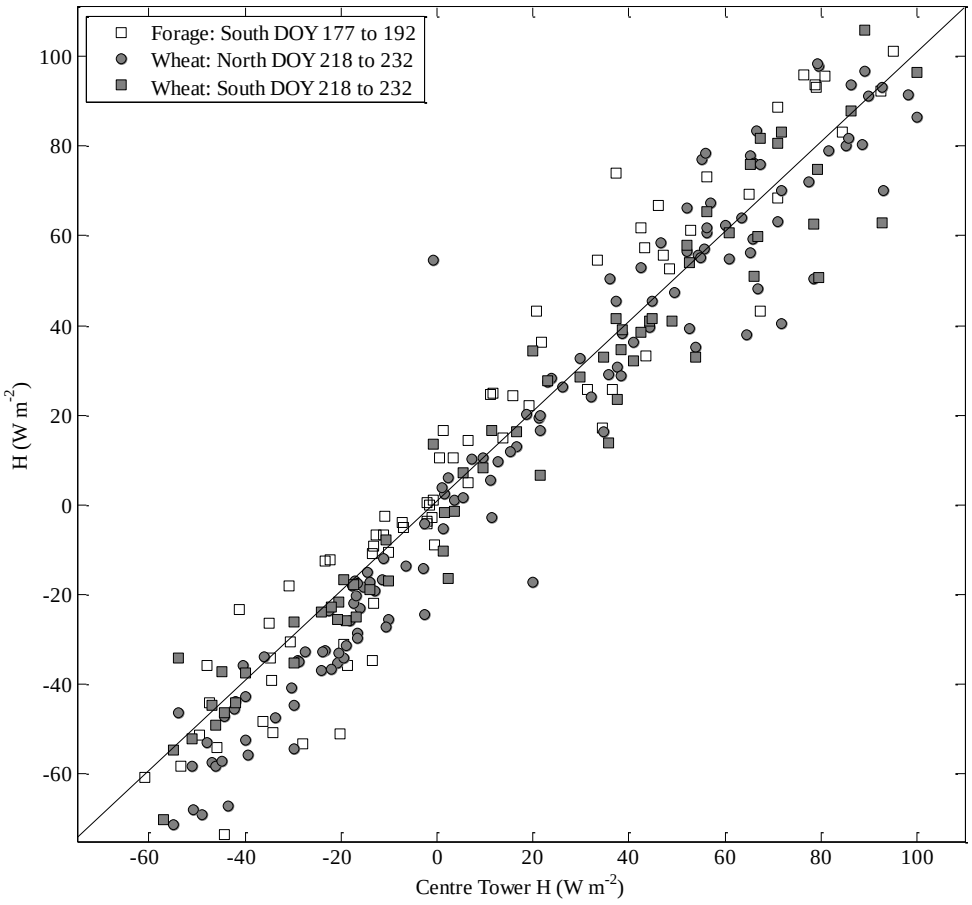

Figure 3.6 Regression three tower comparison of the H 50 m separation in 2014. The black line is a 1:1 reference.

When 100 m apart, Forage values shifted slightly off the 1:1 line compared to the Wheat field (Figure 3.7), and this is reflected in the regression comparison (Table 3.2). Though r^2 values are high (0.91 – 0.94), the Forage intercepts have shifted off zero, 5.13 and 13 W m^{-2} for North-Centre and South-Centre, and -8.15 W m^{-2} for North-South. Wheat maintained high r^2 values (0.93 – 0.96), good slope (1.00 – 1.07), and intercepts closer to 0 W m^{-2} than Forage (-6.33 to -0.09 W m^{-2}). There were no significant differences found among either field's H at 100 m (Forage p = 0.17, Wheat p = 0.3).

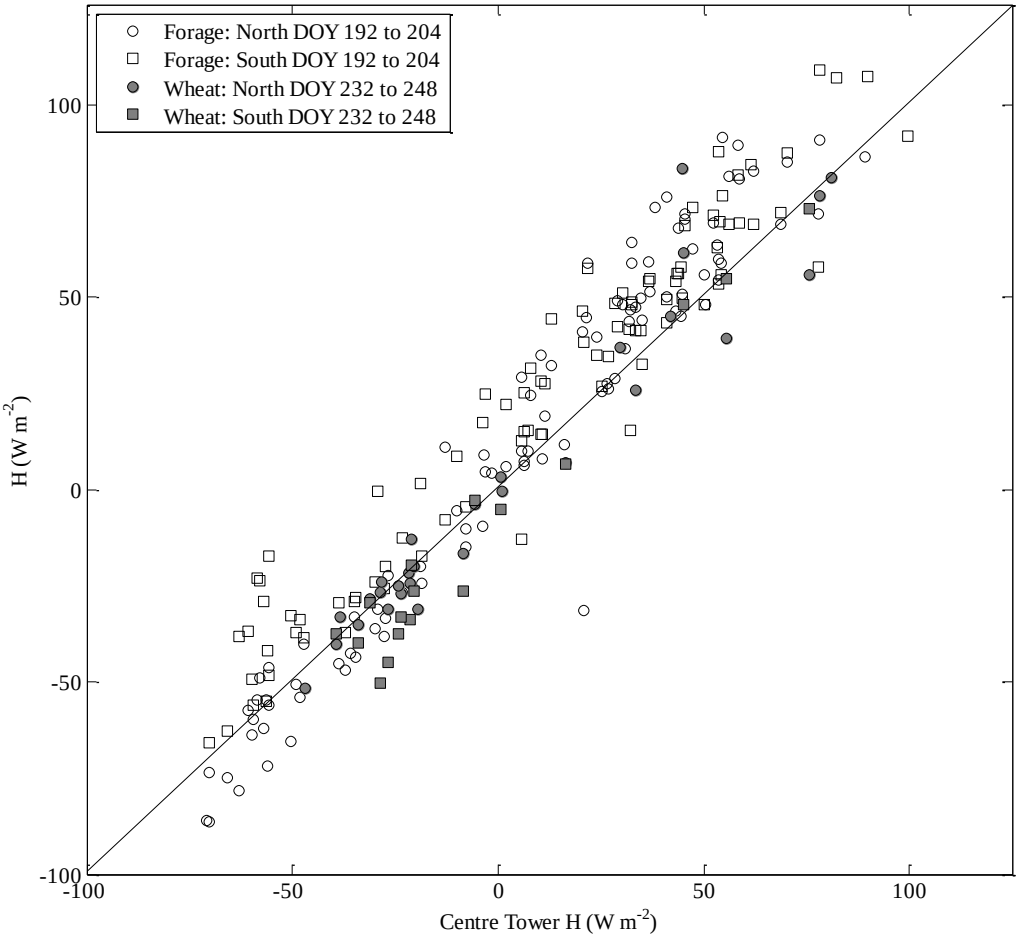

Figure 3.7 Regression three tower comparison of H at the 100 m separation in 2014. The black line is a 1:1 reference.

3.4.1.3 Investigating variability through the Bowen ratio, leaf area index, and footprint analysis. The ratio of H to LE comprises the Bowen ratio, which represents the relative partitioning of turbulent energy over the measured ecosystem. This relationship is examined in Figure 3.8 over two days with continuous flux coverage at Forage. The Bowen ratio was compared at the 100 m separation to examine the maximum spatial variability amongst towers.

On both days winds were predominantly from the North (340 – 25°). DOY 198 was a partially overcast day while DOY 199 was partly cloudy with periodic rain from passing storms. On DOY 198 all three towers correspond tightly throughout the day, and even when there is greater range on DOY 199, all three towers still follow the same distinct, diurnal patterns. This suggests that field characteristics are affecting partitioning similarly at all three towers, despite their distinct footprints, with diurnal trends influencing their magnitude more than spatial effects.

Footprints of each tower separation and field were modelled, and the 100 m separation was examined in Figure 2.2 in conjunction with a leaf area index (LAI) isoline map. There were similarities in footprint shape and differences came primarily from tower placement on field causing different spatial sampling. As shown in Chapter 2.4.2, there were no significant differences among any tower mean footprint LAI. Whole field LAI means for Forage = 3.5 and Wheat = 1.94 were similar to tower footprint LAI values, indicating similarities among crop canopy cover. Semivariograms of each field (Figure 2.3) had a larger range at Forage (200 m) than Wheat (80 m), corresponding to when autocorrelation occurs. Forage had higher variance in its values based on a higher sill (2.05 compared to 0.87 at Wheat).

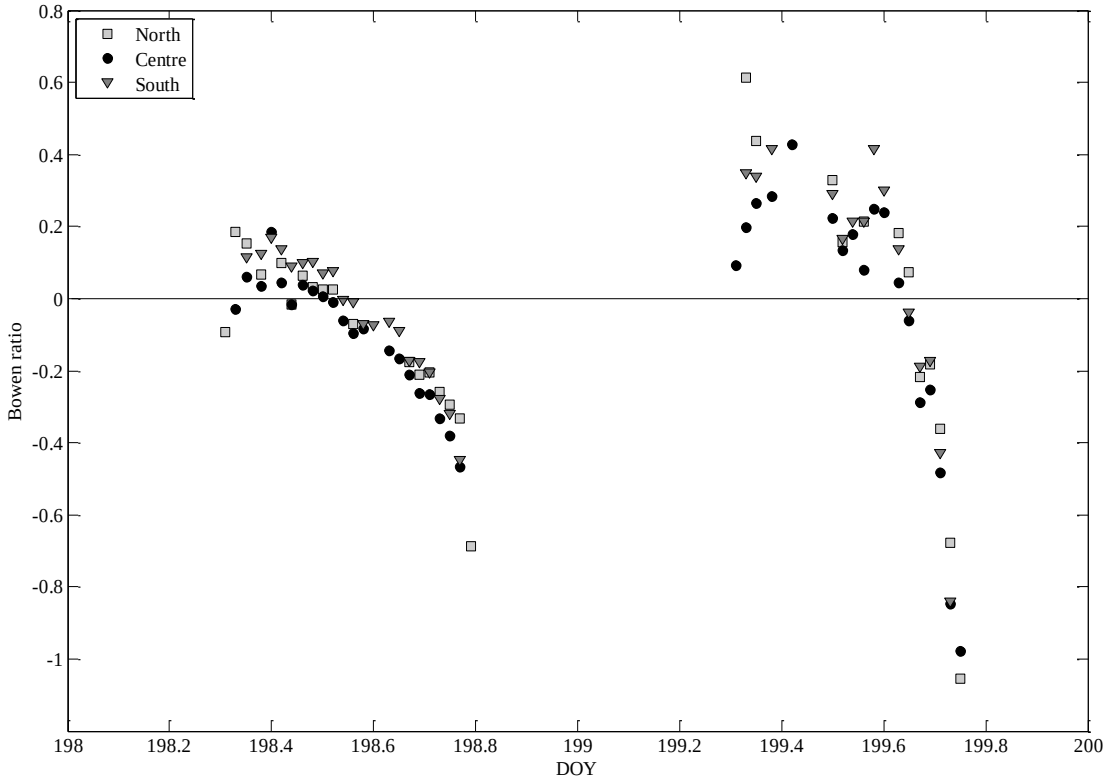

Figure 3.8 The Bowen ratio at the 100 m Forage separation from day of year (DOY) 198 to 200. Ratio excludes LE < 50 W m^{-2}.

3.4.2 Long-term four-tower comparison of virtual heat flux (H_v), 2012 to 2015

We measured H_v at four towers at TGAS during a four-year period, 2012-2015, to examine the capability of multiple flux systems to measure heat flux with a larger dataset. For each year, regression comparisons of H_v at each of the four towers were compared to the combined mean of all towers (Table 3.3). Across all towers and years, r^2 remained quite high (0.95 - 0.98), slopes stayed close to 1 (0.95 - 1.02), and intercepts were within ~±1.5 W m^{-2} of zero.

Table 3.3 Regression comparison of H_v at four towers versus the mean value of all towers each year at TGAS MAN. RMSE is root mean squared error.

	Crop	Tower	r^2	Slope	Intercept ($W\ m^{-2}$)	RMSE ($W\ m^{-2}$)	n
2012	Corn	NE	0.96	0.95	-0.70	12.88	12936
	Corn	SE	0.95	1.08	1.72	17.09	13750
	Corn	NW	0.97	0.97	0.72	11.34	7415
	Corn	SW	0.97	0.99	-1.46	11.00	13747
2013	Soybean	NE	0.98	1.01	0.19	8.50	12409
	Soybean	SE	0.98	0.99	-0.67	8.12	14144
	Soybean	NW	0.97	0.99	0.75	9.75	14357
	Soybean	SW	0.97	1.02	-0.50	8.17	7182
2014	Spring wheat	NE	0.96	1.02	0.64	11.13	14902
	Spring wheat	SE	0.97	1.00	-0.42	9.43	14839
	Spring wheat	NW	0.95	0.95	1.28	12.30	14966
	Spring wheat	SW	0.97	1.02	-1.53	10.09	14738
2015	Soybean	NE	0.96	0.99	0.62	12.75	11748
	Soybean	SE	0.98	0.98	-0.31	9.75	10859
	Soybean	NW	0.97	1.00	0.55	11.62	12143
	Soybean	SW	0.97	1.02	-1.07	11.63	10301

We also did a regression comparison of July, which is the peak of the growing season in Manitoba (Table 3.4). Overall, r^2 values remained high (0.87 - 0.98) at all towers and years but were lower than when the full year was compared. Furthermore, during the 2012 corn year slopes departed more (0.71 - 1.42) than other years (0.85 - 1.04), as did RMSE range which were 12.03 - 22.62 W m^{-2} in 2012 and 5.92 - 12.27 W m^{-2} from 2013-2015. In July 2012 the corn height brought it close to the CSAT3, resulting in a smaller footprint than years with shorter crops.

Table 3.4 Regression comparison of H_v at four towers versus the mean of all towers each year during the month of July at TGAS MAN. RMSE is root mean squared error.

July	Crop	Tower (y)	Mean ($W m^{-2}$)	r^2	Slope	Intercept ($W m^{-2}$)	RMSE ($W m^{-2}$)	n
2012	Corn	NE	26.95	0.87	0.71	-4.15	17.46	1102
	Corn	SE	70.84	0.94	1.42	5.88	22.62	1196
	Corn	NW	33.27	0.96	0.92	0.95	12.03	138
	Corn	SW	49.49	0.95	0.85	-2.54	12.53	1231
2013	Soybean	NE	46.60	0.98	1.02	-0.10	10.00	1271
	Soybean	SE	43.65	0.98	0.95	-0.83	8.22	1177
	Soybean	NW	30.53	0.97	1.04	2.56	11.35	1270
	Soybean	SW	50.07	0.97	0.92	-3.41	8.84	512
2014	Spring wheat	NE	14.89	0.92	0.97	0.09	12.27	1171
	Spring wheat	SE	16.16	0.96	1.01	0.76	8.42	1252
	Spring wheat	NW	9.22	0.97	1.11	5.04	8.62	1259
	Spring wheat	SW	21.37	0.94	0.91	-6.09	9.90	1200
2015	Soybean	NE	24.66	0.95	1.04	0.94	10.78	1219
	Soybean	SE	24.03	0.98	1.02	0.62	5.92	1206
	Soybean	NW	15.45	0.95	1.09	2.80	10.60	1251
	Soybean	SW	27.80	0.94	0.85	-4.33	9.68	1251

3.5 Discussion

3.5.1 Turbulent flux variability at Forage and Wheat fields in 2014

3.5.1.1. Is one tower enough? In the 2014 three-tower comparison of H and LE, we assessed whether fluxes measured at an eddy covariance tower captured the variability present on two fields, and if one tower would be sufficient to represent the field. Generally, LE r^2 values (Table 3.1) were lower than H r^2 (Table 3.2) no matter the crop type or tower position. Apart from South-Centre at Forage, H r^2 values were consistently high across both fields and tower locations while, LE r^2 had large scatter whether co-located (0.69 – 0.90) or 100 m apart (0.54 – 0.82) (Table 3.1). H RMSE was generally

consistent among fields (6 – 12 W m^{-2}) and lower than LE (mean 33.7 W m^{-2}). Hollinger and Richardson (2005) found that H had greater mean difference between paired towers than LE. Mean H values ranged from 5.56 to 25.24 W m^{-2} at Forage and 55.03 to -12.07 W m^{-2} at Wheat. Multiple towers did not capture increased variability for either H or LE, and H had less uncertainty associated with measurements. One tower would have been sufficient for measuring turbulent fluxes at both Forage and Wheat.

3.5.1.2 Sources of variability. Footprints of each tower at the 100 m separation resulted in 50% of tower's fluxes originating from a wholly unique part of the field (Figure 2.2). This increases the potential for spatial sampling differences, particularly in the short term (Lloyd et al. 1997). Our regression comparison of the towers at each field and separation demonstrated how well the eddy covariance method was able to capture the field variability of H and LE. Each field's crop variability was examined in Chapter 2.4.2 through LAI measurements done in a grid across each field. No significant differences were found among any tower's flux footprint area, but small differences in LAI could contribute to NEE differences. The same is possible for both H and LE.

The mean LAI of all tower footprints ranged from 3.08 – 3.79 at Forage and 1.72 – 2.50 at Wheat, while respective field means were 3.50 and 1.94. A difference of 0.98 in LAI was linked to changes in surface energy fluxes of up to 30 – 40 W m^{-2} within 10s of meters in northeastern Colorado, USA (Alfieri and Blanken 2012). This aligns with LE RMSE at both of our fields, however, H RMSE ranged from 6 – 12 W m^{-2}. LAI measures how much foliage there is, but at Wheat during senescence, the amount of foliage didn't change but the stomatal conductance likely decreased. During vegetation transition

periods such as this, LAI may be less reliable a measure of field variability and less representative of H and LE drivers. Measures of stomatal conductance or gridded soil moisture measurements similar to our LAI sampling could provide further insight into drivers and sources of local variability (Verstraeten et al. 2008) to identify whether it contributes to uncertainty in turbulent fluxes.

Wheat measurements occurred in August, which is the latter half of the growing season for spring wheat in southern Manitoba. During the measurement period, the senescing crop caused photosynthetic rates to decline and stop at Wheat. Surface variability most likely resulted from a wet canopy and a drying soil surface from recent rain rather than stomatal controls. Though we did not measure it, field variation for soil or crop moisture may contribute to uncertainty in the turbulent fluxes themselves, despite a visually homogeneous crop.

While regression analyses of H and LE individually suggested that spatial variation played a role in LE particularly, this was less apparent when we examined the Bowen ratio at Forage (Figure 3.8). Potential spatial variability in flux partitioning depends on the sources of LE and H, with canopy controlling this through stomatal conductance. On the Forage field, spatial variability was not great enough to affect the partitioning of energy. It is likely that the canopy was sufficiently developed to behave similarly amongst towers when averaged over our footprint, which is supported by the high mean LAI. Similar diurnal patterns amongst towers (Figure 3.8) indicate that there was generally similar energy partitioning at each tower even when separated. So a single tower was able to represent the energy partitioning at Forage, no matter where towers were located.

3.5.2 Long-term H_v variability and seasonality

Data from TGAS provided a multi-year dataset comparison for H_v. Without a water correction, the entire term originates from the sonic anemometer (CSAT3) alone. H_v retains a weak moisture signal within measurements, but the uncertainty introduced by water vapour corrections was not included.

The results from the long-term data analysis (Table 3.3) showed very little scatter amongst crops or years. The r^2 values for H_v from 2012-2015 were tighter (0.95 – 0.98) compared to the three towers in 2014 measuring H (0.8 – 0.97). Long-term regression intercepts were also all within ±2 W m^{-2} of zero at all towers and years. The remaining variability in annual regression comparisons most likely originates from instrument error with the CSAT3s; our long-term RMSE was within the 5 – 10 W m^{-2}, similar to Mauder et al. (2007).

Our long-term field measurements are below freezing and snow covered for 4-6 months of the year, which creates an anchor of numerous low H values that may improve the regression. The seasonality of H and LE are well-known, driven by changes in vegetation and the state of water. When growing season variability was examined through each year's July data (Table 3.4), differences amongst years were more apparent. While r^2 values were still relatively high (0.87 – 0.98), slope was more variable in July 2012 when corn was grown. RMSE were also twice as much in July 2012. Corn was > 2 m high in 2012 and twice as tall as either soybean or wheat. While crop height was different among years, height of the CSAT3s was constant, resulting in the tall corn crop being much closer to the instrumentation. This reduced the footprint area from which

fluxes originated, subsampling a smaller portion of the field. It may also have affected airflows.

Compared to the annual regression (Table 3.3), the differences in crop footprint and summer regressions (Table 3.4) highlight how measurement period influences the types of uncertainty present. We speculated that crop height differences amongst years could be contributing to greater variation in the 2012 corn than 2013-2015 soybean and spring wheat years. Different crop heights change the zero displacement height and thereby could affect the footprint from which H_v fluxes are generated. Flux footprint models were run for each July 2012 and July 2014 (Chen et al. 2009) with both tall and short crop heights, 2 m and 0.5 m, to examine the effect of crop height (not shown). Both heights were used each year to determine how crop height affected footprint size. In 2012 the 2-m-high crop footprint was 4, 8, and 33% smaller at the 95, 80, and 50% isoline, respectively, than the 0.5-m-crop height. Similarly, the taller crop was 13, 17, and 33% smaller at the same respective isoline in the 2014 footprint models. A corn crop would have a consistently smaller flux footprint than soybeans or spring wheat when measured from the same tower height, resulting in a smaller area contributing to H_v and a greater likelihood that variable parts of the field represent a greater fraction of the measured flux.

3.6 Conclusions

In comparing three towers located on a perennial and an annual field and four years of data with four towers over three annual crops, one tower could measure H on an agricultural field within ~10 W m^{-2} based on RMSE. However, LE regression r^2 had wide

scatter (0.54 - 0.94) across all tower separations at both fields. Diurnal patterns of the 100 m separation showed similar energy partitioning of the Bowen ratio at all 3 towers.

In our longer-term comparison, larger datasets that included frozen, snow-covered winters improved regression comparisons of H_v. When crops were compared in July, the tall corn (> 2 m tall) crop close to the instrumentation had a smaller footprint than shorter crops like soybean or spring wheat (~1 m tall), which contributed to a lower r^2 value, higher RMSE, slopes deviating more from 1, intercepts further from 0 W m^{-2}.

While uncertainty with H was centered on random instrument error of the CSAT3s used, spatially abundant soil moisture measurements to assess stomatal controls may help examine drivers of LE in both annual and perennial cropping systems and during different times of the year. Particular attention must be paid to uncertainty in the shoulder seasons, when crops are establishing or senescing, because of the potential for variability increase across a measurement field and its influence on flux measurements. Furthermore, spatial differences may be less for the Bowen ratio when examining energy partitioning as a whole rather than each flux alone.

3.7 References

Alfieri, J.G., Blanken, P.D. 2012. How representative is a point? The spatial variability of surface energy fluxes across short distances in a sand-sagebrush ecosystem. J. Arid Environ. 87: 42-49.

Amiro, B.D. 1998. Footprint climatologies for evapotranspiration in a boreal catchment. Agric. For. Meteorol. 90: 195-201.

Ben Saïda, A. 2009. Shapiro-Wilk and Shapiro-Francia normality test function. MATLAB Inc. 2012b. Available online: [https://www.mathworks.com/matlabcentral/fileexchange/13964-shapiro-wilk-and-shapiro-francia-normality-tests/content/swtest.m]

Chen, B., Black, T.A., Coops, N.C., Hilker, T., Trofymow, J.A.T., Morgenstern, K. 2009. Assessing tower flux footprint climatology and scaling between remotely sensed and eddy covariance measurements. Boundary-Layer Meteorol. 130: 137-167.

Finkelstein, P.L., Sims, P.F. 2001. Sampling error in eddy correlation flux measurements. J. Geophys. Res. 106(D4): 3503-3509.

Foken, T. 2008. The energy balance closure problem: An overview. Ecol. App. 18: 1351-1367.

Foken, T., Aubinet, M., Finnigan, J.J., Leclerc, M.Y., Mauder, M., Paw U, K.T. 2011. Results of a panel discussion about the energy balance closure correction for trace gases. Bull. Am. Meteorol. Soc. 92: 13-18.

Foken, T., Gothede, M., Mauder, M., Mahrt, L., Amiro, B.D., Munger, J.W. 2004. Post-field data quality control. In: Lee, X., Massman, W., Law, B., editors, Handbook of

micrometeorology: A guide for surface flux measurement and analysis. Kluwer, Dordrecht, the Netherlands. p. 181–208.

Friedrich, K., Mölders, N., Tetzlaff, G. 2000. On the influence of surface heterogeneity on the Bowen-ratio: a theoretical case study. Theor. Appl. Climatol. 65: 181-196.

Glenn, A.J., Amiro, B.D., Tenuta, M., Stewart, S.E., Wagner-Riddle, C. 2010. Carbon dioxide exchange in a northern Prairie cropping system over three years. Agric. For. Meteorol. 150: 908-918.

Glenn, A.J., Amiro, B.D., Tenuta, M., Wagner-Riddle, C., Drewitt,G., Warland, J. 2011. Contribution of crop residue carbon to total soil respiration at a northern Prairie site using stable isotope flux measurements. Agric. and For. Meteorol. 151: 1045-1054.

Glenn, A.J., Tenuta, M., Amiro, B.D., Maas, S.E., Wagner-Riddle, C. 2012. Nitrous oxide emissions from an annual crop rotation on poorly drained soil on the Canadian Prairies. Agric. For. Meteorol. 166-167: 41-49.

Guo, X.F., Cai, X.H., Kang, L., Zhu. T., Zhang, H.S. 2008. Effects of vegetative heterogeneity and patch-scale harvest on energy balance closure and flux measurements. Theor. Appl. Climatol. 96: 281-290.

Hollinger, D.Y., Richardson, A.D. 2005. Uncertainty in eddy covariance measurements and its application to physiological models. Tree Physiol. 25: 873-885.

Kessomkiat, W., Hendricks Franssen, H-J., Graf, A., Vereecken, H. 2013. Estimating random errors of eddy covariance data: An extended two-tower approach. Agric. For. Meteorol. 171-172: 203-219.

Kite, G.W., Droogers, P. 2000. Comparing evapotranspiration estimates from satellites, hydrological models and field data. J. Hydrol. 229: 3-18.

Krishnan, P., Meyers, T.P., Scott, R.L., Kennedy, L., Heuer, M. 2012. Energy exchange and evapotranspiration over two temperate semi-arid grasslands in North America. Agric. For. Meteorol. 153: 31-44.

Kormann, R., Meixner, F.X. 2001. An analytical footprint model for non-neutral stratification. Boundary-Layer Meteorol. 99: 207-224.

Leuning, R., van Gorsel, E., Massman, W.J., Isaac, P.R. 2012. Reflections on the surface energy imbalance problem. Agric. For. Meteorol. 156: 65-74.

Lloyd, C.R., Bessemoulin, P., Cropley, F.D., Culf, A.D., Dolman, A.J., Elbers, J., Heusinkveld, B., Moncrieff, J.B., Monteny, B., Verhoef, A. 1997. A comparison of surface fluxes at the HAPEX-Sahel fallow bush sites. J. Hydrol. 188-189: 400-425.

Maas, S.E., Glenn, A.J., Tenuta, M., Amiro, B.D. 2013. Net CO_2 and N_2O exchange during perennial forage establishment in an annual crop rotation in the Red River Valley, Manitoba. Can. J. Soil Sci. 93: 639-652.

Massman, W.J. 2000. A simple method for estimating frequency response corrections for eddy covariance systems. Agric. For. Meteorol. 104: 185-198.

Mauder, M., Desjardins, R.L., Pattey, E., Worth, D. 2010. An attempt to close the daytime surface energy balance using spatially-averaged flux measurements. Boundary-Layer Meteorol. 136: 175-191.

Mauder, M., Oncley, S.P., Vogt, R., Weidinger, T., Ribeiro, L., Bernhofer, C., Foken, T., Kohsiek, W., De Bruin, H.A.R., Liu, H. 2007. The energy balance experiment EBEX-2000. Part II: Intercomparison of eddy-covariance sensors and post-field data processing methods. Boundary-Layer Meteorol. 123: 29-54.

Melesse, A.M., Nangia, V. 2005. Estimation of spatially distributed surface energy fluxes using remotely-sensed data for agricultural fields. Hydrolog. Processes 19: 2653-2670.

Moncrieff, J.B., Monteny, B., Verhoef, A., Friborg, Th., Elbers, J., Kabat, P., de Bruin, H., Soegaard, H., Jarvis, P.G., Taupin, J.D. 1997. Spatial and temporal variations in net carbon flux during HAPEX-Sahel. J. Hydrol. 188-189: 563-588.

Moore, C.J. 1986. Frequency response corrections for eddy correlation systems. Boundary-Layer Meteorol. 37: 17-35.

Schmid, H.P. 1997. Experimental design for flux measurements: matching scales of observations and fluxes. Agric. For. Meteorol. 87: 179-200.

Tanner, C.B., Thurtell, G.W. 1969. Sensible heat flux measurements with a yaw sphere and thermometer. Boundary-Layer Meteorol. 1: 195-200.

Tenuta, M., Gao, X., Flaten, D., Amiro, B.D. 2016. Lower nitrous oxide emissions from anhydrous ammonia application prior to soil freezing in late fall than spring pre-plant application. J. Environ. Qual. 45:1133-1143.

Verstraeten, W.W., Veroustraete, F., Feyen, J. 2008. Assessment of evapotranspiration and soil moisture content across different scales of observation. Sensors 8: 70-117.

4. DIRECT WHOLE-FARM GREENHOUSE GAS FLUX MEASUREMENTS FOR A BEEF CATTLE OPERATION*

* Published as: Taylor, A.M., Amiro, B.D., Tenuta, M., Gervais, M. 2017. Direct whole-farm greenhouse gas flux measurements for a beef cattle operation. Agric. Ecosyst. Environ. 239: 65-79.

4.1 Abstract

Landscape-scale measurements of greenhouse gas exchange from whole farms can bracket the magnitude of fluxes, identify sources and sinks, and provide data for model development and validation. Greenhouse gas fluxes were measured for an annual cycle on a 123-ha beef-cattle farm in southwestern Manitoba, Canada. Carbon dioxide and methane fluxes were measured from a central eddy covariance flux tower. These measurements were supplemented by a secondary flux tower, and by static chambers that measured carbon dioxide, methane and nitrous oxide fluxes. The farm had 104 backgrounding steers and an additional 160 cow-calf pairs occupied the farm for part of the period. Cattle occupied a winter bale-grazing field, a confined feeding paddock, a summer pasture, and a cereal-crop swath-grazing field in sequence. Cattle within the flux footprint exhibited large respiration and methane fluxes, and the cattle respiration was separated from the land CO_2 exchange. The largest fluxes of nitrous oxide from cattle excreta (urine, manure) were emitted from the confined feeding paddock and from the location of the winter-feed bales, but only the confined feeding paddock had a net emission of methane from excreta. Despite challenges with cattle movements and scaling

in space and time, a greenhouse gas budget was estimated: over the annual cycle, cattle respiration dominated the budget with an emission of 20 t CO_2 equivalent ha^{-1} y^{-1}; CO_2 from the plant/soil system was a net emission of 10 t CO_2 equivalent ha^{-1} y^{-1}; enteric methane was 11 t CO_2 equivalent ha^{-1} y^{-1}; methane from soil/excreta was 0.06 t CO_2 equivalent ha^{-1} y^{-1}; and nitrous oxide from soil/excreta/fertilizer was 4 t CO_2 equivalent ha^{-1} y^{-1}. The farm was a net greenhouse gas source of 46 t CO_2 equivalent ha^{-1} y^{-1} and the plant/soil system was a contributing source in this year, partly because of respiration of imported feed.

4.2 Introduction

In Canada, agriculture contributes about 8% of anthropogenic greenhouse gas emissions (Environment Canada 2015). Methane (CH_4) from cattle production and nitrous oxide (N_2O) from cropping systems are the largest agricultural contributors. Carbon dioxide (CO_2) exchange is also important but the source/sink dynamics on any land area are complex and this is often not included in national greenhouse gas emission inventories unless there has been a change in land management. Agriculture includes a wide range of enterprises, such as dedicated cropping systems (annual, perennial), dedicated animal systems (e.g. cattle, swine, poultry), and a mixture of these. However, some of these enterprises have very specific processes for greenhouse gas exchange. For example, application of nitrogen fertilizers to crops generates N_2O, cattle emit enteric CH_4, and the plant/soil system has an annual cycle of CO_2 exchange in temperate climates.

The beef-cattle production system incorporates many diverse components of greenhouse gas dynamics. Beauchemin et al. (2010) estimated that in Canadian beef

production, 63% of emissions (as CO_2 equivalents) were from enteric methane, 28% were from manure (mostly as N_2O) and 4% were N_2O from cropping systems for feed. These were based on a whole-farm model, which helps to understand the relative components and dynamics of greenhouse gases on complex production systems (e.g., White et al. 2010; Rotz et al. 2011; Foley et al. 2011). Models have advantages to integrate and test hypotheses more easily than setting up specific field experiments. However, direct measurements at different scales help to develop parameters for models and provide data sets for validation and continued model improvement. Several studies have directly measured greenhouse gas fluxes from parts of farms. Often these have measured a single gas, such as CH_4 from individual animals (e.g., Boadi et al. 2002; Beauchemin and McGinn 2005), roaming cattle herds (McGinn et al. 2015), or from confined areas with a high cattle density (e.g., Laubach et al. 2008; McGinn et al. 2009). Similarly, whole-field N_2O emissions (e.g., Wagner-Riddle et al. 2007; Maas et al. 2013) and CO_2 exchange (e.g., Hollinger et al. 2005; Taylor et al. 2013), or all three gases (Bavin et al. 2009; Merbold et al. 2014) have been measured from feed crops.

Micrometeorological techniques, such as eddy covariance or backwards trajectory calculations, are used at scales from meters to kilometers, whereas chambers measure at the sub-meter scale. However, there are challenges using these methods to measure at the whole-farm scale. Most farms have tremendous spatial variability with operations taking place in specific parts of the landscape. Recently Felber et al. (2015) measured CH_4 fluxes from dairy cattle using eddy covariance and described many of the challenges associated with moving point sources on a farm. They further separated net ecosystem exchange of CO_2 into cattle-generated and land-controlled components (Felber et al.

2016a, b), but their system was relatively well constrained in size and animal movements, unlike many large-scale beef cattle operations. Aside from their recent study and measurements over a confined feedlot (Prajapati and Santos 2017), there have been very few attempts to integrate measurements of multiple greenhouse gas fluxes for a whole farm.

Our main objective was to measure the annual cycle of greenhouse gas fluxes (CO_2, CH_4, and N_2O) over a whole farm. Further, we selected a farm operation that raised beef cattle so that we could test our ability to incorporate animal and crop dynamics within a single operation. With this choice, we aimed to determine if the CO_2 flux for the land (soil and plants) system could potentially offset the emissions of CH_4 from cattle and N_2O from soil. As such, we measured individual components at the flux-tower scale (100s m): CO_2 flux that included cattle and land, and CH_4 flux that included enteric emissions from cattle as the main component but also included manure and soil exchange. These flux tower data were supported by chamber measurements to help identify landscape features and practices that controlled the exchange of CO_2, CH_4, and N_2O from soil including animal bedding and excreta (urine, manure).

4.3 Methods

4.3.1 Site description and experimental design

The measurements were conducted on a research farm operated by Agriculture and Agri-Food Canada (Johnson Farm) at Brandon, MB, Canada (49.87528° N, 99.90611°W, 396 m.a.s.l.) on Class 3, low water-holding capacity agricultural land (Manitoba Soils Survey 1974). It is located within the Aspen Parkland ecoregion and the

Stockton District, characterized by undulating glaciolacustrine sand and hummocky landforms with short slopes of gradients of 6-15% (Smith et al. 1998). The soil is a Black Chernozem (Udic Boroll), Marringhurst coarse sandy loam soil on coarse sand and gravelly outwash along the Assiniboine River, and is well- to excessively-drained due to the high porosity of its parent material (Ehrlich et al. 1956). Our site had little overall slope but had land undulations of the order of 2 m. Brandon, MB, has a mean annual temperature of 1.9°C and mean annual precipitation of 472 mm, of which 24% is snowfall (Environment Canada 2014).

The farm has been used for agricultural and livestock research for more than a decade (e.g., Kopp et al. 2004; Legesse et al. 2012). Our study ran from October 2012 to October 2013, encompassing an annual cycle in feed crop and beef cattle production at this location. As in many farms, management practices can be quite complex. During this timeframe, 104 yearling steers were backgrounded (a period of weight-gain after weaning prior to finishing), and in summer 2013, 160 beef cow-calf pairs were added to the farm (Table 4.1).

The feeding strategy for the steers began with winter bale grazing in the southwest pasture (access to 6.1 ha) (Figure 4.1). Approximately 329 large grass-legume hay bales were positioned in rows on the southwest bale-grazing pasture with cross-fencing to limit cattle access until the feed was needed. Deep snow in March 2013 required the steers to be confined in a corral where they were fed more bales of similar composition and had water access, until they were moved to summer southeast pasture (29.6 ha) in June. The southeast summer pasture field had 16 paddocks composed of varying mixtures of forages, and each paddock was cross-fenced and grazed twice over

90 days. Cross-fencing was moved about every 9 days. The cow-calf pairs were introduced in June 2013 to the northwest secondary pasture (10.5 ha), and calves were weaned in early August, after which the cows were moved off site. The weaned

Table 4.1 Livestock and crop management practices. The fields are identified in Figure 4.1.

Date	Field	Event	Value
April 30, 2012	NE	Pre-seed herbicide spray (Round-Up^{TM})	Recommended rate
May 10-14, 2012	NE	Barley (vs. AC Desperado) seeded with Conserva Pak seeder (19 cm row spacing, 2.5 cm depth)	150 kg ha^{-1}
May 10-14, 2012	NE	Oats (vs. Souris) seeded with Conserva Pak seeder	140 kg ha-1
May 26, 2012	NE	Liquid fertilizer applied (28-0-0)	56 kg N ha^{-1}
Jun 15-19, 2012	NE	In-crop herbicide (Refine SG & Agril)	Recommended rate
July 3, 2012	NE	Early barley paddocks swathed	10 cm height
July 5, 2012	NE	Early oats swathed	10 cm height
July 20, 2012	NE	Late barly & oats swathed	10 cm height
October 4, 2012		Steers weighed	104 yearling steers (mean B.W. 225 kg)
October 15, 2012		Main, central micrometeorological tower installation completed	8 m high
Nov 13, 2012	SW	Bales set up in field	279 bales total
Nov 16, 2012	SW	Steers moved from corral to bale-grazing	104 yearling steers
February 22, 2013	NE	First bale field feed consumed, bales added to second pasture	50 bales
Mar 21, 2013	Corral	Bale grazing snowed in, steers confined to water corral	
May 3, 2013	SW	Static-vented chambers installed in field	64 circular chambers
May 8, 2013		Pre-pasture grazing weight	104 yearling steers (mean B.W. 317 kg)
May 13-15, 2013	NE	Barley (vs. AC Desperado) seeded with John Deere 750 seed driller (19 cm row spacing, 2.5 cm depth)	150 kg ha^{-1}
May 13-15, 2013	NE	Oats (vs. Souris) seeded with John Deere 750 seed driller	140 kg ha^{-1}
May 13-15, 2013	NE	Fertilizer application, mid-row banded (46-0-0)	56 kg N ha^{-1}
May 17, 2013	NE	Static-vented chambers installed in field	21 rect. chambers
June 3, 2013		Secondary micrometeorological tower installed on east side of farm	3 m high
June 7, 2013	SE	Steers moved from water corral to pasture	104 yearling steers (mean B.W. 342 kg)
June 7, 2013	Corral	One-time sampling with static-vented chambers	33 circular chambers
June 12, 2013	NE	In-crop herbicide (Refine SG & Agril)	Recommended rate
June 26, 2013	NW	Cow-calf pairs access to water & secondary pasture	160 cow-calf pairs
July 4, 2013	NE	Early barley & early oats swathed	10 cm height
July 24, 2013	NE	Late barley & late oats swathed.	10 cm height
July 31, 2013		Calves weaned from heifers	160 calves (mean B.W. 201 kg)
Aug 12, 2013	NE	Chambers removed from the field	
Aug 13, 2013	NE	Weaned calves moved to swath grazing	10 calves/paddock (mean B.W. 194 kg)
Aug 19, 2013	NW	Heifers removed from the site	160 heifers
Aug 26, 2013	SW	Chambers removed from the pasture	
Sept 9, 2013	SE	All steers moved off site	104 yearling steers (mean B.W. 409 kg)
October 10, 2013	NE	Calves moved off site	160 calves (mean B.W. 209 kg)

calves swath-grazed the northeast field (28.8 ha), which had 16 alternating paddocks of oats and barley with movable cross fencing to ensure that swaths were consumed efficiently. The oats and barley had 56 kg N ha^{-1} applied in a mid-row band during planting with a herbicide treatment about one month later. No fields were irrigated during the period of measurement. Winter bale-grazing steers and the cow-calf pairs had access to the central water corral, while other paddocks had water supplied in field.

Soil characteristics were not significantly different among the fields. In the top 15 cm, the pH (1:2 water) was 7.0, the electrical conductivity was 0.16 mS cm^{-1}, total organic carbon was 17 g kg^{-1}, nitrate was 16 mg N kg^{-1}, phosphate 20 mg P kg^{-1}, potassium was 200 mg K kg^{-1}, and sulphate was 6 mg S kg^{-1} dry soil, based on June to August sampling in 2013.

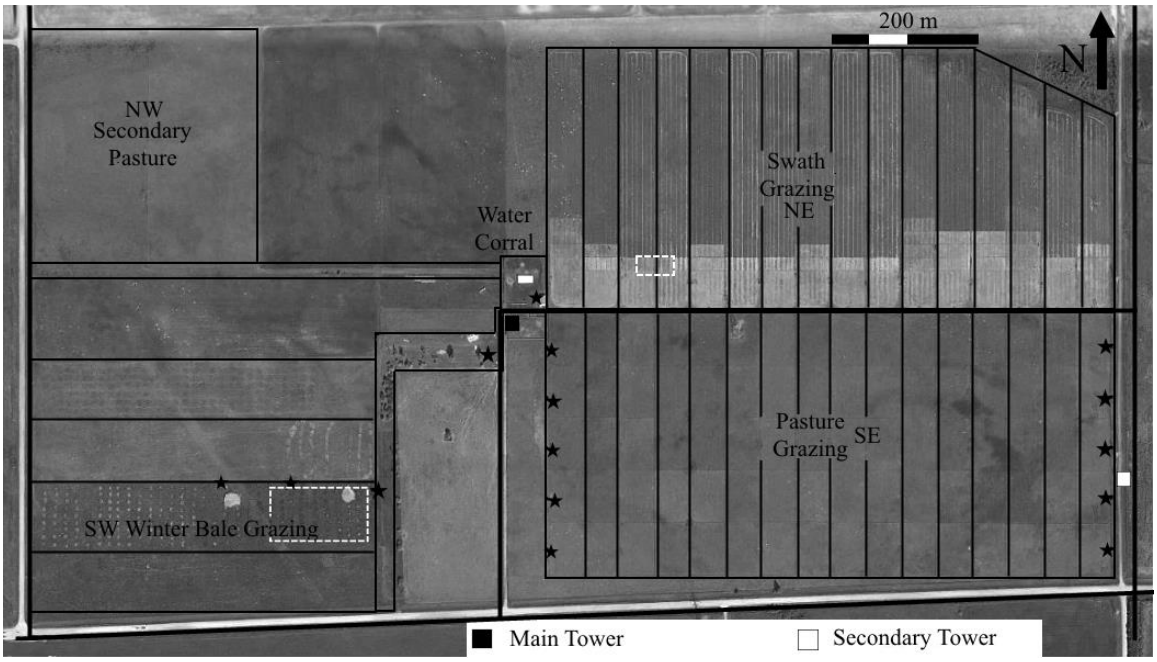

Figure 4.1 Location of operations and instruments. Stars are the locations of four trail cameras moved on farm to track cattle position. White broken lines are static-gas chamber measurement locations. Image from September 14, 2013 (Google, Digital Globe 2016).

4.3.2 Greenhouse gas flux and supporting measurements

The varied nature and scale of farm operations posed some challenges to measure all three greenhouse gases. Our strategy involved a mixture of eddy covariance flux towers and static chamber measurements to understand the relative magnitudes of sources and sinks from different parts of the farm.

4.3.2.1 Micrometeorological measurements. A central main flux tower was installed on October 25, 2012 to measure CO_2 and CH_4 fluxes using eddy covariance. The instrumentation was mounted on a mast attached to scaffolding 8 m above the soil surface, extending 65 cm from the mast. Two 3D sonic anemometer-temperature sensors (CSAT3, Campbell Scientific Inc., Logan, UT, USA) were oriented to the west. A closed-path infrared gas analyzer (IRGA LI-7000 CO_2/H_2O Analyzer, LI-COR Biosciences, Lincoln, NE, USA) protected within a temperature-control housing (University of British Columbia, Biometeorology Group) sampled CO_2 and H_2O. Its gas-sampling intake was 30 cm from the midpoint of the CSAT transducers and was drawn down 3 m of Bev-A-Line IV 3.18 mm I.D. tubing (Cole-Parmer, Vernon Hills, IL, USA) at a flow rate of 8 to 10 L min^{-1} by a diaphragm pump (Model UN815KNDC; KNF Neuberger Inc., Trenton, NJ, USA) located beside the analyzer atop the scaffold. Measurements from the LI-7000 were calibrated automatically every day against a zero-CO_2 and a secondary standard gas calibrated by the Meteorological Services of Canada (Downsview, ON, Canada). A closed-path RMT-200 Fast Methane Analyzer (Los Gatos Research Inc., Mountain View, CA, USA) measured CH_4 concentration. Its intake was located 30 cm from the midpoint of the second CSAT3 transducers, and was drawn down

13 m of 6 mm I.D. tubing by an XDS 35i dry vacuum scroll pump at a nominal flow rate of 28 L min^{-1} (Edwards, Crawley, West Sussex, UK) and through an in-line filter inside the analyzer, located in a temperature-controlled shed below the tower. The diode laser beam cavity pressure was maintained at 18.998 kPa, with the in-line filter changed every 2-3 weeks. Mirrors were cleaned as needed to maintain mirror ring-down. The methane analyzer was calibrated against a zero and known methane concentration of 10.2 μmol mol^{-1} prior to placement in the field. Grid power generation was used for all main tower instrumentation.

A secondary 3-m-high tower was installed on the east side of the farm June 3, 2013 to subsample fluxes from the summer pasture and swath-grazing fields. An open-path infrared gas analyzer (IRGA LI-7500 CO_2/H_2O Analyzer, LI-COR Biosciences) was mounted vertically alongside a CSAT3. An open-path CH_4 analyzer (LI-7700 CH_4 Analyzer, LI-COR Biosciences) was mounted in parallel to the LI-7500 and CSAT3, and was tilted slightly to prevent precipitation from pooling on the mirrors. The washer spray was not used on the LI-7700, because pollen and dust accumulated in the spray liquid on the lower mirror and degraded the signal during testing. The mirrors were cleaned with Kimwipes (Kimberly-Clark Professional, Roswell, GA, USA) and washer fluid daily to biweekly to maintain signal strength. The LI-7700 was calibrated against a known CH_4 standard and a zero prior to installation. A period of flux intercomparison between the Li7700 and RMT-200 analyzers at the main tower gave a slope of 0.96 with negligible offset indicating good agreement (r^2 = 0.85, n=840). The secondary tower was powered by batteries charged by solar panels (Kyocera Solar, Inc., Scottsdale, AZ, USA). High-frequency concentrations and velocities at both towers were recorded at 10 Hz on data

loggers (CR3000 and CR1000, Campbell Scientific Inc.) and were saved to flash memory by an NL 115 card reader (Campbell Scientific Inc.).

Supporting instrumentation at the main tower included air temperature and humidity (HMP45C probe, Vaisala Inc., Woburn, MA, USA, inside Model 41003-5 10-Plate Gill Solar Radiation Shielding, R.M. Young Company, Traverse City, MI, USA), and rainfall (TE525M, Texas Electronics Inc., Dallas, TX, USA) at 1.2 m above the soil surface. Soil temperature was measured at 5-, 10-, and 20-cm depths by chromel-constantan thermocouples installed in a wooden dowel. Vertically installed soil water content reflectometers (CS616, Campbell Scientific Inc.) measured soil moisture from 0-30 cm, and soil heat flux plates (HFT3 REBS Soil Heat Flux Plate, Radiation and Energy Balance Systems Inc., Bellevue, WA, USA) were installed 1 cm beneath the surface. Incoming and outgoing photosynthetically active radiation sensors (LI-190 Quantum Sensor, LI-COR Biosciences) extended from the scaffold 5 m above the surface, as did a net radiometer (CNR1, Kipp & Zonen, Delft, The Netherlands).

Eddy covariance flux data were processed using MATLAB (Mathworks Inc. Natick, MA, USA). High-frequency data were split into 30-minute files, which were despiked and delays adjusted to maximize the flux. No detrending was applied and half-hourly block-averaged cross products were generated with coordinate rotation (Tanner and Thurtell 1969). A storage term was included for flux data from the main tower by calculating the change in concentration over a 30-min period at the tower top and assuming this change applied to the full profile below the sampling height. A storage term was not included for the short secondary tower. Open-path sensors were corrected for density for both heat and water vapour (closed-path for water vapour only) (Webb et

al. 1980); a heating correction was applied to the LI-7500 flux (Burba et al. 2008 Method 4); and a spectroscopic correction was applied to the LI-7700 flux data. The closed-path analyzer fluxes were corrected for high-frequency losses using transfer functions based on model spectra (Moore 1986, Moncrieff et al. 1997, Massman 2000), which typically increased the flux by 30%.

Known shut-downs and calibration times were removed but site visits were not excluded because ranchers, research assistants, and students were on farm daily. All CSAT3 data were excluded when warnings >2000 or when vertical wind velocity > ± 0.5 m s^{-1}. LI-7000 data were excluded when IRGA pressure was > 95 kPa and < 50 kPa, and when [CO_2] variance > 200 μmol mol^{-1} and average [CO_2] < 250 μmol mol^{-1}. LI-7500 data were excluded when the automatic gain control was > 59 based on a histogram of measured values. RMT-200 data were removed when [CH_4] variance > 0.15 (μmol mol^{-1})^2, based on a histogram of measured values, which can indicate if the analyzer restarted. LI-7700 data were excluded when [CH_4] variance was > 0.015 (mmol m^{-3})^2, based on a histogram of values, when the analyzer's received signal strength indicator was < 2%, and when relative humidity was > 88%. A friction velocity (u*) threshold was applied to both towers (0.2 m s^{-1} for main, 0.15 m s^{-1} for secondary), as determined by binning nighttime CO_2 flux into ten equivalent u* bins, with the threshold identified as 80% of the CO_2 flux averaged over the last three bins. After quality control for instrument issues and conditions below the u* threshold, the portion of data retained was 66% and 52% for the main tower CO_2 and CH_4 fluxes, and 62% and 65% for the secondary tower CO_2 and CH_4 fluxes, respectively. This is similar to data capture in most long-term flux studies (Moffat et al. 2007).

Data gaps in CO_2 flux were filled by two methods. Short gaps of less than 2 hours were filled by linear interpolation. Longer gaps in the CO_2 flux were filled using the Fluxnet Canada Research Network model as described by Barr et al. (2004). Briefly, respiration was calculated based on night-time fluxes and corrected for temperature dependency (5-cm soil temperature) using a regression. Gross photosynthesis was calculated using a logistic regression with photosynthetically active radiation during daytime when temperatures were above freezing. The regressions were based on a 100-point moving window, with respiration and gross photosynthesis combining to give net CO_2 flux. We recognized that the presence of cattle could have a very different CO_2 flux than the landscape without cattle. Hence, the longer gaps were filled separately for conditions with and without cattle, based on the exclusion criteria in Section 4.3.3. The gaps were not filled for CH_4 flux, so daily averages are based on the available measurements.

4.3.2.2 Chamber measurements. We positioned chambers to test specific hypotheses related to microsite variation on the landscape. In addition, we used chambers to measure N_2O fluxes because we did not have eddy covariance flux measurements of N_2O at the broader scale. We assumed that most of the N_2O flux would be contributed following nitrogen fertilization of the swath-grazing field or by urine and manure hotspots from cattle deposits. Static-vented chambers (Tenuta et al. 2010) were used on the bale-grazing and swath-grazing fields to measure CO_2, CH_4, and N_2O. The circular chambers used at the post-winter bale grazing site were made of PVC pipe and had an inner diameter of 20 cm. A rubber inner tube gasket was installed on the top of the collars and sides of the lids.

Chambers ranged in height from 10 to 30 cm depending on where they were installed on the field; collars on top of feed needed to be longer to extend through the waste feed and be able to reach the soil surface to create a proper soil-surface seal and minimize lateral diffusion (Hutchinson and Livingston 2001). Collars had a beveled edge to aid installation.

Sixty-four collars were installed at the bale-grazing field on April 29, 2013 (Figure 4.2). Collars were adjusted throughout the spring as the ground thawed and insertion depth ranged from 2 to 10 cm depending on if there were waste feed or feces to cut through. Chamber lids were only used during sampling, had vents to reduce chamber effects on measurements (Hutchinson and Mosier 1981; Hutchinson and Livingston 2001), and were foiled or painted white to increase reflectivity and minimize sunlight impacts on chamber temperature while sampling. Twenty-eight rectangular chambers were installed at the swath-grazing field across row after seeding, with two groups of seven on each of oats and barley (Figure 4.3). They were installed at least 2 m from cross-fencing, 1 m apart to minimize crop trampling, and 2-4 cm into the soil. The number of chambers used aimed to represent the spatial variability of each feeding strategy due to the point source nature of chamber fluxes. Chambers were positioned along the slope gradient to minimize the effect of water pooling during spring runoff. The collars were left in field throughout the sampling periods to reduce insertion disturbance that can create spikes in N_2O fluxes in the initial 24 hours after installation (Muñoz et al. 2011).

Gas sampling was done three times a week in the spring, and two times a week throughout the summer until August 26, 2013 at the bale-grazing field and August 12,

2013 at the swath-grazing field. Gas samples were taken by a 20 mL syringe and needle through a rubber septum in the lid, with the first drawn immediately after the lid was secured on the collar with rubber bands to provide a time zero sample (Rochette and Eriksen-Hamel 2008), and subsequent samples were taken at 20-, 40-, and 60-minute intervals. Exetainer 12 mL glass vials with plastic lids and rubber septa (Labco, UK) sealed with silicone were evacuated and flushed three times with helium prior to being used to store samples until they could be analyzed by gas chromatography (Rochette and Bertrand 2003). At the time of sampling, chamber headspace and air temperature were recorded and a WET sensor (WET-2-K1, Hoskin Scientific Ltd., Burnaby, BC, Canada) provided volumetric moisture content and soil temperature at a 5-cm depth at each collar. Samples were stored on site until they could be transported to the lab for gas analyses following the method of Gao et al. (2015).

Data were processed in R using the HMR statistical package (Pedersen et al. 2010; Pedersen 2012) to estimate the trace gas flux from each chamber sample. While the choice of flux-calculation model can create differences of 20% or greater if fluxes are highly variable (Levy et al. 2011), the model applied (linear, nonlinear) was chosen on a case-by-case basis, per gas, per chamber, per measurement period. Risk of leakage early in the season when the ground was still frozen was minimized using the non-linear flux calculation (Pedersen et al. 2010). For the combined number of chambers at all locations, the application of the HMR package resulted in 23%, 70%, and 53% of N_2O, CO_2, and CH_4 fluxes estimated using a non-linear model, with the remainder estimated using a linear model. The model was not forced to zero, relying on measured values instead. Bale-grazing data were also analyzed by location.

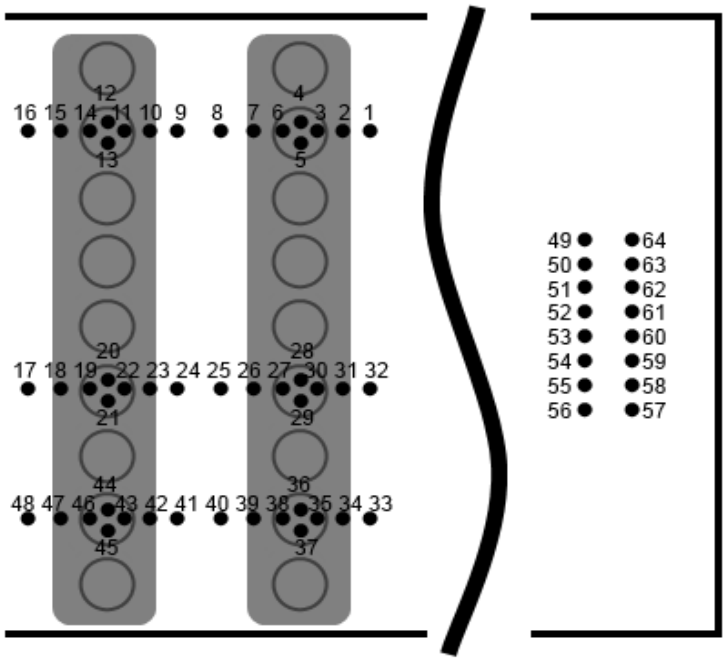

Figure 4.2 Circular collar placement for chamber gas sampling on the post-winter bale grazing pasture. Collars were placed across the bale (grey circles) and the spread of waste feed (grey areas). Collars 49 through 64 followed the slope of the land to provide gas samples of the same pasture where cattle had access, but that were separate from the bale locations.

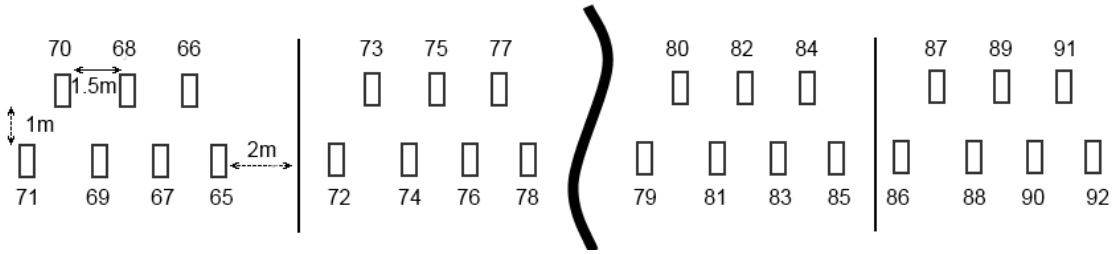

Figure 4.3 Rectangular collar placement for chamber gas sampling pre-swath grazing. Collars groups were located at least 20 m from the farm gate, with two groups of seven collars on each barley and oat swath rotations.

4.3.3 Spatial and temporal considerations

The spatial footprint of the eddy flux measurements was derived using the model of Kormann and Meixner (2001) as parameterized by Chen et al. (2009). The model uses

an analytical solution of the 2D Eulerian advection-diffusion equation with the generated footprint dependent on sensor height, surface roughness length, wind speed and direction, and atmospheric stability. Input data for the model were above-canopy air temperature, sensible heat, latent heat flux, humidity, u*, wind speed, wind direction, standard deviation of the transverse wind speed, and air pressure. Air pressure was set at 98 kPa, otherwise variables were measured or derived from experiment measurements. A domain size of 500 x 500 m with pixel size = 1 m, canopy height = 0.25 m, sensor height = 9 m and 3 m respectively for each tower, and a u* threshold of 0.2 m s^{-1} were used for parameter initialization. Surface roughness length was calculated for each half hour based on measured data where possible.

Cattle moved across the landscape and their presence or absence affected the eddy flux measurement of both CO_2 and CH_4. We used trail cameras to help track the location of cattle, which typically moved as a group to water and feed. Global positioning system collars were not practical for our steers because they were rarely handled, unlike dairy cattle (e.g., Felber et al. 2015). Four trail cameras (Moultrie Game Spy D55-IRXT Infrared Flash Camera, EBSCO Industries, Birmingham AL, USA) were placed at key locations where cattle passed by and were moved as needed to track cattle (Figure 4.1). Cameras originally faced the watering pen, the path to water, the gate at the bale-grazing field, and close to the active bale row in field from mid-November through the spring. In the spring, one camera remained at the water corral, and two followed the active paddocks on the southeast field as the cattle moved through a pasture grazing trial. The cameras were programmed motion sensors and took a photo every half-hour if there was movement, with infrared sensors to detect movement at night. They were able to detect

cattle within 5-10 m in front of the camera's sensor depending on light levels. Photographs were organized and catalogued according to date, time taken, and if there were cattle, people, vehicles present, or if the photo was obscured. This served as a logical index to identify cattle location.

Exclusions were applied to the main tower eddy flux data in the following order to separate cattle respiration contributions from the landscape CO_2 flux. We identified a wind sector where cattle were excluded and calculated a mean CH_4 flux of 0.002 (±0.05 S.D.) μmol m^{-2} s^{-1}. We then used the 1 S.D. value (0.05 μmol m^{-2} s^{-1}) as the threshold below which cattle would not be in the footprint. This is similar to the background agricultural levels (0.032 μmol m^{-2} s^{-1}) measured near a feedlot in Kansas (Prajapati and Santos 2017). Methane fluxes greater than this identified a cattle presence, indicating that the CO_2 flux would include cattle respiration. Cattle presence from trail camera photos was used when the CH_4 analyzer was not running. However, for cases when the CH_4 analyzer was not operating and the trail cameras could have missed cattle presence, we used the maximum summer CO_2 flux = 8.75 μmol m^{-2} s^{-1} as a cattle indicator calculated from a sector with no cattle.

We integrated the main tower eddy covariance and chamber data to estimate the mean CO_2-equivalency for the entire farm. A single day (June 7 when cattle were excluded) of water corral chamber (16 chambers) sampling provided an estimate of the contributions of cattle confinement to soil/excreta N_2O, CO_2, and CH_4 fluxes. Mean chamber fluxes were assigned to the quadrant where measurement occurred, and scaled based on the farm area they represented: 24.9% for each quadrant and 0.5% for the water corral. Main-tower CO_2 flux was separated into cattle respiration and plant/soil based

flux on the data exclusions above. This and the main tower CH_4 flux represented emissions from the whole farm; mobile tower data were not included because of the small footprint and limited sampling period. Lastly, all values were converted to CO_2-equivalency, with global warming potential conversion values of 28 and 265 for CH_4 and N_2O respectively on a mass basis over 100 years that excludes carbon feedbacks (Myhre et al. 2013).

4.4 Results

An average temperature of 1.8 °C and a total precipitation of 512 mm (370 mm as rain) occurred during our 348-day observation period (Figure 4.4). Freezing temperatures were present from November through April. Note the large day-to-day variability in winter temperatures and the short period in June with a substantial amount of rain. A large snowfall in mid-March decreased access to provide feed to cattle in the southwest bale-grazing field, after which the animals were confined in the water corral (Figure 4.1).

4.4.1 Flux tower measurements

Daily average CO_2 flux at the main tower showed consistent net upward (respiration, positive) fluxes for the full period with the exception of a few periods in summer with net downward flux (Figure 4.5). The secondary tower was only operated in the summer and shows net downward flux through most of July and August. The methane flux shows periods of very large emissions corresponding to cattle in the measurement footprint with some correspondence between large respiration and methane fluxes. Plots of the high-frequency concentration signal clearly show coherence between

CO_2 and CH_4 concentrations corresponding to a signal from the cattle (Figure 4.6). In this figure, winter data are shown to minimize concentration fluctuations caused by a land sink or source of either gas.

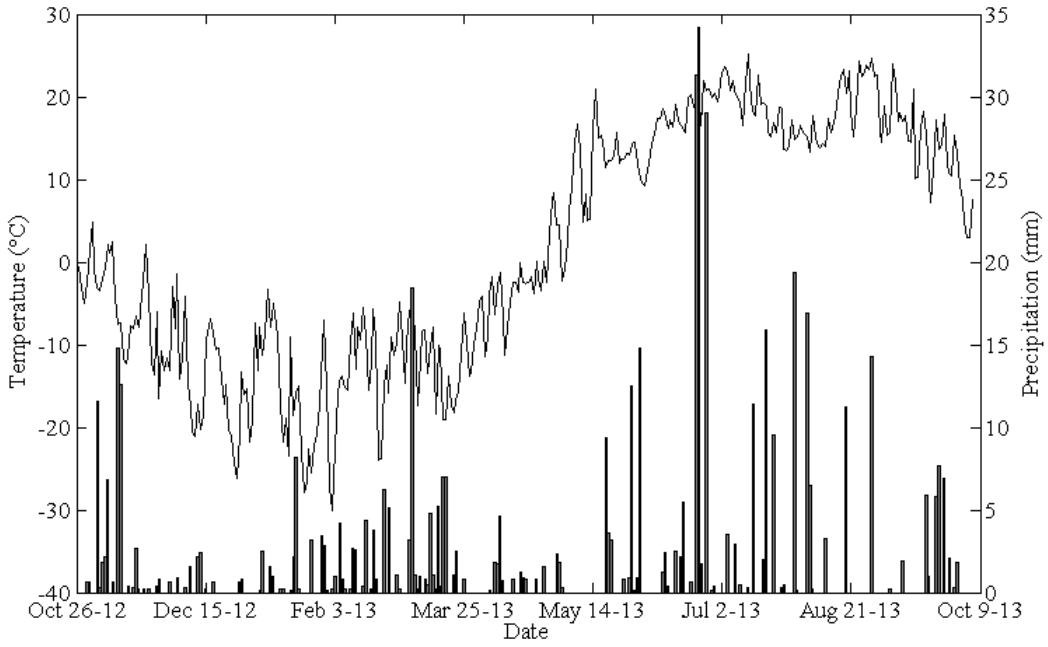

Figure 4.4 Mean daily air temperature and daily precipitation. Rainfall was measured on site and snowfall was measured at the nearby Brandon weather station (Environment Canada 2016).

The integrated flux footprint for the measurement period indicates a reasonable coverage of all wind directions at the main tower (Figure 4.7). However, only the closer parts of the NE swath-grazing field and the SE summer-pasture field were sampled. Further, very little of the SW winter bale-grazing field or NW secondary pasture were sampled. The cattle spent a substantial portion of their time within the closer parts of the footprint because of water access, such that the fluxes shown in Figure 4.5 often included cattle. The secondary tower in the southeast corner of the study area was located

preferentially to capture the summer grazing area, and the footprint indicates this was achieved (Figure 4.7). Note that winds originating from the east outside of the study area

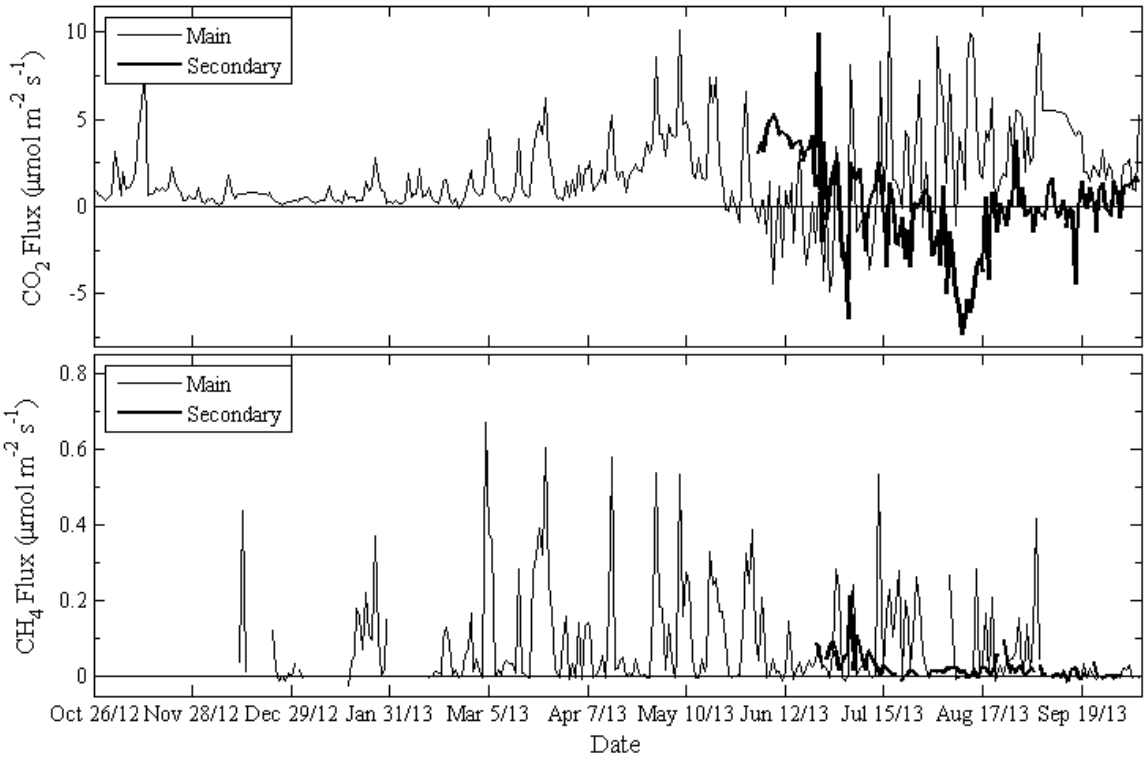

Figure 4.5 Daily averaged CO_2 and CH_4 fluxes at the main and secondary flux towers. Secondary tower fluxes only represent values originating on-farm. Positive values are losses to the atmosphere while negative are uptake by the ecosystem.

were excluded from the secondary tower. Given this footprint climatology, we calculated monthly fluxes as a function of four wind quadrants for the main tower. Methane fluxes clearly show that the cattle were preferentially located in the northeast quadrant from the main tower (Figure 4.8) corresponding to the location of the water corral (Figure 4.1). Cattle presence drove the high respiration fluxes in the NE quadrant (Figure 4.8). The SE and NW quadrants had sufficient pasture growth to overcome cattle respiration and have

net carbon uptake in June and July. This productivity was partly driven by a large June precipitation event (Figure 4.4). In spring to summer, cattle occupied the SE summer-pasture field and cow-calf pairs grazed the NW quadrant; methane fluxes show their location, although movement to water still results in dominant methane fluxes from the NE quadrant.

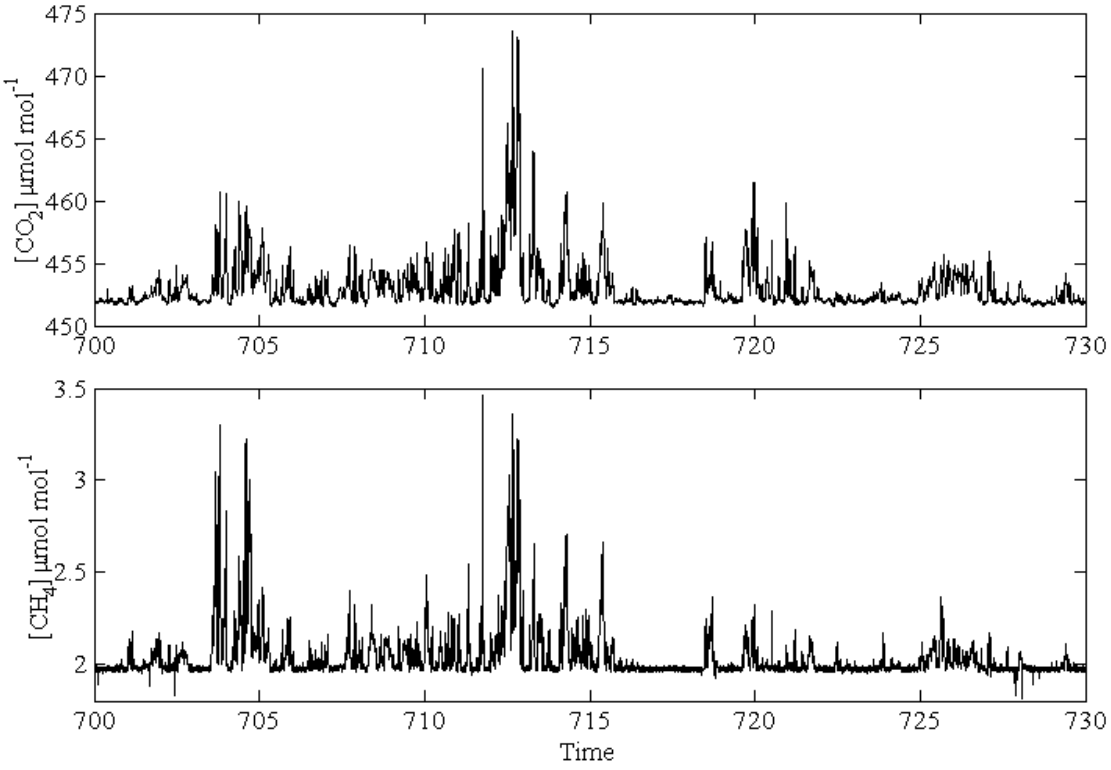

Figure 4.6 High-frequency concentrations of CO_2 and CH_4 on March 24, 2013 (DOY 83) at 07:00 – 07:30, mean air temp = -8.7°C. Data were cross-correlated to adjust for signal lag.

The methane flux indicated cattle presence, so we devolved the CO_2 flux to remove periods when cattle respiration dominated the plant/soil CO_2 exchange (Figure 4.9). The land CO_2 flux signal without cattle had a pattern that is more familiar for temperate ecosystems with a carbon sink from late May to late July, and respiration

dominating for the rest of the year. The measurement signal of the combination of cattle respiration and land CO_2 exchange was variable because of the sampling of animals moving throughout the footprint, which in turn, changed with meteorological conditions. There appears to be a seasonal bias in our ability to capture cattle respiration in Figure 4.9; during summer (May through August), cattle respiration is moderated by soil and vegetation respiration fluxes, whereas cattle were missing from part of the footprint in December and January so low respiration fluxes were measured.

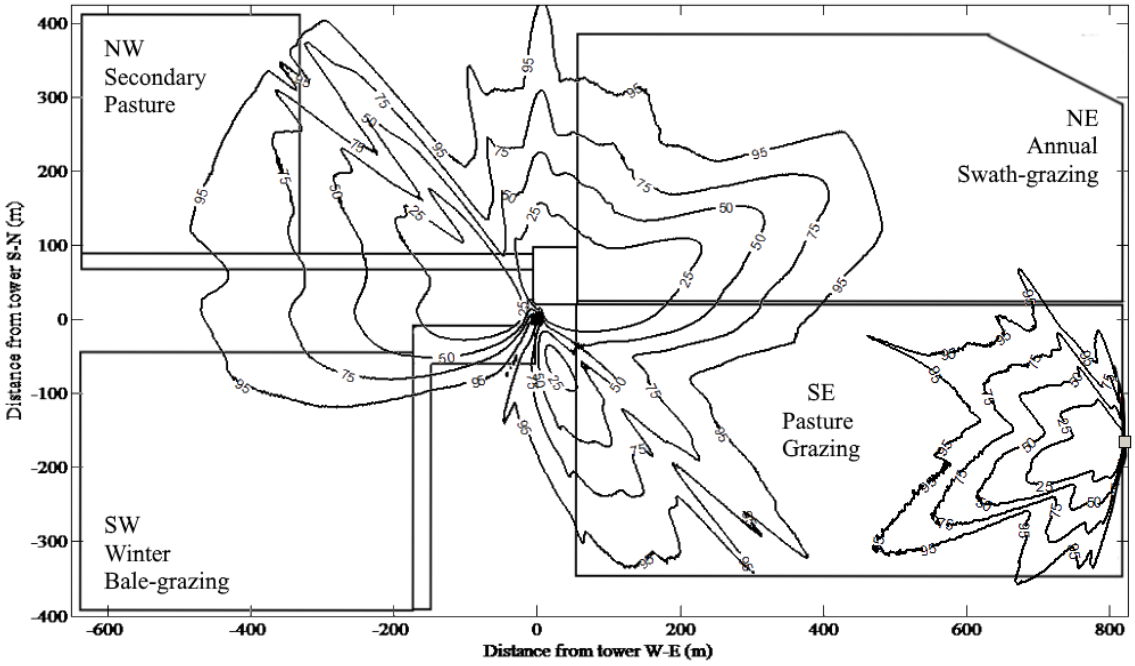

Figure 4.7 Main and secondary tower flux footprints for the duration of each tower's installment. Lines are scale field boundaries. Fluxes originating off farm were excluded from the secondary tower's footprint calculation. Isolines represent the area from which the percent of each tower's fluxes originate from. The dark box is the main tower, while the grey box is the secondary tower.

The measurement of both CO_2 and CH_4 flux at the same location provided an opportunity to observe the ratio of CH_4 to animal respiration flux, similar to the concentration ratio measured by Bai et al. (2016). For the case where both CH_4 and CO_2

originate from cattle oral sources, this ratio could inform about the timing of enteric CH_4 emissions related to animal metabolism. We selected data using the criteria that there

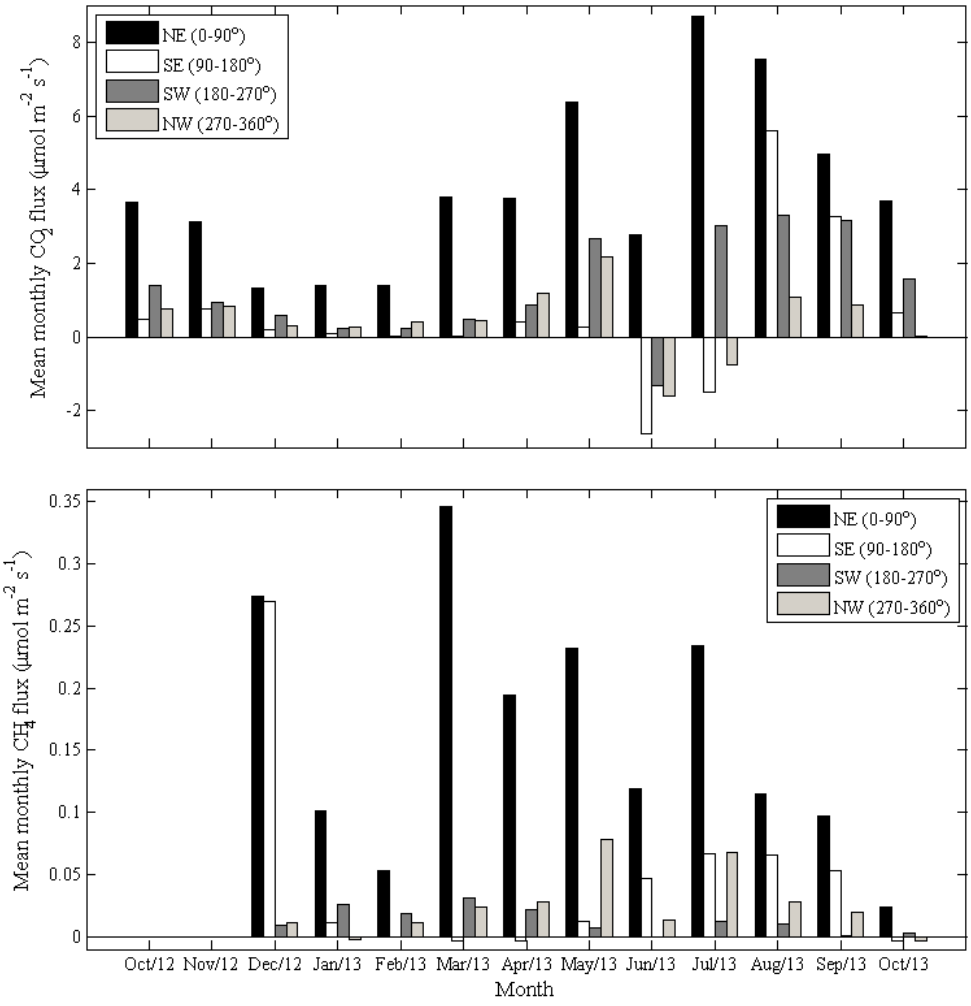

Figure 4.8 Mean monthly fluxes at the main tower by farm quadrant. For CH_4 flux, December 2012 and October 2013 are incomplete months, with 19 and 9 days respectively, whereas October 2012 and 2013 are incomplete months for CO_2 flux, having 7 and 9 days respectively. Positive values are emissions to the atmosphere, while negative are uptake into the ecosystem.

should be sufficient CH_4 flux to ensure cattle were in the footprint (>0.05 µmol CH_4 m^{-2} s^{-1}) and that CO_2 flux was dominated by animal respiration (> 8.75 µmol CO_2 m^{-2} s^{-1}). Further, we used only measured periods, without gap-fill. For conditions with frozen

temperatures, the CO_2 flux is entirely respiration; for warmer temperatures, we only used night-time CO_2 flux to eliminate photosynthesis. Figure 4.10a shows the time trend of the ratio based on 30-min measurements. The ratios varied by about a factor of two on any given day, and the diurnal trend in Figure 4.10b shows that the ratio was often smaller at night. The summer ratios tended to be lower than winter, even accounting for the summer measurements being night-time only. The measurements included two populations of animals: steers measured by both the main and secondary tower, and cow-calf pairs measured at the main tower. During summer, the ratios for the steers and cow-calf pairs were similar, although there were two high points in each population of data.

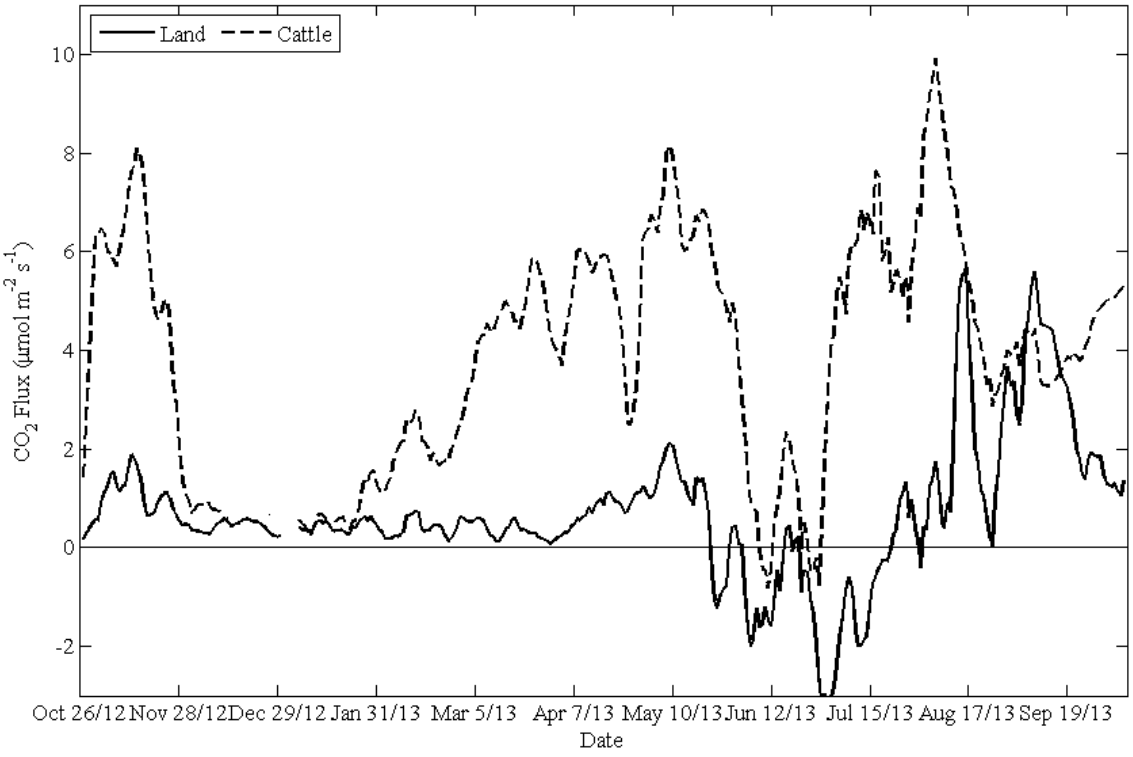

Figure 4.9 Mean daily gap-filled CO_2 flux from the main tower with (Cattle) and without (Land) cattle respiration contributions. Positive values are upward fluxes. Values were smoothed with a 5-point moving average.

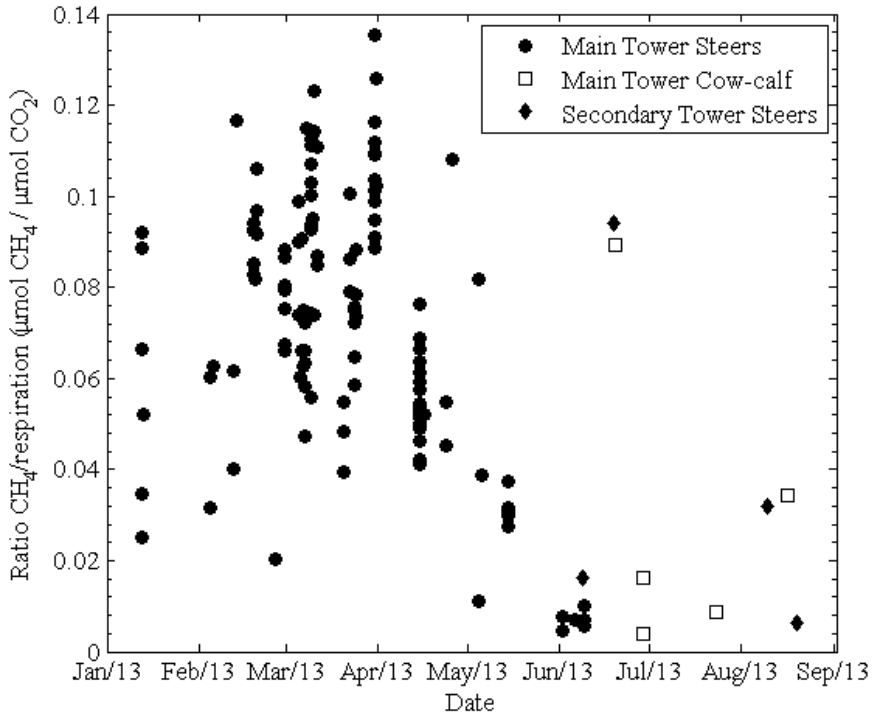

Figure 4.10a Methane to respiration flux ratio when cattle were in the flux tower footprint. Values are the ratio of 30-min fluxes.

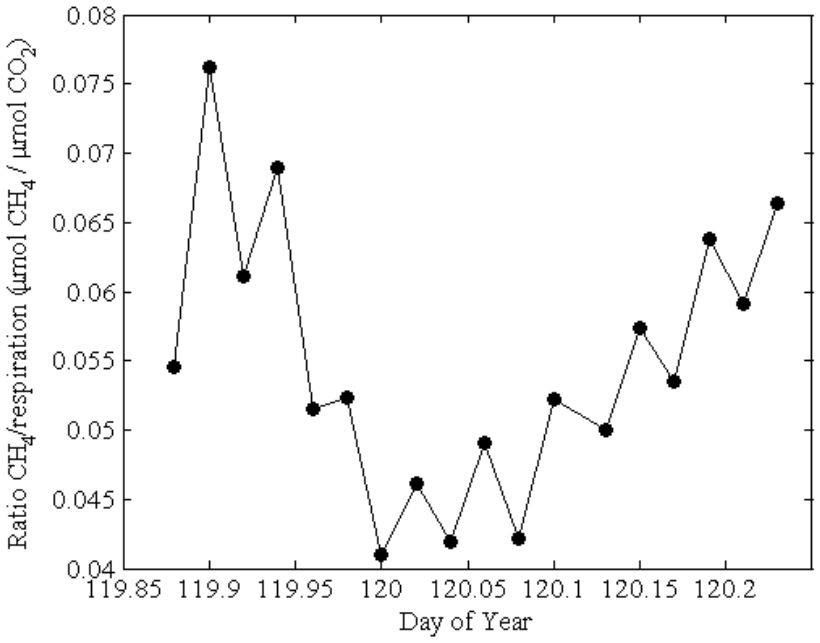

Figure 4.10b Methane to respiration flux ratio for overnight April 29-30, 2013 at the main tower. Values are the ratio of 30-min fluxes.

4.4.2 Chamber measurements

The NE swath-grazing field had nitrogen fertilizer application on May 14 and we captured the post-fertilizer N_2O flux that began shortly following fertilization until the beginning of July (Figure 4.11). This event preceded the highest soil respiration flux that increased as the soil warmed (Figure 4.11). Similarly, the strength of the soil CH_4 sink tended to be greatest from mid-June to mid-July in this field. Soil nitrogen analyses showed ammonium concentrations at their highest level on May 16 just after fertilizer application, with the highest nitrate levels during the July sampling (Table 4.2). Soil temperature ranged from 15 to 27 ºC during the measurements.

At the winter bale-grazing field, the N_2O flux was clearly greatest at sampling locations where hay bales had been located (Figure 4.12). Fluxes between the bales and in a control area without bales were relatively small. The on-bale flux event started in the middle of May when near-surface (5-cm depth) soil temperatures were above 10 °C and continued until late July. Ammonium and nitrate concentrations were much higher at the bale locations than in other parts of the field (Table 4.2). Further, there was a progression of high ammonium concentrations early in the season and then declining into July, whereas the nitrate concentration was relatively constant from late May into July. Respiration fluxes tended to be similar among locations, although the bale location had a slightly greater flux in the later part of the summer. The bale locations tended to be a weaker CH_4 sink compared to the other locations (Figure 4.12).

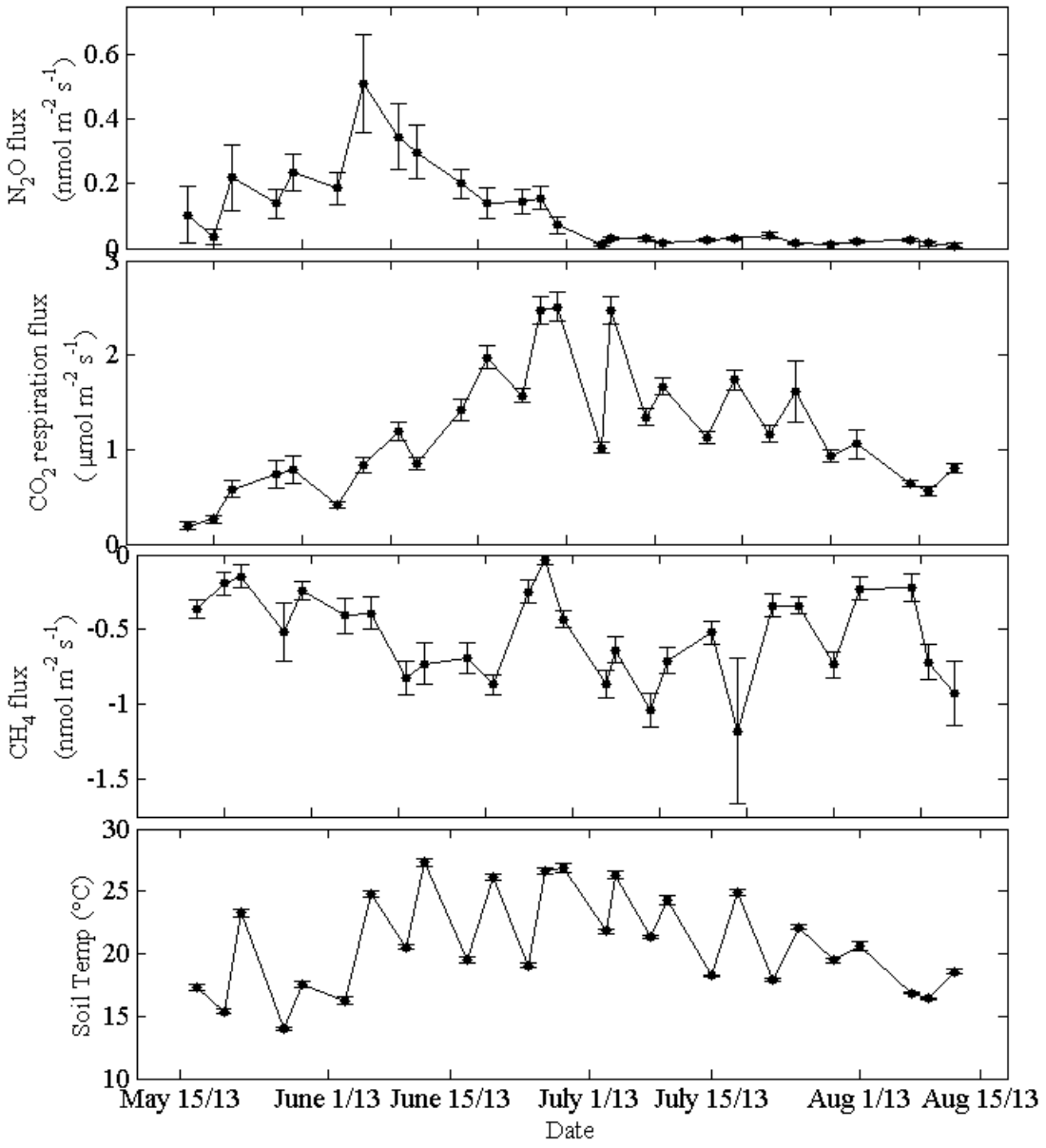

Figure 4.11 Chamber N_2O, CO_2, CH_4 fluxes, and soil temperature pre-swath grazing on the NE field, from May 17, 2013 through August 12, 2013. Each point is a mean of 28 chambers. Error bars are ±1 SE. Seeding and mid-row banded fertilizer were done on May 15, 2013. Barley and oats were swathed early (July 4, 2013) and late (July 24, 2013) depending on paddock, after which chambers were reinstalled until calves were introduced.

Table 4.2 Soil nitrogen at Bale-grazing and Swath-grazing fields in 2013 (means ± S.E.).

Location	NO_{2-} + NO_{3-}-N Bale (mg kg^{-1} oven dry soil)			NH_{4+}-N Bale (mg kg^{-1} oven dry soil)		
(0-15 cm Depth)	May 9	May 30	Jul 16	May 9	May 30	Jul 16*
Bale	9 ±2.8a	24 ±12a	20 ±10a	81 ±44a	54 ±38a	4.2 ±8.8
Between	14 ±4.9ab	5.9 ±3.7b	6.9 ±1.8b	12 ±14b	7.8 ±6.7b	1.6 ±3.4
No Bale	11 ±5.1b	7.5 ±11b	6.4 ±1.7b	9.5 ±8.6b	6.2 ±3.1b	0.6 ± 0.3
	NO_{2-} + NO_{3-}-N Swath (mg kg^{-1} oven dry soil)			NH_{4+}-N Swath (mg kg^{-1} oven dry soil)		
Depth (cm)	May 16	Jun 20	Jul 12	May 16	Jun 20	Jul 12
0 - 15	11 ±3.5	23 ±20	3.8 ±2.3	54 ±86	10 ±11	2.3 ±1.8

Letters represent differences between location, not date.

* No significant differences between locations.

4.4.3 Estimates of whole-farm greenhouse gas exchange

The measurements of individual greenhouse gas components from different parts of the farm were combined to arrive at a whole-farm estimate. We did this by integrating the flux tower measurements for three sources: 1) CO_2 from cattle respiration (defined as the gap-filled CO_2 respiration flux when cattle were in the footprint minus the land-only component of respiration), 2) enteric CH_4 emissions from cattle, and 3) CO_2 from the plant/soil land base. We then complemented these with chamber measurements of CH_4 and N_2O from animal excreta, nitrogen fertilizer application, and "general soil". This last general soil category represents a measurement that was not specifically identified with enhanced nitrogen deposition from synthetic fertilizer or animals. Note that soil respiration measured by our chambers is already captured in the CO_2 flux-tower measurement.

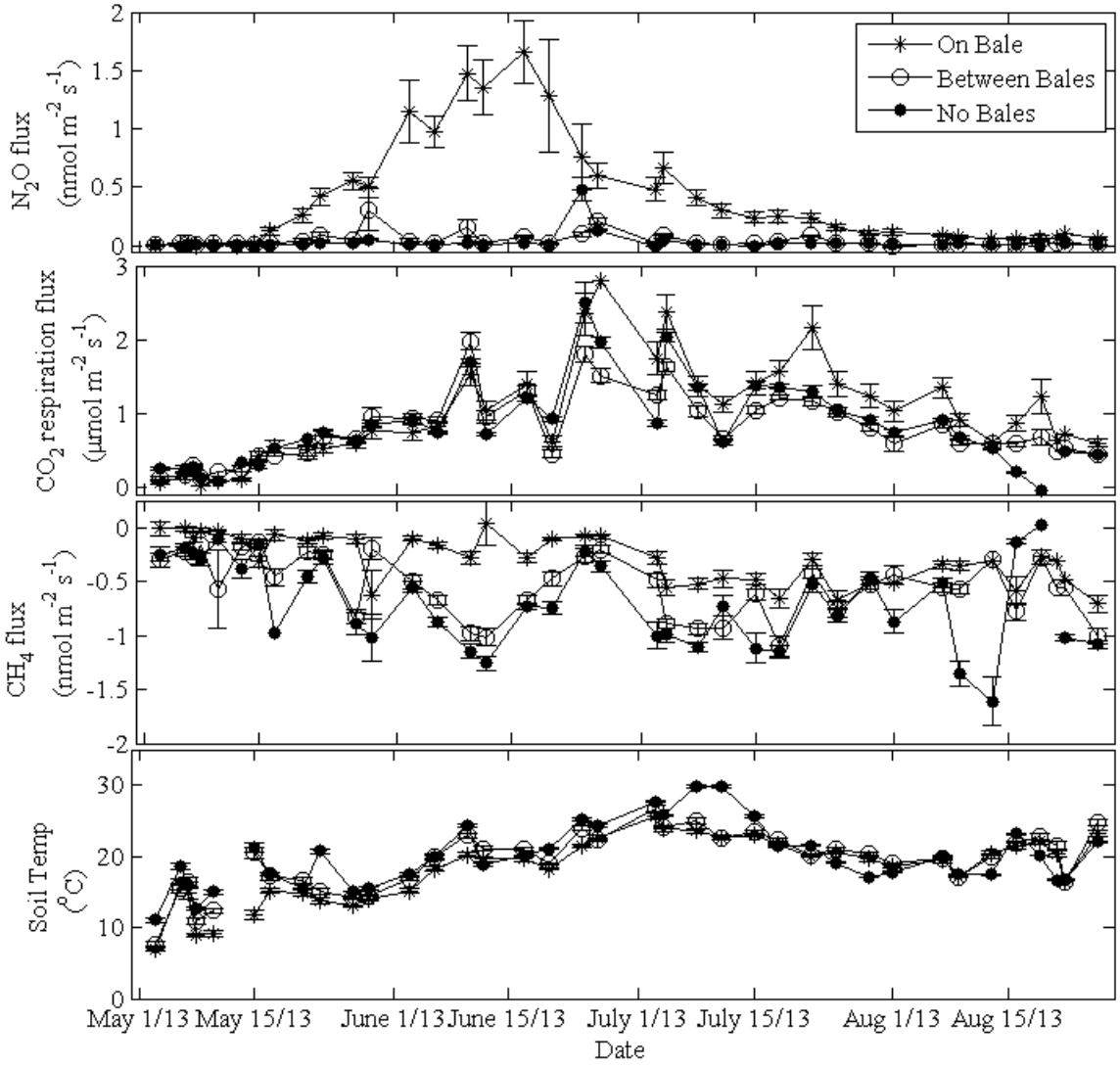

Figure 4.12 Chamber N_2O, CO_2, CH_4 flux and soil temperature on pasture post-winter bale grazing from May 3, 2013 to Aug 28, 2013 (SW field). Each point represents the mean of the chambers included. On Bale and Between Bales each had 24 chambers, while no-bale locations had 16. Error bars are ±1 SE.

Table 4.3 presents the flux measurements by gas and source. Cattle respiration averaged 1.5 µmol m^{-2} s^{-1} and the land component was also a CO_2 source of 0.7 µmol m^{-2} s^{-1}, based on the separation of processes before gap filling. If we maintained continuous gap-filling without cattle/land separation, the average CO_2 flux was 1.8 µmol m^{-2} s^{-1}. Enteric CH_4 emissions averaged 0.08 µmol m^{-2} s^{-1}. The excreta and bedding emissions in

the water corral were about 0.2 μmol CH_4 m^{-2} s^{-1}, far exceeding the soil sink of about -5 x 10^{-4} μmol CH_4 m^{-2} s^{-1}, but the water corral only covered a small area. Further, these fluxes were not continuous throughout the year, and we estimate that the net CH_4 excreta/soil effect was a small emission of 4 x 10^{-4} μmol CH_4 m^{-2} s^{-1} averaged over the year. Nitrous oxide emissions were about 0.009 μmol N_2O m^{-2} s^{-1} from excreta and about 1 x 10^{-4} μmol N_2O m^{-2} s^{-1} from fertilizer addition, again not constant throughout the year. The N_2O flux scaled over space and time was a net emission of about 0.001 μmol N_2O m^{-2} s^{-1}. Whole-farm emissions incorporating global warming potential factors indicated emissions of 46 t CO_2e $ha^{-1}y^{-1}$, dominated by cattle respiration.

Table 4.3. Whole-farm greenhouse gas flux estimates (mean ± S.E.).

	CO_2		CH_4		N_2O
Farm field	Cattle respiration (μmol m^{-2} s^{-1})	Plant-soil (μmol m^{-2} s^{-1})	Enteric (μmol m^{-2} s^{-1})	Soil-manure (nmol m^{-2} s^{-1})	Soil-manure (nmol m^{-2} s^{-1})
NE	1.47 ±0.034 (whole field)	0.70 ±0.034 (whole field)	0.078 ±1.8E-3 (whole field)	-0.538 ±0.028	0.114 ±0.011
SE				*-0.51 ±0.02*	*0.0406 ±4.6E-3*
SW				-0.475 ±0.012	0.175 ±0.012
NW				*-0.51 ±0.02*	*0.0406 ±4.6E-3*
Water corral				257.1 ±103.2	9.21 ±3.3E-3
Spatial scaled means (μmol m^{-2} s^{-1})*	1.47 ±0.034	0.70 ±0.034	0.078 ±1.8E-3	5.25E-4 ±5.46E-4	2.4E-3 ±2.9E-5
Temporally weighted means (μmol m^{-2} s^{-1})†	1.47 ±0.034	0.70 ±0.034	0.078 ±1.8E-3	4.13E-4 ±6.5E-4	0.0012 ±1.2E-5
Net CO2-equivalent (t CO2e ha^{-1} $year^{-1}$)‡	20.37 ±0.48	9.78 ±0.47	11.14 ±0.25	0.058 ±0.092	4.4 ±0.04

Variability is reported as SEM and italics are estimated values based on chamber measurements.

* Spatial scaling data obtained from the field-by-field means, where each was multiplied by the weighting of how much space each location occupied (0.24875 for each quadrant and 0.005 for the water corral)

† Subsequently, the spatially weighted mean from each field location was averaged based on 116 days for SW, NW, and SE quadrants, 87 days for NE, and 182.5 for the water corral.

‡ Global warming potential of 28 for CH_4 and 265 for N_2O by mass (Myhre et al. 2013).

4.5 Discussion

4.5.1 Spatial and temporal challenges

4.5.1.1 Flux tower sampling. The spatial variability of fields and the moving cattle herd posed challenges to integrating greenhouse fluxes in space and time. Ideally, there

would be multiple flux towers on the farm to measure each field uniformly. This could work well for static parts of the landscape (plants and soil), but the moving cattle will always have a varying footprint. Figure 4.7 suggests that we could have chosen a higher measurement height to have a larger spatial footprint on the farm to better capture herd-scale emissions. However, these are long-term average footprints and short-term conditions could result in flux sources/sinks from beyond the farm boundaries. This is especially an issue during stable night conditions when footprints can originate from many hundred meters from the tower, possibly sampling fluxes from outside the farm.

The methane flux measurements helped to identify cattle presence on the landscape and their respiration was sufficiently great to swamp the plant/soil CO_2 flux through much of the year. It took a substantial photosynthetic uptake in June through August to overcome the cattle respiration flux (Figures 4.5, 4.9). Frozen winter conditions resulted in low soil respiration such that cattle activity easily dominated total respiration. The cattle impact was also sufficiently great that the high-frequency signal for methane flux and sensible heat flux in winter were sometimes correlated, similar to the methane and CO_2 correlation shown in Figure 4.6. This is because of a low background sensible heat flux in our winter environment. Global-positioning sensors could have helped determine cattle location, but matching location with the flux footprint can be a challenge. Felber et al. (2015, 2016a) had a much more constrained dairy cattle system with good position knowledge, but they acknowledged the challenge with these moving point sources. In our study, the combination of moving cattle, shifting wind direction, and changes in atmospheric turbulence made our landscape integration poorly constrained.

We estimated the plant/soil CO_2 flux to be about 265 g C m^{-2} y^{-1} (average of 0.7 μmol m^{-2} s^{-1}, Table 4.3) when excluding cattle during our gapfilling. Felber et al. (2016a) estimated CO_2 flux gapfilling uncertainty with and without cattle inclusion of about 40-50 g C m^{-2} y^{-1} for a much more constrained dairy farm (20 cows on 3.6 ha). If we calculate CO_2 flux without excluding cattle during gapfilling, the net emission is 605 g C m^{-2} y^{-1}, with the difference of 340 g C m^{-2} y^{-1} caused by cattle respiration. This is much less than the 557 g C m^{-2} y^{-1} given in Table 4.3 based on separate gap-filling of cattle periods. The cattle presence was sufficiently great to likely increase our CO_2 flux uncertainty to much more than 100 g C m^{-2} y^{-1} making it difficult to determine if the plant/soil system was a source or a sink.

Skinner (2008) expressed concern over the large shifts in instantaneous fluxes when cattle were near a tower, potentially invalidating the stationarity requirement for eddy covariance. However, the issue of stationarity is usually caused by non-steady conditions in the wind field, potentially invalidating the averaging of instantaneous velocity-scalar cross product deviations from the mean. We did not quality-control the data for stationarity but there was no pattern in CO_2 flux, CH_4 flux, or the variance in the CH_4 concentration with the standard deviation of wind direction when cattle were present, a good indicator of changing source/sinks over a 30-min averaging period. Similarly, Felber et al. (2016a) also did not include a filter for stationarity in their measurements over cattle.

Some sectoral patterns emerged for both CH_4 and CO_2 exchange (Figure 4.8). The upward CO_2 flux in the SW quadrant in July was likely caused by decomposition of remaining winter-feed bales, because cattle were seldom in the footprint (low CH_4

fluxes). The water corral located in the NE sector was dominated by cattle presence and showed the highest fluxes for both CH_4 and CO_2 (respiration). As a reference, beef cattle heifers typically respire about 2000 L CO_2 d^{-1} per head (Boadi et al. 2002) and beef steers emit about 160 L CH_4 d^{-1} per head (Wilson et al. 2010). There is also a diurnal emission variation of the order of a factor of two for CH_4 (e.g., McGinn et al. 2008). For the case where our 104 animals were located in the water corral to the north of our main tower (Figure 5.1, corral area is 0.62 ha), we could expect maximum fluxes of the order of 17 μmol CO_2 m^{-2} s^{-1} and 1.3 μmol CH_4 m^{-2} s^{-1}. This scaling is not exactly correct because the flux footprint is often larger than the corral area, but this shows that our daily measured fluxes were less than these maximum amounts (Figures 4.5, 4.9).

A few studies have looked at the ratio of enteric methane to respiration. Bai et al. (2015) calculated an average concentration ratio of 0.028 μmol CH_4 μmol^{-1} CO_2 for beef cattle in Australia with a range of 0.008 to 0.044 μmol CH_4 μmol^{-1} CO_2. Felber et al. (2016a) calculated a flux ratio of 0.07 μmol CH_4 μmol^{-1} CO_2 for dairy cattle. Our data indicate substantial diurnal variation in the flux ratio with most data being between 0.01 and 0.12 μmol CH_4 μmol^{-1} CO_2 (Figure 4.10). The diurnal variation (Figure 4.10b) cannot be easily attributed to a single process, because the timing of feed intake, digestion, feed quality, and cattle activity were not measured, all of which contribute to variability in both CH_4 and CO_2 cattle emissions (Laubach and Kelliher 2005, Dijkstra et al. 2011, Laubach et al. 2013). However, our ratios as a function of time suggest that more measurements with better monitoring of animal activities are needed, which was not evident from the plots of concentrations or fluxes reported by Bai et al. (2015), Felber

et al. (2016b), or Prajapati and Santos (2017). Refinement of how these processes change CH_4 flux could allow for it to be modelled from CO_2 respiration flux measurements.

4.5.1.2 Chamber sampling. Our main goal was to use the chambers to capture N_2O flux, which was not measured through eddy covariance. Chambers are useful for capturing spatial differences to contextualize temporal emissions (Molodovskaya et al. 2011), particularly if there are enough to reflect the variability of the location. Minimum detection levels for chamber fluxes are usually of the order of 0.5 to 1 nmol N_2O m^{-2} s^{-1} (Parkin et al. 2012; Duran and Kucharik 2013), and our emission events in both the swath-grazing and winter bale-grazing field clearly exceeded these (Figures 4.11, 4.12). Note that the frozen winter conditions in Manitoba cause negligible winter N_2O fluxes as shown in Figures 4.11 and 4.12, and at other Manitoba sites (e.g., Tenuta et al. 2016).

4.5.1.2.1 Swath-grazing field. Nitrous oxide emissions from annual cropping systems in Manitoba are episodic, dominated by an event during spring thaw and a second event following nitrogen fertilizer application (Glenn et al. 2012; Maas et al. 2013). Our chamber measurements on the swath-grazing field were designed to capture the nitrogen fertilizer application event that typically accounts for more than three-quarters of the total annual N_2O emissions from cropped fields (Tenuta et al. 2016). Our sampling missed the smaller thaw event, which would have occurred prior to our spring measurements (Figure 4.11). We had sufficient precipitation (Figure 4.4) immediately following fertilizer application in mid-May to sustain N_2O emissions for about six weeks. Late-June soil sampling showed increased NO_3^- concentrations (Table 4.2), and it is likely that these

were even higher at the time of peak N_2O emissions in the beginning of June. It is possible that some of these emissions were contributed by the legacy of cattle excreta from the previous fall, but we do not have soil nitrogen measurements prior to fertilizer application on this field to estimate this contribution. However, the N_2O flux on this field was more than twice that on the no-bale sections of the bale-grazed field, indicating that nitrogen fertilizer application was more important than distributed cattle excreta (Figure 4.12, Table 4.3). Soil CO_2 emissions gradually increased as the soil warmed and crop roots developed, peaking in late June (Figure 4.11). CH_4 flux was a minor sink, with greater uptake in late July and August. This is consistent with other measurements of a net sink for CH_4 in well-drained agricultural soils in Manitoba (Dunmola et al. 2010).

4.5.1.2.2 Bale-grazing field. The chamber measurements on the winter bale-grazing field were designed to estimate excreta contributions to greenhouse gas emissions. As such, we hypothesized that the location of cattle excreta would not be random. For example, a survey of Canadian beef operations (Sheppard et al. 2015) observed cattle congregated on pasture about one-quarter of the time, depositing urine and feces unevenly causing a patchy nitrogen distribution (Oenema et al. 1997). Bale grazing deposition created a more predictable pattern that was reflected in our chamber measurements of N_2O, with emissions higher on the bales than elsewhere (Figure 4.12). Emissions from the on-bale locations were higher and of greater duration than the post-fertilizer N_2O emissions (Figure 4.11) and were clearly the main source of emissions compared to between-bale and no-bale locations. It is likely that the preferential

movement of cattle around the bales and subsequent manure/urine deposition were a larger contributor to field variability than potential landscape effects.

It is clear that the N_2O emissions were negligible during frozen winter conditions and the on-bale flux did not start until air temperatures reached 10°C. This is consistent with other over-wintering cattle studies (Hynšt et al. 2007; Hörtnagl and Wohlfahrt 2014), although our environment tends to be a little more extreme than most cattle-rearing regions globally, with almost half the year spent frozen (Figure 4.4). For cattle excreta, urine is a larger driver of N_2O emissions than feces (Tremorin et al. 2012). Nitrifying organisms can be slow growing, so urine and faeces patches can take weeks to completely nitrify, mineralizing organic N over long periods of time (Oenema et al. 1997), relating to the N content of the original waste (Bolan et al. 2004). The high on-bale emissions from mid-May to late June corresponded to higher moisture than the other two chamber locations. This was caused by the bedpack and residual bale material, whose porous nature held more moisture and contributed to greater N_2O emissions from residual urine and dung. N_2O emissions positively correlated with higher soil NO_3^- concentrations (Table 4.2), as found in other studies (e.g., Hynšt et al. 2007; Gao et al. 2015).

Unlike the N_2O flux, CO_2 emissions were similar among chamber measurement locations, although the on-bale locations tended to have higher respiration later in the season, having more straw material to decompose (Figure 4.12). The on-bale locations had less net CH_4 uptake than the other locations, likely because emissions from manure offset the mineral soil uptake. However, CH_4 manure emissions were not large enough to

create a net upward flux, indicating that our flux tower CH_4 emissions did not have a component from this field.

4.5.1.2.3 Water corral. The water corral hosted all cattle at some point as the sole location for water access in winter for steers and cow-calf pairs in summer. It was also a confined area for steers from mid-March to early June as access to feed. The frequent visits and confinement created a zone of about 0.62 ha with substantial excreta deposits. Confinement of beef cattle for at least part of the year is common on the Canadian Prairies, although two-thirds of operations practiced extensive winter grazing in 2011, a substantial increase since 2005 (Sheppard et al. 2016). These excreta in the corral emitted large amounts of both N_2O and CH_4, typically orders of magnitude more than measured in the open fields (Table 4.3). However, this was only for a small area of the farm and the scaled emissions are minor compared to CO_2 and enteric CH_4 fluxes. Manure from confined areas is typically spread on fields during the frost-free period in Canada (winter spreading is generally not permitted) but the manure can be stockpiled or composted first, each process having different emissions of greenhouse gases. At our site, manure was not spread during our measurement period so these emissions were not captured.

4.5.2 The value of whole-farm flux measurements

Attempts to measure whole-farm greenhouse gas exchange are rare, especially for systems that involve cattle, enabling this study to provide insight on combining flux measurement techniques on a dynamic farm. Eddy covariance has been used to measure CH_4 fluxes from cattle over pasture (Detto et al. 2011; Baldocchi et al. 2012) and feedlots

(Prajapati and Santos 2017); and backward trajectory analysis is a common method to measure CH_4 fluxes from confined cattle (e.g., McGinn et al. 2008; Harper et al. 2011). Although several studies have measured CO_2 flux over grazed lands (e.g., Skinner 2008, Taylor et al. 2013), these did not explicitly include the cattle presence during the flux measurements. Our study was less constrained than a recent study on a small dairy farm in Switzerland (Felber et al. 2015, 2016a), with a larger domain (123 ha and 100+ animals compared to 3.6 ha and 20 animals in Switzerland) and less control over animal movement. Our farm included both backgrounding steers and cow-calf pairs for a short period. In Canada, beef operations average 65 cows and backgrounding operations average 31 steers (Sheppard et al. 2015). However there is tremendous variability: farms can have very few cattle or have over 500 cows or more than 100 steers; extensive farms can be more than 1800 ha in size whereas small operations may only be 20 ha (Alemu et al. 2016). Hence, the diversity among farms makes it difficult to extrapolate our data because there is no "typical" farm. In the farm taxonomy of Alemu et al. (2016), our operation would be classed as a large cow-calf backgrounding operation. Additional direct measurements of greenhouse gas budgets for a range of farm systems are needed to characterize sinks and sources.

Our methods employed both eddy covariance and chamber measurements, capturing different flux footprints of different scales, ranging from excreta, bale waste feed, cattle paddock, cattle herd, to farm net exchange. Our secondary flux tower was of limited use to help with our whole-farm accounting, although it clearly showed that fields without cattle had different CO_2 flux than the main tower footprint with cattle (Figure 4.5). Chambers identified winter grazing bales as N_2O hotspots the following spring and

summer, whose fluxes may not have been captured through micrometeorological methods because of the wind direction dependent flux source area. They also helped to constrain the magnitude of the N_2O flux on the farm, which showed as being small compared to CO_2 and CH_4 fluxes, but important after the large global warming potential for N_2O was included (Table 4.3). Beauchemin et al. (2010) estimated that manure N_2O accounted for 20% of all greenhouse gas emissions from the cow-calf herd in western Canadian beef production based on an 8-year production cycle. They did not include the carbon balance (plant/soil CO_2 flux, or cattle respiration) in their analysis, but their ratio of manure N_2O to enteric CH_4 flux for the cow-calf operation was about 0.38 in CO_2 equivalents, similar to our ratio of 0.4 (Table 4.3). Our field measurements averaging 0.4 nmol N_2O m^{-2} s^{-1} were similar to other measurements in Manitoba that ranged from 0 to 0.3 nmol N_2O m^{-2} s^{-1} (Tremorin et al. 2012), and our water corral measurements were the same as maximum fluxes of about 10 nmol N_2O m^{-2} s^{-1} measured in Europe (Flessa et al. 1996; Maljanen et al. 2007).

Cattle respiration clearly exceeded plant/soil CO_2 exchange (Table 4.3) and some of the carbon imbalance was made up by importing feed for winter bale grazing and for the period during which the cattle were confined to the corral. The carbon imported as feed was 329 large bales (76 t C) (Table 4.1) for the base winter feeding but many more bales were brought into the water corral during confinement during the March to June period. We estimate the gross primary production for the plant/soil system at about 700 g C m^{-2} y^{-1}, about the same as measured on a hay field in Manitoba (Taylor et al. 2013). Scaling to the full farm (123 ha), this represents about 400 t C fixed as net primary productivity (assuming 50% autotrophic respiration) in that year. The annual weight gain

by the 104 steers was about 19 t live weight (Table 5.1). However, without improved export and import data, we cannot do a net ecosystem carbon budget similar to Felber et al. (2016b).

4.6 Conclusions

Eddy covariance towers and static-vented chamber campaigns were used to measure the temporal and spatial variability of CO_2, CH_4, and N_2O on a Canadian beef farm for almost a full year. Although the flux tower footprints did not sample the full farm, they covered a sufficient area to estimate average fluxes. Cattle dominated the greenhouse gas budget through both respiration of CO_2 and enteric emissions of CH_4. The land contribution to CO_2 flux was often swamped by the cattle presence. Cattle excreta (urine and manure) contributed about 10% of the total greenhouse emissions (as CO_2 equivalent), and this would be 18% if we did not include cattle respiration. The highest N_2O fluxes from cattle excreta occurred in a water corral where cattle congregated for extended periods and at on-bale locations in the field following winter grazing. These were larger than the N_2O flux from a field where nitrogen fertilizer was added for annual crops used for swath grazing. With the exception of the water corral, the rest of the land base was a sink for CH_4, even where manure was present in the hay-bale winter grazing area. The farm supported a large number of cattle in a relatively small area and included imported feed. Overall, the farm was a greenhouse gas source because the plant/soil system was only a sink for a short part of the year.

To our knowledge, this is the first whole-farm measurement of greenhouse gases over an annual cycle where beef cattle were part of the operation. For future studies,

additional flux towers to measure individual fields with better footprint coverage would help, which would also improve sectoral averaging of fluxes from different management practices across a farm. We measured both CO_2 and CH_4 fluxes from our eddy covariance towers and it is likely that the very small N_2O fluxes would only be detectable following the nitrogen fertilizer application or over the small water corral; hence, chambers may still be better to estimate the N_2O flux from this farm. Our use of CH_4 fluxes as the main determinant of animal presence likely has some advantage over global positioning system locators because matching up animal locations is not trivial for large areas with many moving animals. However, knowing the number of animals in the footprint would allow an estimate of greenhouse gas flux per animal. Lastly, we needed better information on the lateral transfers at the farm gate to account for movement of feed and cattle to arrive at net biome production or a net carbon/greenhouse gas budget for the farm.

4.7 References

Alemu, A.W., Amiro, B.D., Bittman, S., MacDonald, D., Ominski, K.H. 2016. A typological characterization of Canadian beef cattle farms based on a producer survey. Can. J. Animal Sci. 96: 187-202.

Bai, M., Flesch, T.K., McGinn, S.M., Chen, D. 2015. A snapshot of greenhouse gas emissions from a cattle feedlot. J. Environ. Qual. 44: 1974-1978.

Bai, M., Griffith, D.W.T., Phillips, F.A., Naylor, T., Muir, S.K., McGinn, S.M., Chen, D. 2016. Correlations of methane and carbon dioxide concentrations from feedlot cattle as a predictor of methane emissions. Anim. Prod. Sci. 56: 108-115.

Baldocchi, D., Detto, M., Sonnentag, O., Verfaillie, J., Teh, Y.A., Silver, W., Kelly, N.M. 2012. The challenges of measuring methane fluxes and concentrations over a peatland pasture. Agric. For. Meteorol. 153: 177-187.

Barr, A.G., Black, T.A., Hogg, E.H., Kljun, N., Morgenstern, K., Nesic, Z. 2004. Inter-annual variability in the leaf area index of a boreal aspen-hazelnut forest in relation to net ecosystem production. Agric. For. Meteorol. 126: 237-255.

Bavin, T.K., Griffis, T.J., Baker, J.M., Venterea, R.T. 2007. Impact of reduced tillage and cover cropping on the greenhouse gas budget of a maize/soybean rotation ecosystem. Agric. Ecosyst. Environ. 134: 234-242.

Beauchemin, K.A., Janzen, H.H., Little, S.M., McAllister, T.A., McGinn, S.M. 2010. Life cycle assessment of greenhouse gas emissions from beef production in western Canada: A case study. Agric. Sys. 103: 371-379.

Beauchemin, K.A., McGinn, S.M. 2005. Methane emissions from feedlot cattle fed barley or corn diets. J. Anim. Sci. 83: 653-661.

Boadi, D.A., Wittenberg, K.M., Kennedy, A.D. 2002. Validation of the sulphur hexafluoride (SF_6) tracer gas technique for measurement of methane and carbon dioxide production by cattle. Can. J. Anim. Sci. 82: 125-131.

Bolan, N.S., Saggar, S., Luo, J., Bhandral, R., Singh, J. 2004. Gaseous emissions of nitrogen from grazed pasture processes, measurements and modelling, environmental implications, and mitigation. Adv. Agron. 84: 39-120.

Burba, G.G., McDermitt, D.K., Grelle, A., Anderson, D.J., Xu, L. 2008. Addressing the influence of instrument surface heat exchange on the measurements of CO_2 flux from open-path gas analyzers. Global Change Biol. 14: 1854-1876.

Chen, B., Black, T.A., Coops, N.C., Hilker, T., Trofymow, J.A., Morgenstern, K. 2009. Assessing tower flux footprint climatology and scaling between remotely sensed and eddy covariance measurements. Boundary-Layer Meteorol. 130: 137-167.

Detto, M., Verfaillie, J., Anderson, F., Xu, L., Baldocchi, D. 2011. Comparing laser-based open- and closed-path gas analyzers to measure methane fluxes using the eddy covariance method. Agric. For. Meterol. 151: 1312-1324.

Dijkstra, J., Oenema, O., Bannink, A. 2011. Dietary strategies to reducing N excretion from cattle: implications for methane emissions. Curr. Opin. Environ. Sustain. 3: 414-422.

Dunmola, A.S., Tenuta, M., Moulin, A.P., Yapa, P., Lobb, D.A. 2010. Pattern of greenhouse gas emission from a Prairie Pothole agricultural landscape in Manitoba, Canada. Can. J. Soil Sci. 90: 243-256.

Duran, B.E.L., Kucharik, C.J. 2013. Comparison of two chamber methods for measuring soil trace-gas fluxes in bioenergy cropping systems. Soil Sci. Soc. Am. J. 77: 1601–1612.

Ehrlich, W.A., Pratt, L.E., Poyser, E.A. 1956. Report of reconnaissance soil survey of Rossburn and Virden map sheet areas. Manitoba Soil Survey, Manitoba Department of Agriculture. Available: http://sis.agr.gc.ca/cansis/publications/surveys/mb/mb6/index.html [Online]

Environment Canada. 2014. Canadian Climate Normals 1971-2000, Available: http://climate.weather.gc.ca/climate_normals/index_e.html#1971 [Online]

Environment Canada. 2015. National Inventory Report 1990-2013: Executive Summary. Environment Canada, Gatineau, QC, Canada.

Environment Canada, 2016. Daily Data Report: Brandon A, Manitoba. Available http://climate.weather.gc.ca/climateData/dailydata_e.html [Online]

Felber, R., Münger, A., Neftel, A., Ammann, C. 2015. Eddy covariance methane flux measurements over a grazed pasture: effect of cows as moving point sources. Biogeosciences 12: 3925-3940.

Felber, R., Neftel, A., Ammann, C. 2016a. Discerning the cows from the pasture: quantifying and partitioning the NEE of a grazed pasture using animal position data. Agric. For. Meteorol. 216: 37-47.

Felber, R., Bretscher, D., Münger, A., Neftel, A., Ammann, C. 2016b. Determination of the carbon budget of a pasture: effect of system boundaries and flux uncertainties. Biogeosciences 13: 2959-2969.

Flessa, H., Dörsch, P., Beese, F., König, H., Bouwman, A.F. 1996. Influence of cattle wastes on nitrous oxide and methane fluxes in pasture land. J. Environ. Qual. 25: 1366-1370.

Foley, P.A., Crosson, P., Lovett, D.K., Boland, T.M., O'Mara, F.P., Kenny, D.A. 2011.Whole-farm systems modelling of greenhouse gas emissions from pastoral suckler beef cow production systems. Agric. Ecosyst. Environ. 142: 222-230.

Gao, X., Asgedom, H., M. Tenuta, M., Flaten, D. 2015. Enhanced efficiency urea sources and placement effects on nitrous oxide emissions. Agron. J. 107: 265-277.

Glenn, A.J., Tenuta, M., Amiro, B.D., Maas, S.E., C. Wagner-Riddle, C. 2012. Nitrous oxide emissions from an annual crop rotation on poorly drained soil on the Canadian Prairies. Agric. For. Meteorol. 166-167: 41-49.

Harper, L.A., Denmead, O.T., Flesch, T.K. 2011. Micrometeorological techniques for measurement of enteric greenhouse gas emissions. Anim. Feed Sci. Technol. 166-167: 227-239.

Hollinger, S.E., Bernacchi, C.J., Meyers, T.P., 2005. Carbon budget of mature no-tillecosystems in North Central Region of the United States. Agric. Forest Meteorol. 130: 59–69.

Hörtnagl, L., Wohlfahrt, G. 2014. Methane and nitrous oxide exchange over a managed hay meadow. Biogeosciences 11: 7219-7236.

Hutchinson, G.L. A.R. Mosier, A.R. 1981. Improved soil cover method for field measurement of nitrous oxide fluxes. Soil Sci. Soc. Am. J. 45: 311-316.

Hutchinson, G.L., Livingston, G.P. 2001. Vents and seals in non-steady-state chambers used for measuring gas exchange between soil and the atmosphere. Eur. J. Soil Sci. 52: 675-682.

Hynšt, J., Miloslav, Š., Brůček, P., Petersen, S.O. 2007. High fluxes but different patterns of nitrous oxide and carbon dioxide emissions from soil in a cattle overwintering area. Agric. Ecosyst. Environ. 120: 269-279.

Kopp, J.C., Wittenberg, K.M., McCaughey, W.P. 2004. Management strategies to improve cow-calf productivity on meadow bromegrass pastures. Can. J. Anim. Sci. 84: 529-535.

Kormann, R. Meixner, F.X. 2001. An analytical footprint model for non-neutral stratification. Boundary-Layer Meteorol. 99: 207-224.

Laubach, J., Kelliher, F.H. 2005. Methane emissions from dairy cows: Comparing open-path laser measurements to profile-based techniques. Agric. For. Meteorol. 135: 340-345.

Laubach, J., Kelliher, F.M., Knight, T.W., Clark, H., Molano, G., Cavanagh, A. 2008. Methane emissions from beef cattle - a comparison of paddock-and animal-scale measurements. Austr. J. Exper. Agri. 48: 132-137.

Laubach, J., Bai, M., Pinares-Patiño, C.S., Phillips, F.A.,Naylor, T.A., Molano, G., Rocha, E.A.C., Griffith, D.W.T. 2013. Accuracy of micrometeorological techniques for detecting changes in methane emissions from a herd of cattle. Agric. For. Meteorol. 176: 50-63.

Legesse, G., Small, J.A., Scott, S.L., Kebreab, E., Crow, G.H., Block, H.C., Robins, C.D., Khakbazan, M., McCaughey, W.P. 2012. Bioperformance evaluation of various summer pasture and winter feeding strategies for cow-calf production. Can. J. Anim. Sci. 92: 89-102.

Levy, P.E., Gray, A., Leeson, S.R., Gaiawyn, J., Kelly, M.P.C., Cooper, M.D.A., Dinsmore, K.J., Jones, S.K., Sheppard, L.J. 2011. Quantification of uncertainty in trace gas fluxes measured by the static chamber method. Eur. J. Soil Sci. 62: 811-821.

Maas, S.E., Glenn, A.J., Tenuta, M., Amiro, B.D. 2013. Net CO_2 and N_2O exchange during perennial forage establishment in an annual crop rotation in the Red River Valley, Manitoba. Can. J. Soil Sci. 93: 639-652.

Maljanen, M., Martikkala, M., Koponen, H.T., Virkajärvi, P., Martikainen, P.J. 2007. Fluxes of nitrous oxide and nitric oxide from experimental excreta patches in boreal agricultural soil. Soil Biol. Biochem. 39: 914-920.

Manitoba Soils Survey. 1974. Manitoba South Park: Canada Land Inventory Soil Capability for Agriculture. Printed by the Surveys and Mapping Branch, Department of Energy, Mines and Resources, Ottawa. (Map) [Accessed October 19, 2013] Available Online at:
<http://sis.agr.gc.ca/cansis/publications/maps/cli/1m/agr/cli_1m_agr_manitoba.jpg> [Online]

Massman, W.J. 2000. A simple method for estimating frequency response corrections for eddy covariance systems. Agric. For. Meteorol. 104: 185-198.

McGinn, S.M., Chen, D., Loh, Z., Hill, J., Beauchemin, K.A., Denmead, O.T. 2008. Methane emissions from feedlot cattle in Australia and Canada. Australian J. Exper. Agric. 48: 183-185.

McGinn, S.M., Beauchemin, K.A., Flesch, T.K., Coates, T. 2009. Performance of a dispersion model to estimate methane loss from cattle in pens. J. Environ. Qual. 38: 1796-1802.

McGinn, S.M., Flesch, T.K., Coates, T.W., Chen, D.L., Bai, M., Bishop-Hurley, G. 2015. Evaluating dispersion modeling options to estimate methane emissions from grazing beef cattle. J. Environ. Qual. 44: 97-102.

Merbold, L. Eugster, W., Stieger, J., Zahniser, M., Nelson, D., Buchmann, N. 2014. Greenhouse gas budget (CO_2, CH_4, N_2O) of intensively managed grassland following restoration. Global Change Biol. 20: 1913-1928.

Moffat, A.M., Papale, D., Reichstein, M., Hollinger, D.Y., Richardson, A.D., Barr, A.G., Beckstein, C., Braswell, B.H., Churkina, G., Desai, A.R., Falge, E., Gove, J.H., Heimann, M., Hui, D., Jarvis, A.J., Kattge, J., Noormets, A., Stauch, V.J. 2007. Comprehensive

comparison of gap-filling techniques for eddy covariance net carbon fluxes. Agric. For. Meteorol. 147: 209-232.

Molodovskaya, M., Warland, J., Richards, B.K., Öber, G., Steenhuis, T.S. 2011. Nitrous oxide from heterogeneous agricultural landscapes: source contribution analysis by eddy covariance and chambers. Soil Sci. Soc. Am. J. 75: 1829-1838.

Moncrieff, J.B., Massheder, J.M., de Bruin, H., Elbers, J., Friborg, T., Heusinkveld, B., Kabat, P., Scott, S., Soegaard, H., Verhoef, A. 1997. A system to measure surface fluxes of momentum, sensible heat, water vapour and carbon dioxide. J. Hydrol. 188-189: 589-611.

Moore, C.J. 1986. Frequency response corrections for eddy correlation systems. Boundary-Layer Meteorol. 37: 17-35.

Muñoz, C., Saggar, S., Berben, P., Giltrap, D., Jha, N. 2011. Influence of waiting time after insertion of base chambers into soil on produced greenhouse gas fluxes. Chil. J. Agr. Res. 71, 610-614.

Myhre, G., Shindell, D., Breon, F-M., Collins, W., Fuglestvedt, J., Huang, J., Koch, D., Lamarque, J-F., Lee, D., Mendoza, B., Nakajima, T., Robock, A., Stephens, G., Takemura, T., Zhang, H., 2013. Anthropogenic and Natural Radiative Forcing, in: Stocker, T.F., Qin, D., Plattner, G.K., Tignor, M., Allen, S.K., Boschung, J., Nauels, A.,

Xia, Y., Bex, V., Midgley, P.M. (Eds), Climate Change 2013: The physical science basis. Contribution of working group I to the fifth assessment report of the Intergovernmental Panel on Climate Change. Cambridge University Press, Cambridge, UK and New York, NY, USA. pp 661-731.

Oenema, O., Velthof, G.L., Yamulki, S., Jarvis, S.C. 1997. Nitrous oxide emissions from grazed grassland. Soil Use Manage. 13: 288-295.

Parkin, T.B., Venterea, R.T., Hargreaves, S.K. 2012. Calculating the detection limits of chamber-based soil greenhouse gas flux measurements. J. Environ. Qual. 41: 705–715.

Pedersen, A.R. 2012. HMR: Flux estimation with statistic chamber data. R package version 0.3.1. Avalable: http://CRAN.R-project.org/package=HMR [Online]

Pedersen, A.R., Petersen, S.O., Schelde, K. 2010. A comprehensive approach to soil-atmosphere trace-gas flux estimation with static chambers. Eur. J. Soil Sci. 61, 888-902.

Prajapati, P., Santos, E.A. 2017. Measurements of methane emissions from a beef cattle feedlot using the eddy covariance technique. Agric. For. Meteorol. 232: 349-358.

Rochette, P., Bertrand, N. 2003. Soil air sample storage and handling using polypropylene syringes and glass vials. Can. J. Soil Sci. 83: 631-637.

Rochette, P., Eriksen-Hamel, N.S. 2008. Chamber measurements of soil nitrous oxide flux: are absolute values reliable? Soil Sci. Soc. Amer. J. 72: 331-342.

Rotz, C.A., Corson, M.S., Chianese, D.S., Montes, F., Hafner, S.D., Jarvis, R., Coiner, C.U. 2011. The Integrated Farm System Model. Reference manual, Version 3.4. Pasture systems and watershed management research unit. Agricultural Research Service, USDA.

Sheppard, S.C., Bittman, S., Donohoe, G., Flaten, D., Wittenberg, K.M., Small, J.A., Berthiaume, R., McAllister, T.A., Beauchemin, K.A., McKinnon, J., Amiro, B.D., MacDonald, D., Mattos, F., Ominski, K.H. 2015. Beef cattle husbandry practices across Ecoregions of Canada in 2011. Can J. Anim. Sci. 95: 304-321.

Sheppard, S.C., Bittman, S., Ominski, K.H., MacDonald, D., Amiro, B.D. 2016. Changes in land, feed and manure management practices on beef operations in Canada between 2005 and 2011. Can J. Anim. Sci. 96: 252-265.

Skinner, R.H. 2008. High biomass removal limits carbon sequestration potential of mature temperate pastures. J. Environ. Qual. 37: 1319-1326.

Smith, R.E., Veldhuis, H., Mills, G.F., Eilers, R.G., Fraser, W.R., Lelyk, G.W. 1998. Terrestrial ecozones, ecoregions, and ecodistricts, An ecological stratification of Manitoba's landscapes. Technical Bulletin 98-9E. Land Resource Unit, Brandon Research Centre, Agriculture and Agri-Food Canada, Winnipeg, MB. Available:

http://sis.agr.gc.ca/cansis/publications/ecostrat/provDescriptions/mbteee/mbteee_report.pdf [Online]

Tanner, C.B., Thurtell, G.W. 1969. Sensible heat flux measurements with a yaw sphere and thermometer.TR Ecom 66-G22-F.Department of Soil Science, University of Wisconsin, Madison, Wisconsin.

Taylor, A.M., Amiro, B.D., Fraser, T.J. 2013. Net CO_2 exchange and carbon budgets of a three-year crop rotation following conversion of perennial lands to annual cropping in Manitoba, Canada. Agric. For. Meteorol. 182-83: 67-75.

Tenuta, M., Mkhabela, M., Tremorin, D., Coppi, L., Phipps, G., Flaten, D., Ominski, K. 2010. Nitrous oxide and methane emission from a coarse-textured grassland soil receiving hog slurry. Agric. Ecosys. Environ. 138: 35-43.

Tenuta, M., Gao, X., Flaten, D.N., Amiro, B.D. 2016. Late fall application of anhydrous ammonia reduces emissions of nitrous oxide compared to spring pre-plant application in Manitoba. J. Environ. Qual. 45:1133-1143.

Tremorin, D.G., Mkhabela, M., Tenuta, M., Flaten, D.N., Ominski, K.H. 2012. Nitrous oxide emissions from dung and synthetic urine of cattle grazing forage grass fertilized with hog slurry. Anim. Feed Sci. Technol. 177: 225-236.

Wagner-Riddle, C., Furon, A., McLaughlin, N.L., Lee, I., Barbeau, J., Jayasundara, S., Parkin, G., von Bertoldi, P., Warland, J. 2007. Intensive measurement of nitrous oxide emissions from a corn-soybean-winter wheat rotation under two contrasting management systems over 5 years. Global Change Biol. 13: 1722-1736.

Webb, E.K, Pearman, G.I., Leuning, R. 1980. Correction of flux measurements for density effects due to heat and water vapor transfer. Quart. J.R. Meteorol. Soc. 106: 85-106.

White, T.A., Snow, V.O., King, W.McG. 2010. Intensification of New Zealand beef farming systems. Agric. Syst. 103: 21-35.

Wilson, C., Undi, M., Tenuta, M., Wittenberg, K.M., Flaten, D., Krause, D.O., Entz, M.H., Holley, R., Ominski, K.H. 2010. Pasture productivity, cattle productivity and metabolic status following fertilization of a grassland with liquid hog manure: A three-year study. Can. J. Anim. Sci. 90: 233-243.

5. SYNTHESIS

5.1 Significance and implications

Agroecosystems have diverse management practises and systems that contribute to flux cycles in a variety of ways. This thesis looked at the capability of eddy covariance in capturing site variability of cropping systems fluxes and of a whole beef cattle farm. Chapter 2 evaluated our ability to capture the spatial variability of NEE over an agricultural field with a single eddy covariance flux tower, and measured field variability with gridded LAI measurements. Chapter 3 evaluated the capability of eddy covariance to represent spatial variability, but for H, LE, and Bowen ratio energy partitioning. It also examined H for a longer period and during multiple cropping seasons. Chapter 4 focused on gas fluxes with large spatial variation, examining how well we might be able to measure the variability of a complex beef cattle farm, combining both eddy covariance and chamber gas measurements.

5.1.1 Spatial representation of eddy covariance flux measurements over agricultural fields

Both chapter 2 and 3 generally found that increasing the number of eddy covariance flux towers on a field did not capture more of a field's variability. Regression analysis comparisons showed how r^2 of NEE over a forage slightly worsened the further towers moved apart, to a maximum distance of 100 m. Senescence had a larger impact on a spring wheat crop and made accounting for NEE spatial variation difficult. LE regression r^2 had consistent but high scatter. H was well represented by one tower, though

tower and instrument height must be adjusted dependent upon crop height to prevent obstruction or interference from tall crops and maintain an appropriate footprint size.

Mean field LAI was comparable to the subsampled tower footprint mean LAI. Minimum and maximum LAI suggested that footprints could have under- or over-represent the field LAI depending on tower placement. To address this, the North 100 m footprints of each field were repositioned on the gridded LAI colour map to simulate what values would have been captured if towers had been placed where LAI was predominantly low or high. At Forage, the high LAI footprint mean was 4.1 and the low LAI footprint mean was 2.4, while Wheat high and low footprint LAI were 2.6 and 1.8, respectively. Both minimum and maximum potential mean footprint LAI at both fields are comparable to the field means of 3.50 at Forage and 1.94 at Wheat (Table 2.2). Given the tower footprint sizes for our fields and separations, our flux towers would have captured a representative portion of the crop canopy no matter where they were positioned on field, so long as the footprint remained over the sample crop. It also indicates that another factor is driving differences among towers measuring NEE.

One of the primary assumptions of eddy covariance is that measurements are over a homogeneous surface, though most studies do not verify this. Based on 30-minute fluxes, this thesis determined that NEE RMSE was ~30%, LE was ~25- 44%, and H was ~10% whether co-located or separated. Multiple towers did not increase this, suggesting that one tower was enough to capture flux variability. Previous research has shown how annual and perennial crops affect CO_2 exchange in different ways across seasons (Taylor et al. 2013). These chapters also highlight the role of crop type in flux uncertainty, where

LAI had smaller values for spring wheat than the forage, and corn height contributed to smaller footprints than either soybeans or spring wheat when measuring H_v.

Both of these chapters highlight the need to include spatial accounting when using eddy covariance to measure gas or energy fluxes and ensure that tower measurements are representative of the surfaces that they measure. While a single measure of field variability helps this, continuous or repeated temporal measurements are necessary to gauge how a field changes within and among seasons. This combined with flux footprint modelling may help determine not only if the variability of a measured space influences fluxes, but if fluxes are representative of the field and cropping system.

Overall, H had the best goodness of fit when three towers were compared short term and four towers compared long-term. NEE and LE were more greatly affected by tower separation and field variability. However, NEE RMSE ranged from 1 – 4 μmol m^{-2} s^{-1} and H RMSE ranged 6 – 12 W m^{-2} no matter the field or tower separation, suggesting that though some differences are present, the real world application of this uncertainty did not amount to large flux differences amongst towers. LE RMSE had a wide range of 16 – 58 W m^{-2} that was not particularly bound by tower separation, but may relate more to the larger range of values present at the Forage field than Wheat. As well, when Bowen ratio energy partitioning was examined over a diurnal basis, the effects of field variability played less of a role. All three towers at the Forage field in 2014 had consistent patterns throughout the day, despite the differences found when H and LE were examined in regression separately.

5.1.2 The challenge of measuring the greenhouse gas budget of a complex beef cattle farm

While two chapters examined how the eddy covariance method represented the field variability of NEE, LE, and H, another chapter focused on applying the method to a complex farm with known variability of crop, field, cattle, feeding strategy, and source origin. The one tower method examined in the first two chapters was expanded to find better ways to quantify exchange of CO_2, CH_4, and N_2O. We saw eddy covariance as an integral component of capturing the fluxes of a complex, real world beef cattle farm, so we incorporated a secondary tower, as well as three campaigns of static-vented chamber measurements. Using chambers on winter bale grazing, summer swath grazing, and within the confinement/water corral incorporated N_2O measurements into the experiment and helped capture spatially variant fluxes that may be missed by the tower.

Variability from moving sources like cattle is complex, because they do not emit CH_4 and CO_2 uniformly, and can often move outside of the tower's flux footprint. Chapter 4 found that we could use CH_4 measurements as a tracer to isolate CO_2 respiration contributions from cattle, allowing us to see the impacts of cattle separate from the landscape fluxes. Strategically placed field cameras, which can potentially predict animal position with a similar level of accuracy as GPS collars (Benevenutti et al. 2015), were combined with background CH_4 concentration levels and allowed for CH_4 fluxes originating from cattle to be identified. Correlating flux patterns between CH_4 and CO_2 were also identified in the winter, when landscape CO_2 flux is very low. This allowed the CO_2 respiration fluxes cattle to be separated from landscape CO_2 fluxes.

Sampling chambers found that positions on field where there were bales during the previous winter's bale grazing emitted significantly more N_2O for longer periods of time than elsewhere on the field. Chambers were located outside of the main eddy covariance tower's footprint, and emissions may have been entirely missed by tower measurements if a fast response N_2O gas analyser had been available. Chambers helped to capture seasonal emissions resulting from animal behaviour that caused field emission patchiness. The largest N_2O emissions were from excreta/manure in the confinement pen near the eddy covariance tower.

Combining the chamber data with the eddy covariance tower measurements enabled us to estimate a CO_2, CH_4, and N_2O budget and subsequent CO_2-equivalency for the farm during the year-long measurement period. Cattle respiration contributions of CO_2 and enteric CH_4 dominated the budget, and the farm was a net carbon source. The small size of the farm with such a large number of cattle, in addition to the large amount of feed imported, played a role in the farm being a source of of 46 t CO_2e $ha^{-1}y^{-1}$. A study examining the larger farm system and including the fields where feed was grown may help to ameliorate the impact of cattle respiration through perennial field carbon fixation, but it is unlikely a beef cattle farm could be carbon neutral because of CH_4 emission and CO_2 respiration contributions. This is of particular concern in Canada currently because of the drive by governments and producers to reward perennial cropping systems feeding into beef cattle operations as carbon sinks or carbon neutral, when they may not be when lifecycle greenhouse gas exchange is examined.

5.2 Project limitations

Generally it is not possible to use more than one tower in most studies. Eddy covariance and micrometeorological researchers are prohibited by financial costs and the technical expertise required for establishing measurement sites and for continued upkeep and management. This thesis helps determine the spatial uncertainty applicable when drawing conclusions from single eddy covariance tower measurements of NEE, LE, and H over agroecosystems. However, conclusions drawn from our study are limited by the fields over which experiments were applied, which were flat agricultural sites with clay soils.

A challenge in both Chapters 2 and 3 was that we had not anticipated having difficulties with the CSAT3's accuracy/deviation over time, since they were not factory calibrated prior to our experimentation. When measurements were compared, for example, air temperature measurements amongst towers varied by up to 10°C at a given time. Without a known 'correct' CSAT3, it introduced some limitations in both of the 3-tower comparisons. Unfortunately, post-experiment factory calibration did not provide the needed information to correct measured values. How much an instrument changes over time is a unique characteristic and cannot be standardized. This reinforced the necessity of proper instrument calibration for the start of any experiment, but also within long-term monitoring sites. Additionally, Wheat South exhibited some drift when fluxes were below zero, separate from the regression comparison. It is possible that drift in the CSAT3 instrumentation occurred from the beginning of measurements to the end at each site, as evidenced by Figure 3.7. Whether factory calibration would aide this is unknown, but our regression correction to the stationary Centre tower could not account for this.

Characterizing our sites with LAI focused on variability in the vegetation, which neglects soil contributions. Including spatially sampled chamber measurements would have given a way to quantify soil respiration source terms as well. Particularly, at the Wheat site when the crop had already senesced, soil respiration measurements would have allowed for spatial sampling of the soil CO_2 source.

Both Chapter 2 and 3 would have benefited from a spatial measurement of soil moisture to better examine potential causes of variability in NEE, H, and LE fluxes. This was particularly relevant when analysing Chapter 3, because of how stomatal controls affect plant physiology and therefore canopy cover and potential energy exchange, and the importance of the water balance in cropping system. A direct measure of stomatal conductance would be most helpful. Methods to spatially quantify soil moisture are ongoing, through projects such as NASA's SMAPVEX which uses remote sensing to measure soil moisture, and has been recently undergone ground validation (Ojo 2017). However, satellite imagery may have too coarse a pixel size or measured too infrequently to gauge the field variability of short eddy covariance towers.

Tracking individual cattle movement with GPS collars was not possible in our study because the steers on farm were rarely handled and skittish. Our trail cameras were partially successful, but could not capture continuous presence or the amount of cattle, preventing us from calculating emission intensity factors. Felbert et al. (2015) and (2016) used GPS collars to track dairy cattle with some success. However, cameras have been shown to be nearly equivalent to GPS tracking when identifying cattle location (Benevenutti et al. 2015). Had they been placed more strategically, such as overhead to look down on cattle congregation areas, we may have captured cattle numbers and

location better. The development of photo recognition software will also benefit this type of tracking and reduce the huge time sink of manually cataloguing the photographs (Benevenutti et al. 2015). Measuring these complex systems sacrifices control and increases uncertainty, but may better represent what happens farms on all across Canada, and the uncertainty involved with measuring and modelling their budgets.

5.3 Integrating spatial and temporal phenomena into future flux work

Future eddy covariance studies should endeavour to include measures of site variability focusing on driving forces for fluxes, quantify the uncertainty associated with them, and the effect on conclusions drawn from the data. Tower footprints of eddy covariance towers have been compared to estimates of gross primary productivity (GPP) derived from Lidar vegetation classification maps (Chen et al. 2009), and upscaled flux data to predict GPP, ecosystem respiration, NEE, LE, and H on a global scale (Jung et al. 2011). For field-scale eddy covariance studies, satellite imagery may not be available as often as needed, can be hindered by cloud cover, and may be cost prohibitive.

An unmanned aerial vehicle (UAV) was not available for use during our experiments, but they are gaining popularity. They allow for multi-spectral imaging of research sites at potentially lower cost, finer resolution, and greater frequency than other remote sensing techniques like aeroplane or satellite. Multi-copters in particular are suited to characterizing field studies with lower measurement towers because imaging is over a smaller area and at a higher resolution. Currently there are weight restrictions related to instruments and power needs, but pyranometers, radiometers, cameras, infrared, or lightweight thermal imaging are available (Anderson and Gaston 2013). As technology progresses, more possibilities will open up, necessitating research into how

they can be used to create spatial maps of fields and quantify the relationships with carbon, water, and energy exchange in conjunction with flux footprint modelling.

Measurements such as these could establish baselines of site variability, with daily or weekly imagery taken on a regular schedule to map spatial changes of the field. Multi-spectral band cameras available on UAVs also allow for time-averaged normalized difference vegetation index (NDVI), which relates to plant vigor and is most useful in species where biomass is proportional to photosynthetic rates (Gago et al. 2015), and thereby carbon flux too. Other indices derived from reflectance could provide insight for plant water status, and be useful when measuring H and LE. The price and availability of multi-copter UAVs may not only be beneficial for researchers, but for producers as well, because of their ease of use and the ability to quickly investigate their fields (Gago et al. 2015).

It was observed in data from Chapter 4 (not included) that cattle created a diurnal trend in H that could be isolated during the winter because of low background H, providing another avenue through which they influence fluxes. Further research into this, how to capture cattle variability and track movement in relation to fluxes are needed to ensure quantification of management practises and greenhouse gas contributions are as accurate as possible. Research combining field studies such as ours with per-animal CO_2 respiration and enteric emission measurement would be useful to identify if field techniques can accurately predict emissions per animal.

Our research found a relationship between cattle CO_2 respiration and CH_4 enteric emission. Enteric methane is shown to be influenced by a wide range of factors, including but not limited to feed intake, quality and type, animal size and age, growth rate, and

environmental conditions (Broucek 2014), but the amount of CO_2 exhaled by cattle at the same time may not be easily separated from environmental fluxes. Further work could refine our understanding of this relationship to examine if there is an equation or model that allows one to be gap-filled from measurement of the other. We must determine whether one has a more consistent relationship than the other, such as modelling CO_2 respiration from enteric CH_4 or vice versa, and if it varies by gender, feed regime, or otherwise. It could also be integrated with micrometeorological techniques to allow more complete, gap-filled estimates of whole farm emissions. Studies where CO_2 is measured over cattle must also account for respiration as part of their greenhouse gas balance. Current CO_2 gap-filling methods are based on GPP and ecosystem respiration, and if used, will miss fluxes from cattle respiration.

Eddy covariance flux measurements are the micrometeorological standard for measuring fluxes of NEE, LE, and H, and over time have incorporated corrections for different confounding factors, such as spectral corrections, de-spiking, or the Webb-Pearman-Leuning correction for open-path sensors. These increase our measurement accuracy and improve understanding of how agricultural systems impact greenhouse gases and energy exchange. The research herein will further help us understand how spatial variability influences flux cycling and the uncertainty associated with the data as it is carried forward in modelling scenarios and for best management practise recommendations. Incorporating spatial accounting or CH_4 gap-filling methods with flux research will add another layer of certainty to our measurements and in the recommendations made to refine our agricultural flux policies and how to address the anthropogenic impacts of the production systems.

5.4 References

Anderson, K., Gaston, K.J. 2013. Lightweight unmanned aerial vehicles will revolutionize spatial ecology. Front Ecol. Environ. 11: 138-146.

Benvenutti, M.A., Coates, T.W., Imaz, A., Flesch, T.K., Hill, J., Charmley, E., Hepworth, G., Chen, D. 2015. The use of image analysis to determine the number and position of cattle at a water point. Comput. Electron. in Agric. 118: 24-27

Broucek, J. 2014. Production of methane emissions from ruminant husbandry: A review. J. Environ. Protect. 5: 1482-1493

Chen, B., Black, T.A., Coops, N.C., Hilker, T., Trofymow, J.A., Morgenstern, K. 2009. Assessing tower flux footprint climatology and scaling between remotely sensed and eddy covariance measurements. Boundary-Layer Meteorol. 130: 137-167.

Felber, R., Münger, A., Neftel, A., Ammann, C. 2015. Eddy covariance methane flux measurements over a grazed pasture: effect of cows as moving point sources. Biogeosciences 12: 3925-3940.

Felbert, R., Neftel, A., Ammann, C. 2016. Discerning the cows from the pasture: quantifying and partitioning the NEE of a grazed pasture using animal position data. Agric. For. Meteorol. 216: 37-47.

Gago, J., Douthe, C., Coopman, R.E., Gallego, P.P., Ribas-Carbo, M., Flexas, J., Escalona, J., Medrano, H. 2015. UAVs challenge to assess water stress for sustainable agriculture. Agric. Water Manage. 153: 9-19.

Jung, M., Reichstein, M., Margolis, H.A., Cescatti, A., Richardson, A.D., Arain, M.A., Arneth, A., Bernhofer, C., Bonal, D., Chen, J., Gianelle, D., Gobron, N., Kiely, G., Kutsch, W., Lasslop, G., Law, B.E., Lindroth, A., Merbold, L., Montagnani, L., Moors, E.J., Papale, D., Sottocornola, M., Vaccari, F., Williams, C. 2011. Global patterns of land-atmosphere fluxes of carbon dioxides, latent heat, and sensible heat derived from eddy covariance, satellite, and metorological observations. J. Geophys. Res. 116: 1-16.

Ojo, E.R. 2017. *In situ* and modelled soil moisture determination and upscaling from point-based to field scale. The University of Manitoba. Winnipeg, MB, Canada. Available online: [https://mspace.lib.umanitoba.ca/handle/1993/32026]

Taylor, A.M., Amiro, B.D., Fraser, T.J. 2013. Net CO_2 exchange and carbon budgets of a three-year crop rotation following conversion of perennial lands to annual cropping in Manitoba, Canada. Agric. For. Meteorol. 182-83: 67-75.